

UC Merced

UC Merced Electronic Theses and Dissertations

Title

Metal-Catalyzed Hydroboration of Unsaturated Bonds (C=C, C=N, C=O) and Alkylation of Nitriles

Permalink

<https://escholarship.org/uc/item/7m10c7ds>

Author

Singh, Arpita

Publication Date

2022

Peer reviewed|Thesis/dissertation

UNIVERSITY OF CALIFORNIA, MERCED

Metal-Catalyzed Hydroboration of Unsaturated Bonds (C=C, C=N, C=O) and Alkylation of Nitriles

By
Arpita Singh

A dissertation submitted in partial satisfaction of the requirements for the degree of

Doctor Of Philosophy

In

Chemistry

In the

Graduate Division

Of the

University of California, Merced

Committee in charge:

Prof. Ryan Baxter, Chair
Prof. Michael Findlater
Prof. Kristin M. Hutchins
Prof. Rebeca Arevalo

August 2022

Chapter 1 © *ACS Catal.* **2018**, 8, 7, 6186–6191.

Chapter 2 © *Polyhedron* **2019**, 159, 365-374; *Asian J. Org. Chem.* **2020**, 9, 416-420;
Nat. Catal. **2020**, 3, 154-162.

Chapter 3 © (<https://doi.org/10.1021/acs.organomet.1c00690>)

Chapter 4 © 2022 Arpita Singh

The Dissertation of Arpita Singh is approved, and it is acceptable in quality and form for publication on microfilm and electronically:

Dedication

In loving memory of my beloved father

Table of Contents

List of Tables.....	vii
List of Figures	viii
List of Schemes	xi
List of Abbreviations.....	xii
Acknowledgements.....	xiii
Curriculum Vita	xiv
Abstract	xvii
I. NICKEL-CATALYZED 1,4-REGIOSELECTIVE HYDROBORATION OF <i>N</i>-HETEROARENES.....	1
1.1. Introduction	1
1.2. Results and Discussion	4
1.3. Conclusion	12
1.4. Experimental Section	12
1.4.1. General considerations	12
1.4.2. General procedure for the hydroboration of pyridines.....	12
1.4.4. General procedure for ligand exchange reactions	12
1.4.5. Kinetics study and general procedure of kinetics experiments	13
1.5. Appendix.....	14
1.6. References.....	27
II. METAL-CATALYZED HYDROBORATION OF ALKENES AND AMIDES.....	29
2.1. Introduction	29
2.2. Iron-catalyzed hydroboration of alkenes	29
2.3. Lanthanum-catalyzed hydroboration of amides	37
2.4. Conclusion	44
2.5. Experimental Section	44
2.5.1. General considerations	44
2.5.2. General procedure for hydroboration of terminal alkenes.....	44
2.5.3. General procedure for synthesis of [BIAN]Fe-Styrene complex (M5)	44
2.5.4. Kinetic isotope effect experiment for hydroboration of styrene.....	45
2.5.5. General procedure for the formation of lanthanum polyoxometalate (POM).....	45
2.5.6. General procedure for deoxygenation of 3° amides.....	45
2.5.7. Gram scale reaction for hydroboration of 3° amide.....	45
2.5.8. General procedure for C-N bond activation reactions.....	45

2.5.9. General procedure for kinetic studies.....	46
2.6. Appendix.....	47
2.7. References.....	63
III. COBALT-CATALYZED ALKYLATION OF NITRILES WITH ALCOHOLS	68
3.1. Introduction	68
3.2. Results and Discussion	69
3.3. Conclusion	75
3.4. Experimental Section	75
3.4.1. General considerations	75
3.4.2. General procedure for alkylation of nitriles.....	75
3.5. Appendix.....	76
3.6. References.....	79
IV. METAL-CATALYZED HYDROBORATION OF CARBONATES AND SEMI-HYDROGENATION OF ALKYNES	82
4.1. Metal-catalyzed hydroboration of carbonates	82
4.2. Copper-catalyzed semi-hydrogenation of alkynes.....	84
4.3. Conclusion	86
4.4. Experimental Section	86
4.4.1. General procedure for hydroboration of carbonates with $\text{La}_4\text{O}(\text{acac})_{10}$	86
4.4.2. General procedure for hydroboration of carbonates with NaHBET_3	86
4.4.3. General procedure for semi-hydrogenation of alkynes.....	86
4.5. Appendix.....	87
4.6. References.....	97
Appendix: Copyrights.....	99

List of Tables

Table 1.1. Optimization of reaction parameters with various phosphine ligands	4
Table 1.2. Optimization of reaction parameters with various commercially available Ni sources	5
Table 1.3. Nickel-catalyzed regioselective 1,4-hydroboration of N-heteroarenes	7
Table 2.1. Optimization of reaction conditions using styrene as the model substrate	33
Table 2.2. Optimization of hydroboration of amides using various lanthanum salts	39
Table 2.3. Optimization of reaction with various polynuclear lanthanide-diketonato clusters	40
Table 2.4. Scope of hydroboration of amides	41
Table 2.5. Modulating bond activation by changing the R group	42
Table 3.1. Base screening for alkylation of nitriles	70
Table 3.2. Optimization of the reaction conditions for nitrile alkylation	71
Table 3.3. Comparison between Co(acac) ₃ and CoCl ₂ /BIAN	72
Table 4.1. Optimization of hydroboration of carbonates	83
Table 4.2. Optimization of semi-hydrogenation of alkynes	85

List of Figures

Figure 1.1. Examples of commercialized drug molecules comprised of 1,4-DHP as central components.....	1
Figure 1.2. Some of the precatalysts used for dearomatization of pyridines.	3
Figure 1.3. a) Structure of Ni(acac) ₂ -PCy ₃ (19) b) Structure of Ni(acac) ₂ -PCy ₂ Ph (20).....	9
Figure 1.4. Reaction of 17 with Pcy ₃	10
Figure 1.5. Displacement of PCy ₃ with 3,5-Lutidine from 18	10
Figure 1.6. Reaction profile of reduction of 3,5-lutidine by HBPin in the presence of 14/L3 (■), 17 (●) and 18 (▲).	11
Figure 1.7. ¹ H NMR for Initial hydroboration of pyridine in the presence of Ni(acac) ₂ and NaOtBu at R.T.	14
Figure 1.8. ¹ H NMR for Initial hydroboration of pyridine in the presence of Ni(acac) ₂ and SNaOtBu at 50 °C	15
Figure 1.9. ¹ H NMR of reaction mixture for hydroboration of pyridine at T= 1hr. (a) Ni(acac) ₂ /PCy ₃ ; (b) Ni(acac) ₂ /PCy ₂ Ph; (c) Ni(acac) ₂ /PCy ₃ ; and (d) free pyridine. The (*) represents the peak for diborylated 1,4- DHP.	16
Figure 1.10. (a) ¹¹ B NMR of stoichiometric reaction of Ni(acac) ₂ (25.69 mg, 0.1 mmol), and HBpin (12.80 mg, 14.51 uL, 0.1 mmol) in benzene-d ₆ ; (b) ¹¹ B NMR of reaction of Ni(acac) ₂ (25.69 mg, 0.1 mmol), and HBpin (76.79 mg, 87.06 uL, 0.6 mmol) under standard catalytic condition in benzene-d ₆	17
Figure 1.11. Stoichiometric reaction of pyridine (7.91 mg, 8.08 uL, 0.1 mmol), and HBpin (12.80 mg, 14.51 uL, 0.1 mmol) in benzene-d ₆ . (a) ¹ H NMR at T= 1 hr; (b) ¹¹ B NMR at T= 1hr.....	18
Figure 1.12. Stoichiometric reaction of pyridine (7.91 mg, 8.08 uL, 0.1 mmol), and PCy ₃ (23.83 mg, 24.34 uL, 0.1 mmol) in benzene-d ₆ . (a) ¹ H NMR at T= 1 hr; (b) ³¹ P NMR at T= 1hr.	19
Figure 1.13. Stoichiometric reaction of HBpin (12.80 mg, 14.51 uL, 0.1 mmol), and PCy ₃ (23.83 mg, 24.34 uL, 0.1 mmol) in benzene-d ₆ . (a) ¹ H NMR at T= 1 hr; (b) ¹¹ B NMR at T= 1 hr; (c) ³¹ P NMR at T= 1 hr.....	20
Figure 1.14. Stoichiometric reaction of pyridine (7.91 mg, 8.08 uL, 0.1 mmol), HBpin (12.80 mg, 14.51 uL, 0.1 mmol), and PCy ₃ (23.83 mg, 24.34 uL, 0.1 mmol) in Benzene-d ₆ . (a) ¹ H NMR at T= 1 hr; (b) ¹¹ B NMR at T= 1 hr.....	21
Figure 1.15. Plot of [Ni] vs. reaction rate (<i>K</i> _{max}), the reaction follows 1 st order dependence on [Ni].	22
Figure 1.16. Plot of [3,5-lutidine] vs. reaction rate (<i>K</i> _{max}), the reaction follows 0 th order dependence on [3,5-lutidine].....	23
Figure 1.17. Plot of [HBpin] vs. reaction rate (<i>K</i> _{max}), the reaction follows first order dependence on HBpin till 1.5 equiv. [HBpin], and then 0 th order at higher concentration.....	24
Figure 1.18. ¹ H NMR comparison for hydroboration of 3,5-lutidine. (a) Ni(acac) ₂ /PCy ₃ ; (b) Zn(acac) ₂ /PCy ₃ ; (c) Zn(acac) ₂	25
Figure 1.19. (a) ¹ H NMR of 16g ; (b) ¹³ C NMR of 16g	26
Figure 2.1. Prominent examples of redox non-innocent ligands.....	30
Figure 2.2. A well understood example serving to illustrate the concept of redox non-innocence.	31
Figure 2.3. Representative examples of iron complexes utilized for hydroboration of alkenes. ...	32
Figure 2.4. Iron pre-catalysts used for hydroboration of alkenes.....	33
Figure 2.5. Crystal structure of M5	35
Figure 2.6. Mechanism for the hydroboration of alkenes	36
Figure 2.7. Resonance stabilization of amides	37

Figure 2.8. Selected examples of catalysts for hydrofunctionalization of amides	38
Figure 2.9. Synthesis of polynuclear lanthanide-diketonato clusters	38
Figure 2.10. POMs with various lanthanide elements. (a) La (39) ; (b) Y (40) ; (c) Gd (41) ; (d) Eu (42) ; (e) Er (43) . All hydrogen and carbon atoms have been omitted for clarity.	39
Figure 2.11. Reaction intermediate presumed to be catalytically inactive species 49	43
Figure 2.12. Top diagram shows the GC-Mass of ion mass of alkyl boronate, as a function of time. Bottom diagram is mass spectrum taken at RT = 9.36 min.	47
Figure 2.13. The GC-Mass of reaction mixture. Top diagram shows ion mass of product as a function of time. Bottom diagram is mass spectrum taken at RT = 9.23 min.	48
Figure 2.14. Crystal data and structure refinement for [La] (39).....	49
Figure 2.15. Crystal data and structure refinement for [Y] (40).	49
Figure 2.16. Crystal data and structure refinement for [Gd] (41).....	50
Figure 2.17. Crystal data and structure refinement for [Eu] (42).	50
Figure 2.18. Crystal data and structure refinement for [Er] (43).....	51
Figure 2.19. Crystal data and structure refinement for (49).....	51
Figure 2.20. Plot of [Catalyst] Vs. reaction rate (K_{max}), the reaction follows 1 st order till 3 mol % catalyst loading. [Substrate] rate order assessment Varying concentration of Substrate while keeping Catalyst and HBpin constant.	52
Figure 2.21. Plot of [Substrate] Vs. reaction rate (K_{max}), the reaction follows 0 th order dependence on the substrate.....	53
Figure 2.22. Plot of [HBpin] Vs. reaction rate (K_{max}), the reaction follows 1 st order dependence on HBpin till 2 equiv. [HBpin], and then 0 th order at higher concentration.	54
Figure 2.23. ¹ H NMR of [BIAN]Fe-Styrene complex (M5).....	55
Figure 2.24. ¹ H NMR of DBpin, * represents product, (▲) represents mesitylene, (●) represents THF and (◆) represents pinacol.....	56
Figure 2.25. ¹¹ B NMR of DBpin	57
Figure 2.26. ¹ H NMR of 39	58
Figure 2.27. ¹³ C NMR of 39	59
Figure 2.28. ¹ H NMR of stoichiometric reaction. (Top): ¹ H NMR of 39 + 44a heated at 50 °C for 1hr; (Middle): ¹ H NMR of 44a ; (Bottom): ¹ H NMR of 39 . The (*) in the inset shows the shifts in the peak of 44a after heating with 39	60
Figure 2.29. ¹ H NMR of stoichiometric reaction. (Top): ¹ H NMR after heating (49) + 44a at 50°C for 2 hrs; (Bottom): ¹ H NMR of (49).	61
Figure 2.30. ¹¹ B NMR of stoichiometric reaction. (Top): ¹¹ B NMR after heating (49) + 44a at 50°C for 2 hrs; (Bottom): ¹¹ B NMR of (49).....	62
Figure 3.1. Representative examples of drugs containing the α-alkylated nitrile moiety.	68
Figure 3.2. Representative examples of pre-catalysts used for alkylation of nitriles..... Error! Bookmark not defined.	
Figure 3.3. ¹ H NMR of 3-(4-chlorophenyl)-2-(4-(trifluoromethyl)phenyl)propanenitrile (60ac) 76	76
Figure 3.4. ¹³ C NMR of 3-(4-chlorophenyl)-2-(4-(trifluoromethyl)phenyl)propanenitrile (60ac)	77
Figure 3.5. ¹⁹ F NMR of 3-(4-chlorophenyl)-2-(4-(trifluoromethyl)phenyl)propanenitrile (60ac)78	78
Figure 4.1. Selected examples of pre-catalysts for hydroboration of carbonates.....	83
Figure 4.2. Pre-catalysts used for semi-hydrogenation of alkynes.....	85
Figure 4.3. ¹ H NMR for hydroboration of dimethyl carbonate with La(acac) ₃	87
Figure 4.4. ¹¹ B NMR for hydroboration of dimethyl carbonate with La(acac) ₃	88

Figure 4.5. ^1H NMR for hydroboration of dimethyl carbonate with NaHBET_3 , ● represents NaHBET_3 and * represents internal standard	89
Figure 4.6. ^{11}B NMR for hydroboration of dimethyl carbonate with NaHBET_3	90
Figure 4.7. ^1H NMR for progress of hydroboration of ethylene carbonate with NaHBET_3 , ● represents NaHBET_3 and ♦ represents the products 67 and 68b	91
Figure 4.8. ^1H NMR of stoichiometric reaction of HBpin and ethylene carbonate	92
Figure 4.9. ^{11}B NMR of stoichiometric reaction of HBpin and ethylene carbonate	93
Figure 4.10. ^{11}B NMR of stoichiometric reaction of NaHBET_3 and ethylene carbonate.....	94
Figure 4.11. ^1H NMR of semi-reduction of diphenylacetylene in DMF, * represents Z-alkene, ● represents E-alkene	95
Figure 4.12. ^1H NMR of semi-reduction of diphenylacetylene in THF and 4, 4-ditertiarybutyl-2,2'-bipyridyl, * represents Z-alkene, ● represents E-alkene.	96

List of Schemes

Scheme 1.1. Preliminary screening of pyridine (15a) and picoline substrates (15b-d) in hydroboration catalysis employing Ni(acac) ₂ / PR ₃	6
Scheme 1.2. Left: Preparation of 17 . Right: Solid-state structure of 17	8
Scheme 1.3. Left: Preparation of 18 . Right: Solid-state structure of 18	9
Scheme 2.1. Substrate scope for hydroboration of alkenes	34
Scheme 2.2. Method for the preparation of M5	35
Scheme 3.1. Substrate scope for alkylation of nitriles.....	74
Scheme 4.1. Substrate scope for lanthanum-catalyzed hydroboration of carbonates.....	84
Scheme 4.2. General reaction for hydroboration of carbonates with NaHBET ₃	84

List of Abbreviations

Ar	aryl
BIAN	bis(arylamino)acenaphthene
hmbs	hexamethyldisilazane
NMP	N-Methylpyrrolidone
bs	broad singlet (NMR)
°C	degree Celsius
Cy	cyclohexyl, -C ₆ H ₁₁
THF	tetrahydrofuran
DCM	dichloromethane
s	singlet (NMR)
d	doublet (NMR)
t	triplet (NMR)
m	multiplet (NMR)
dd	doublet of doublets (NMR)
h	hour(s)
Me	methyl, -CH ₃
Et	ethyl, -CH ₂ CH ₃
<i>i</i> Pr	isopropyl, -CH(CH ₃) ₂
Ph	phenyl, -C ₆ H ₅
<i>t</i> Bu	tert-butyl, -C(CH ₃) ₃
Ph	phenyl, -C ₆ H ₅
R	organic substrate
ee	enantiomeric excess
equiv.	equivalent(s)
MHz	mega Hertz
Mol	mole(s)
NMR	nuclear magnetic resonance
GC-MS	gas chromatography-mass spectrometry
<i>o</i>	ortho
<i>m</i>	meta
<i>p</i>	para
t	time
RT	room temperature
T	temperature
INS	internal standard
n.c.	no conversion
n.d.	not determined

Acknowledgements

The process of earning a doctorate is long and arduous, and it is undoubtedly not done singlehandedly. First and foremost, I would like to thank almighty for his choicest blessings and making this possible.

I would like to thank several people for their influence on my scientific career. I would like to extend my deepest gratitude and profound respect to my research advisor Prof. Michael Findlater for allowing me to conduct research in the lab and use the resources. His guidance, mentorship, and motivation has played a vital role during my Ph.D. I am honored to be his graduate student and I feel very privileged to be a part of his diverse research group. I really appreciate his advice and insights on the professional matters, especially when I felt lost and couldn't take an appropriate decision for myself. As I leave the Findlater lab for future endeavors in my career, I acknowledge his impact on my way of approaching challenges in science and never being afraid to try new things.

I am grateful to several faculty members including my research exam and dissertation committee members. I would like to thank Dr. Andrew Harned and Dr. Anthony Cozzolino for providing suggestions regarding my research projects in my qualifying exam. I am thankful to my dissertation committee members both at UC Merced and Texas Tech University, Dr. Ryan Baxter, and Dr. Rebeca Arevalo, and Dr. Kristin Hutchins for serving on my committee and providing feedback on my research. I am thankful to Dr. Christine Isborn for her help in the admission process at UC Merced.

I appreciate the funding sources NSF, Welch, Texas Tech, and UC Merced for the financial assistance and resources. My notable thanks to the International Office of Affairs and Department of Chemistry, Texas Tech for awarding me several fellowships during my Ph.D. I would also like to extend my deepest gratitude to graduate committee members of Chemistry and Biochemistry at UC Merced for providing me Dissertation Incentive Award.

I would like to thank my previous group members, Dr. Sem Tamang, Dr. Anu Saini, Dr. Sara Haghighi, Dr. Deepika Bedi. I really appreciate the time they took out to provide suggestions about my chemistry. I am highly indebted to them for their efforts in training me to be a good scientist. I am grateful to my current group members Dr. Andrew King, Dr. Miguel Chacon, Aida, Aneelman, and Koto, for their love, support and friendship.

My sincere thanks to the staff of Chemistry and Biochemistry both at Texas Tech and UC Merced: Dr. Kazimierz Surowiec, Dr. Piotr Dobrowolski, Dr. Daniel Unruh, Jeanne Bertonazzi, Scott Hiemstra, Jerry Franco, Quentin Vaughn, Dr. David Rice, Robin Trayler for their help and support.

Thanks to my amazing mother and brother for their continuous and relentless love. They are my pillars of strength, and this wouldn't have been possible without them. I am grateful to my parents for the knowledge and love they instilled in me. I am forever indebted to them for giving me the opportunities and experiences so that I can excel in life.

Finally, I would like to thank my friends Siddharth, Sakshi, Amandeep and Lovedeep for their love and support.

Curriculum Vita

EDUCATION

University of California (Transferred) Ph.D. in organic and organometallic chemistry	Merced, California Aug 2022
Texas Tech University (Moved to University of California, Merced) Ph.D. in organic and organometallic chemistry	Lubbock, Texas Jul 2021
Panjab University Master's in organic chemistry (H.S.)	Chandigarh, India May 2015
Panjab University Bachelors's in chemistry (H.S.)	Chandigarh, India May 2015

RESEARCH EXPERIENCE

Graduate Researcher at University of California, Merced Jul 2021-Present

- Initiated, designed, and executed experiments using cobalt and bis(imino)acenaphthene (BIAN) ligand to carry out the alkylation of nitriles with alcohols.

Graduate Student at Texas Tech University Jan 2017-Jul 2021

- Modified the synthesis of bis(imino)acenaphthene (BIAN) ligands which lessened the reaction time considerably (from 1 day to 1 hour).
- Synthesized several metal complexes of transition metals (iron, cobalt, nickel, ruthenium, iridium, zinc); analyzed and characterized them with NMR, IR, and X-Ray crystallography techniques.
- Designed and optimized iron-based catalytic system for the regioselective hydroboration of alkenes and alkynes; synthesized plausible intermediates to study the mechanism.
- Developed a catalytic system for the dearomatization of pyridines to produce 1,4-dihydropyridines; synthons in pharmaceutical drugs.
- Collaborated with a cross-functional team to synthesize substrates and optimize lanthanum-based catalytic system to reduce amides and esters; isolated reaction intermediates and ran kinetics experiments to gain in-depth knowledge of the mechanism.

Additional projects: Hydroboration of carbonates, Semi hydrogenation of alkynes, Preparation of POCOP ligands and their iridium complexes

Master's student at Panjab University Jul 2013-May 2015

- Developed a greener method for synthesizing amides, circumventing the prior functionalization of substrates.
- Gained hands-on experience in simple techniques such as distillation, TLC preparation, and analyzing TGA, NMR, IR, and GC data.

MENTORSHIP EXPERIENCE

Mentor at Texas Tech University Jan 2017-Jul 2021

- Instructed chemistry majors' students about experiments involving multi-step synthesis, organometallic complexes, purification, and isolation; analyses using FT-IR, NMR, GC-MS, TLC, and column chromatography techniques.
- Supervised and guided students in weekly lab experiments, monitored student performances, and ensured lab safety guidelines.
- Delivered organic chemistry recitation classes to several sections comprising 100 students each; helped them understand and solve problems related to their course and conducted quizzes periodically to check the performance.

Lecturer at Dev Samaj College for Women

Jul 2015-Dec 2016

- Presented organic chemistry lectures and experiments to undergraduate classes, designed quizzes, conducted oral and practical examinations.

PUBLICATIONS

- **Singh, A.**; Bedi, D.; Findlater, M. Iridium complexes of POCOP and PONOP pincer Ligands. *Inorg. Synth.* (Submitted).
- **Singh, A.**; Findlater, M. Cobalt catalyzed alkylation of nitriles with alcohols *Organometallics*. **2022** (ASAP Articles)
[10.1021/acs.organomet.1c00690](https://doi.org/10.1021/acs.organomet.1c00690)
- Tamang, S.; **Singh, A.**; Bedi, D.; Bazkiaei, A.R.; Warner, A.A.; Glogau, K.; McDonald, C.; Unruh, D.K.; Findlater, M. Polynuclear lanthanide-diketanato clusters for the catalytic hydroboration of carboxamides and esters. *Nat. Catal.* **2020**, *3*, 154-162.
- **Singh, A.**; Haghighi, S.S.; Smith, C.R.; Unruh, D.K.; Findlater, M. Hydroboration of Alkenes and Alkynes Employing Earth - Abundant Metal Catalysts. *Asian J. Org. Chem.* **2019**, *9*, 416-420.
- Larson, P.J.; Wekesa, F.S.; **Singh, A.**; Smith, C.R.; Rajput, A.; McGovern, G.P.; Unruh, D.K.; Cozzolino, A.F.; Findlater, M.; Synthesis, characterization, electrochemical properties and theoretical calculations of (BIAN) iron complexes. *Polyhedron* **2019**, *159*, 365-374.
Tamang, S.; **Singh, A.**; Unruh, D.K.; Findlater, M. Nickel-Catalyzed Regioselective 1,4-Hydroboration of N-Heteroarenes. *ACS Catal.* **2018**, *8*, 6186-6191.

AWARDS AND FELLOWSHIPS

- | | |
|---|---------------------|
| • CBC Chemistry Department Dissertation Incentive Award | Jan 2022-May 2022 |
| • Study Abroad Competitive Fellowship | May 2021 - Jul 2021 |
| • Study Abroad Competitive Fellowship | May 2020 - Aug 2020 |
| • Robert Goodin Research Fellowship | May 2019 - Aug 2019 |
| • Tex Syn IV Speed-Talk Award | May 2019 |
| • Summer RA Department Fellowship | May 2018 - Aug 2018 |
| • Department Provost Fellowship | Jan 2017 - Jan 2018 |

CONFERENCES ATTENDED

- | | |
|--|----------|
| • ACS National Meeting in San Diego | Mar 2022 |
| • International Webinar | Dec 2020 |
| • ACS Fall 2020 Virtual Meeting & Expo | Aug 2020 |

- GIDW 2020 Virtual Poster Event July 2020
- RSC Online Twitter Conference Mar 2020
- ACS South-West Regional Meeting, El Paso Nov 2019
- Tex Syn IV, Waco, TX May 2019
- ACS National Meeting in Boston, MA Aug 2018
- ACS South-West Regional Meeting, Lubbock Oct 2017

POSTER PRESENTATIONS

- Cobalt-catalyzed alkylation of nitriles with alcohols (ACS National Meeting, 2022)
- Iron-catalyzed hydroboration of alkenes and alkynes. (GIDW 2020 Virtual Poster Event, 2020)
- Polynuclear Lanthanide-diketonato cluster: Catalytic hydroboration of carboxamides and esters. (RSC Online Twitter Conference, 2020)
- Hydroboration of Alkenes and Alkynes Employing Earth - Abundant Metal Catalysts. (Tex Syn IV, 2019)
- Unprecedented catalytic reactivity of Lanthanides in deoxygenation of amides. (Department of Chemistry Graduate Student Poster Competition, 2019)
- Nickel catalyzed 1,4-selective Hydroboration of pyridines and *N*-heteroarenes. (ACS National Meeting, 2018)
- Synthesis, Characterization and Applications of Fe-BIAN Complexes in the Hydrosilylation of Ketones and Imines. (Department of Chemistry Graduate Student Poster Competition, 2017)

ORAL PRESENTATIONS

- Polynuclear Lanthanide-diketonato clusters: Catalytic hydroboration of carboxamides and esters (ACS National Meeting, 2022)
- Nuclear Magnetic Resonance-A tool to elucidate structure (Dev Samaj College For Women, Ferozepur, Punjab, India, Dec 2020)
- Iron-catalyzed hydroboration of alkenes and alkynes. (ACS Fall 2020 Virtual Meeting & Expo, Aug 2020)
- Polynuclear Lanthanide-diketonato cluster: Catalytic hydroboration of carboxamides and esters. (ACS SWRM, 2019)
- Hydroboration of Alkenes and Alkynes Employing Earth - Abundant Metal Catalysts. (Tex Syn IV, 2019)
- Synthesis and characterization of Fe(II)-BIAN complexes. (ACS SWRM, 2017)

ORGANIZATIONS

- Chemistry Graduate Student Organization (CGSO)
- American Chemical Society (ACS)

LEADERSHIP SKILLS

Secretary - Chemistry Graduate Student Organization, Texas Tech

Abstract

Metal-Catalyzed Hydroboration of Unsaturated Bonds (C=C, C=N, C=O) and Alkylation of Nitriles

Arpita Singh, Doctor of Philosophy, University of California Merced, 2022

Advisor: Prof. Michael Findlater

Transformations of organic substrates into more valuable chemical targets is an exciting and fruitful avenue of investigation. Such transformations can be achieved using catalytic or stoichiometric reactions. Catalysts play an indispensable role in industrial chemistry; it is believed that ~80 percent of all manufactured products involved the use of catalysis at some point during synthesis. Moreover, approximately 90 percent of all industrial chemicals made worldwide use catalysts within the manufacturing process. Catalysis can be broadly divided into different categories: homogenous catalysis, heterogeneous catalysis, organocatalysis and, enzymatic catalysis. Homogenous and heterogeneous catalysis may both involve the use of metals to carry out a chemical transformation.

Many organic transformations are catalyzed by precious metals; noble metals like iridium (Ir), palladium (Pd), platinum (Pt), rhodium (Rh) typically afford good regio- and stereo-selectivity. The price, scarcity, and toxicity of precious metals are motivating factors driving the use of earth-abundant metals in catalysis. The replacement of precious metals with base metals will also help reduce the cost of the end-product.

The metal-catalyzed hydroboration reaction is an example of homogenous catalysis and has been well studied for 45 years. In a typical hydroboration reaction, hydrogen and boron are added across a pi-bond, most typically those found in C=C, C=N and, C=O bonds. Hydroboration can accommodate mild reagents, reaction conditions and can tolerate a variety of functional groups. The substituted boron group may also act as a 'functional handle' to potentially allow formation of a new C-C bond or introduce an alternative functional group such as an alcohol, amide, amine, or halogen.

In the first part of this dissertation, we report the 1,4-regioselective hydroboration of N-heteroarenes using a nickel-based catalyst system. Commercially available Ni(acac)₂ was used in conjunction with tricyclopentylphosphine (PCyp₃) to carry out hydroboration of pyridines to afford 1,4-dihydropyridines (1,4-DHPs) with yields of up to 96%. To the best of our knowledge, our catalyst system represents the first successful example of 1,4-selectivity for para-substituted pyridines.

The second part of this dissertation describes the hydroboration of alkenes using a BIAN (bis-arylimino)acenaphthene supported iron complex and hydroboration of amides using a lanthanum-based catalyst. The products obtained after the hydroboration of alkenes, i.e., alkyl boronates, can potentially be used as coupling partners in Suzuki-Miyaura chemistry. The products obtained after hydroboration of amides, i.e., amines, are important molecules in both the pharmaceutical agriculture industries.

The third part of the dissertation discusses the alkylation of nitriles employing alcohols. We have utilized our well-explored BIAN ligands in conjunction with commercially available cobalt(II) chloride to carry out the transformation. α -alkylated nitriles obtained from alkylation of

nitriles have a number of applications as they are essential synthons in the synthesis of several drug molecules, including isoaminile and phenylalkylamines.

The final part of the dissertation deals with the hydroboration of carbonates. We disclose an operationally convenient method for the hydroboration of carbonates. Commercially available $\text{La}(\text{acac})_3$ was employed in the hydroboration of carbonates to afford diols and methanol as the reduction products. The results of our lanthanum-based catalytic system were compared with previously reported NaHBET_3 -catalyzed hydroboration of carbonates.

I. NICKEL-CATALYZED 1,4-REGIOSELECTIVE HYDROBORATION OF N-HETEROARENES

Modified with permission from *ACS Catal.* **2018**, 8, 7, 6186–6191.
Sem Raj Tamang, Arpita Singh, Daniel K. Unruh, Michael Findlater*
(<https://pubs.acs.org/doi/abs/10.1021/acscatal.8b01166>)

1.1. Introduction

The dearomatization of N-heteroarenes to afford dihydropyridines (DHPs) is an important transformation as it provides a pathway to a range of substrates which are biologically useful e.g., nicotinamide adenine dinucleotide (NADH).¹ In alternative uses, related compounds are used as Ca²⁺ channel blockers and as building blocks in the development of new drugs to treat cardiovascular disease. Nifedipine (**1**), Amlodipine (**2**), and Nimodipine (**3**) are all used to treat a variety of diseases.² Moreover, 1,4-DHPs are also known to serve as reducing agents in organocatalysis by functioning as organohydride donors,³ and they are also products of the multicomponent Hantzsch ester synthesis³⁻⁴ which are of potential use as NADH mimics.⁵⁻⁶

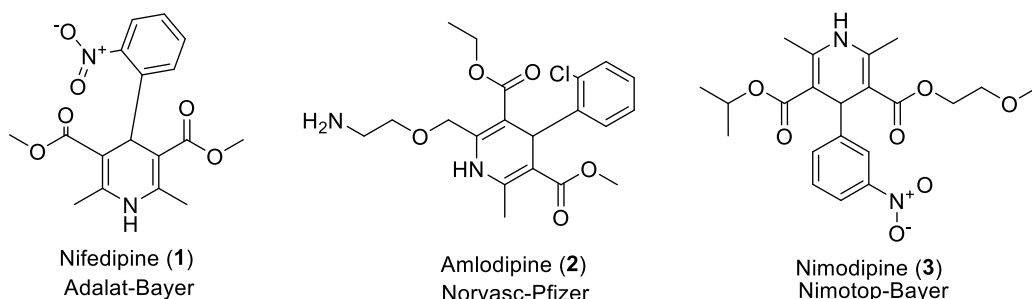


Figure 1.1. Examples of commercialized drug molecules comprised of 1,4-DHP as central components.

Thus, a range of methods have been reported which allow synthetic access to DHPs, though achieving regioselectivity remains a challenge. Typically, regioselectivity may be achieved employing multistep procedures which utilize metal hydrides like LiAlH₄, NaBH₄ or alkali metals or mixtures of products (1,2- and 1,4-DHPs) requiring separation are observed.⁷⁻⁹ For example, the hydrogenation of pyridines require harsh conditions and are susceptible to over-reduction to piperidine products.¹⁰ Another disadvantage of using more traditional reducing agents are a lack of chemo- and regioselectivity, and low functional group tolerance.¹¹ Hydroboranes and hydrosilanes have been used extensively as surrogates for H₂ in transition metal catalyzed reduction chemistry. These reducing agents use relatively mild conditions, don't require specialized equipment and the introduction of boron and silicon moieties allows for further elaboration of the reduction products. Therefore, the development of a mild and regioselective method based upon earth abundant metals would be desirable.¹²

In 2011, Hill and co-workers published the seminal work on the utilization of hydroboration in the reduction of pyridines to afford a mixture of 1,2- and 1,4-reduction products using a β -diketiminato *n*-butylmagnesium complex (**4**).¹³ However, the Mg based catalyst suffered from a lack of chemoselectivity as hydroboration of C=O groups occurred preferentially over the desired N-heteroarene hydroboration. In 2012, Suginome *et al.* reported Rh-catalyzed hydroboration¹⁴ of pyridines where they employed [Rh(cod)Cl]₂ (**5**) to yield 1,2-DHP's. This catalytic system gave moderate to good yields and was successful towards the hydroboration of multi-substituted pyridines. This was the first example of dearomative reduction of pyridines employing a transition metal catalyst. In 2012, Marks and co-workers reported the La-catalyzed¹⁵ dearomatization of pyridines and N-heteroarenes employing [Cp*₂LaH] (**6**) as catalyst. The catalytic system had a wide functional group tolerance and worked well for substrates having both electron withdrawing and donating groups to yield 1,2-regioselective products in moderate to excellent yields. Marks and co-workers also observed that the reaction proceeds faster if electron withdrawing groups are attached at the C4 position and no reaction was observed for substrates bearing substituents at the C2 position. In 2012, Crudden and co-workers reported the metal free dearomative reduction of C=N bond moieties employing a borenium salt¹⁶ bearing a tetravalent boron anion [DABCOBpin]⁺BH(C₆F₅)₃⁻ (**7**). Inspired by the emerging frustrated lewis pair (FLP) chemistry, Wang and coworkers¹⁷ employed a bulky organoborane Ar^F₂BMe (Ar^F = 2,4,6-tris(trifluoromethyl)phenyl) (**8**) to carry out the 1,4-regioselective hydroboration of the pyridines. The reaction proceeded well at 25 °C to afford the corresponding products in moderate to good yields. In 2016, Gunathan and co-workers² employed Ru based catalyst (**9**) in the presence of HBPin to carry out the hydroboration of pyridines. The Ru based catalytic system could tolerate alkyl, aryl, heteroaryl, ester, amine, amide, alkoxy, and acyloxy functional groups. In 2017, NacNacZnH (**10**) (NacNac = [Ar'NC(Me)CHC(Me)NAr'], Ar' = 2,6-Me₂C₆H₃) was employed by Nikonov and co-workers¹⁸ to carry out regioselective hydrosilylation and hydroboration of pyridines. The catalytic activity of the complex was not only limited to pyridines, it was also extended to difficult substrates like phenanthroline. Later, in 2017 Wang¹⁹ and co-workers employed dinitrogen bridged diiron complex [Cp*(Ph₂PC₆H₄S)Fe]₂(μ -N₂) (**11**) to successfully carry out the 1,2-regioselective hydroboration of pyridines. In the same year, Wright and co-workers carried out boronium-catalyzed hydroboration of pyridines that was initiated by the readily available ammonium salt, NH₄BPH₄. The catalytic system was versatile and both 1,2 and 1,4 could be obtained by tuning the polarity of the solvent.¹³ In 2019, Wang and co-workers utilized air stable half sandwich nickel (II) complex of phosphinophenolato ligand, Cp*Ni(1,2-Ph₂PC₆H₄O) (**12**) for the activation of HBpin and reduction of N-heteroarenes via hydroboration. The catalyst presented 1,2 regioselectivity for dihydropyridines; also the oxygen atom in the phosphinophenolato ligand played a crucial role in the hydroboration reaction.²⁰ In 2019, Park and coworkers exploited KO^{*t*}Bu in conjunction with 18-crown-6 (**13**) for 1,4-regioselective hydroboration of pyridines; outer sphere mechanism was proposed for the reaction.²¹ Later in 2019, Zhang and coworkers employed potassium hydride to carry out the hydroboration of N-heteroarenes; 1,2-regioselective products were obtained for quinolines. In this report, 5 examples for hydroboration of pyridines were also reported and 1,4-selective products were obtained with majority of the pyridines.²²

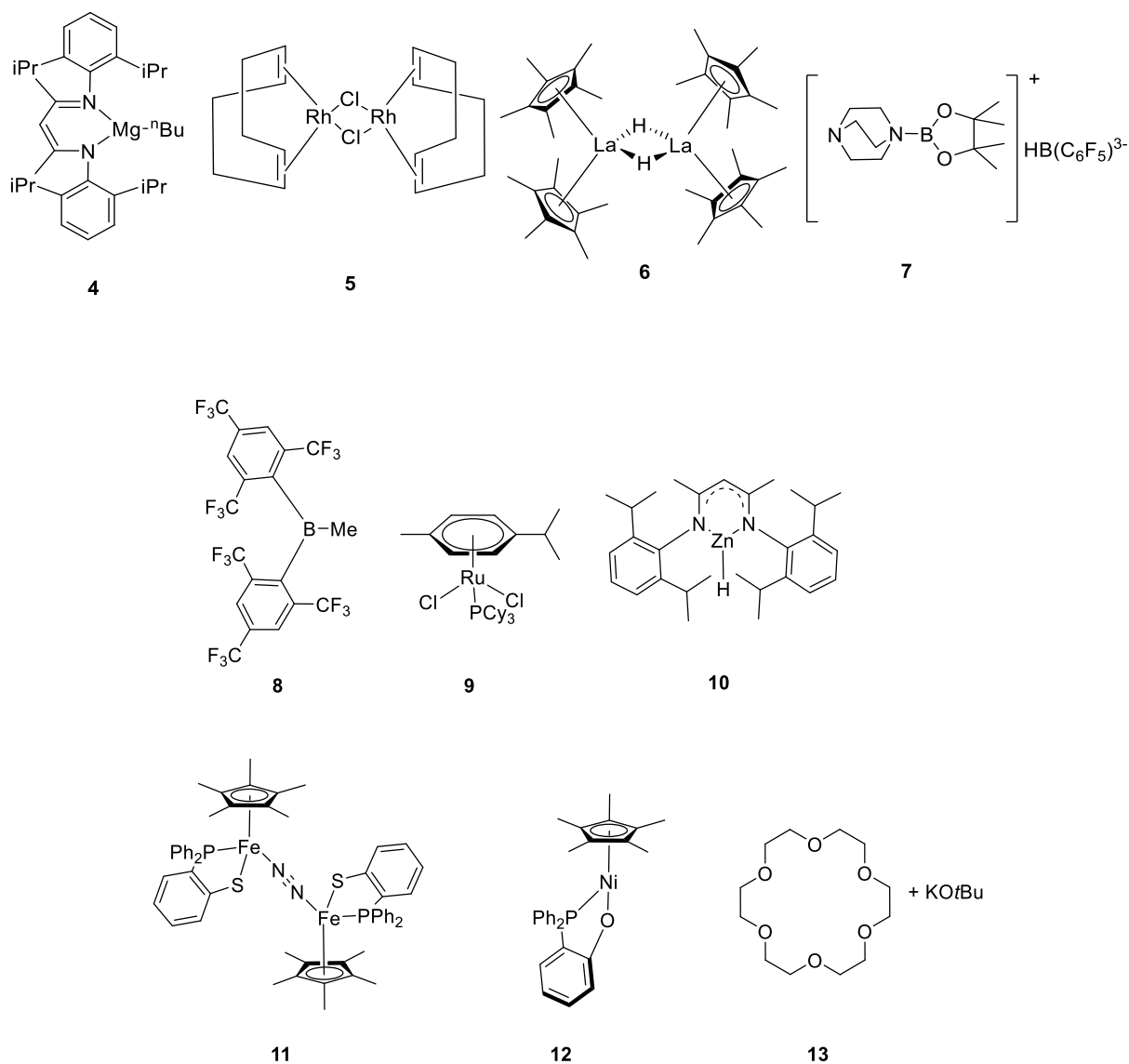


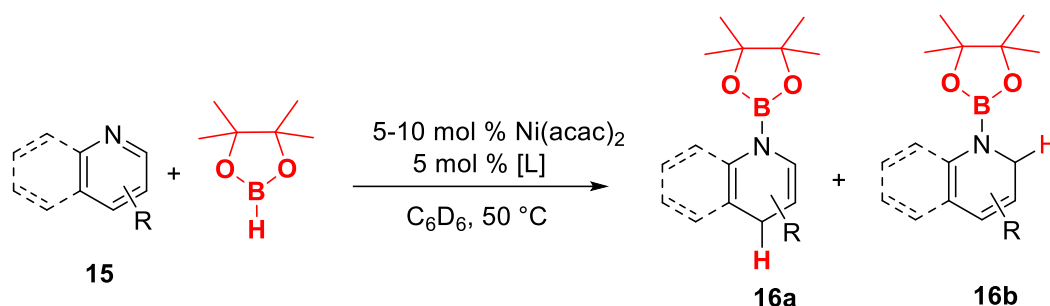
Figure 1.2. Some of the pre-catalysts used for dearomatization of pyridines.

The development of regioselective methods based upon earth-abundant (Fe)¹⁹ and even metal-free (borane and phosphane) catalysts are particularly noteworthy. Earth-abundant transition-metal catalysis have recently garnered much attention,²³ and nickel has emerged as a leading nonprecious metal alternative.²⁴ Thus, regioselective reduction of N-heteroarenes utilizing nickel is significant and desirable. Considerable progress has already been made in nickel-catalyzed reduction of unsaturated hydrocarbons such as ketones,²⁵ esters,²⁶ amides,²⁷ and nitriles.²⁸

1.2. Results and Discussion

Herein, we report the first nickel-based catalyst system for the 1,4-regioselective hydroboration of *N*-heteroarenes in good to excellent yields. Preliminary experiments focused on the ability of commercially available nickel salts to perform the hydroboration of pyridine with HBpin in benzene-*d*₆. Little to no activity was observed using Ni(acac)₂ (**14**, 10 mol %), even after prolonged reaction times at elevated temperatures (24 hrs at 50 °C). Initial attempts at reaction optimization focused on the use of additives e.g. employing NaOtBu resulted in improved activity and afforded a mixture of 1,2- and 1,4-*N*-borylated dihydropyridines (2:1) at room temperature (**Figure 1.7**). Further experiments revealed that upon addition of tricyclohexylphosphine, nickel loading could be lowered to 5 mol % with no concomitant erosion in substrate conversion. (**Figure 1.9**). Additionally, the use of phosphine ligand afforded enhanced 1,4-regioselectivity with no need for salt additives (**Table 1.1**).

Table 1.1. Optimization of reaction parameters with various phosphine ligands



Entry	[L]	(hrs)	Conversion of 15a (%) ^a	Ratio (16a: 16b) ^a
1 ^b	-	15	<5	18:82
2	PMe ₃	15	14	25:75
3	Dppe	15	13	27:73
4	PPhCl ₂	15	0	-
5	[(CH ₃) ₂ CH] ₂ PCl	15	2	n.c.
6	[(CH ₃) ₂ CH]PCl ₂	15	0	-
7	(CH ₃) ₃ CPCl ₂	15	0	-
8	PCy ₃	1	100	100:0
9	PPh ₃	15	5	35:65
10	PCy ₂ Ph	2	100	100:0
11	PCyPh ₂	15	36	79:21
12	P(Cyp) ₃	1	100	100:0
13 ^c	-	4	63	40:60
14 ^d	-	1	63	89:11

Reaction conditions: HBpin (0.6 mmol), pyridine (0.5 mmol), Ni(acac)₂ (5 mol %), [L] (5 mol %), C₆D₆ (0.7 mL), 50 °C; (a) Conversion and ratio of 1,4-dihydropyridine to 1,2-dihydropyridine were determined via ¹H NMR analysis; (b) Ni(acac)₂ (10 mol %) at room temperature; (c) Ni(acac)₂ (10 mol %), NaOtBu (20 mol %) at room temperature; (d) Ni(acac)₂ (10 mol %), NaOtBu (20 mol %) at 50 °C. (e) n.c.– no conversion

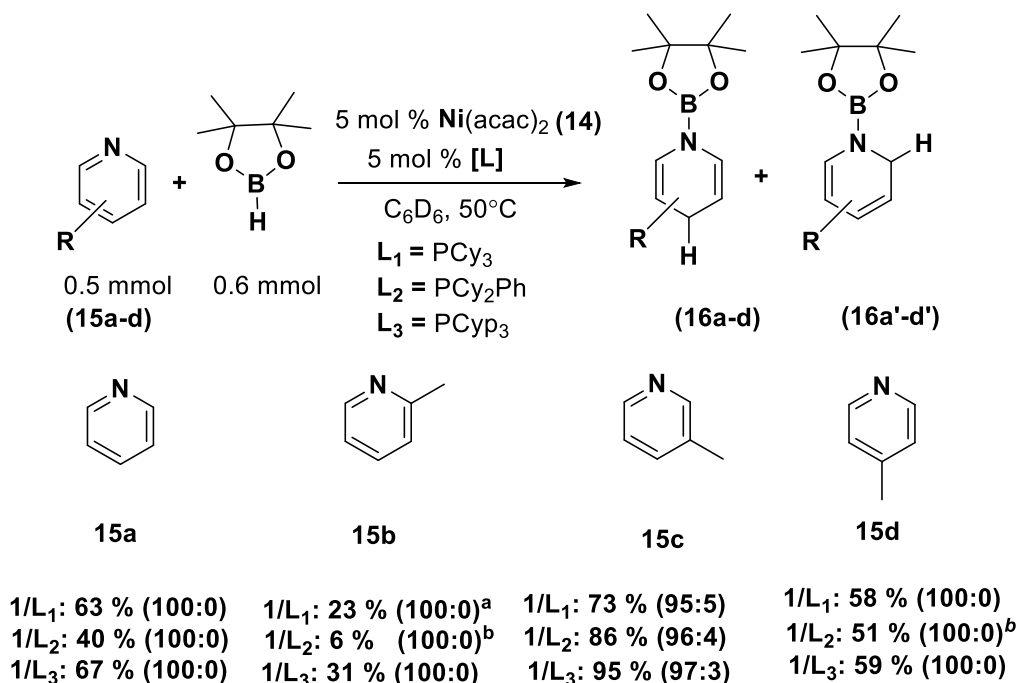
Various commercially available Ni salts were tested for this transformation, Ni(acac)₂ still gave the best results for this transformation (**Table 1.2**).

Table 1.2. Optimization of reaction parameters with various commercially available Ni sources

Entry	[Ni]	t (hrs)	Yield (%)	Ratio (16a: 16b) ^a
1	Ni(acac) ₂	1	67 (20%) ^b	100:0
2	Ni(TMHD) ₂	10	30 (13) ^c	100:0
3	Ni(OTf) ₂	10	26	74:26
4	NiCl ₂	10	0	-
5	Ni(COD) ₂	1	24 (27%) ^b	100:0

Reaction conditions: HBpin (0.6 mmol), pyridine (0.5 mmol, [Ni] (5 mol %), [L] (5 mol %), C₆D₆ (0.7 mL), 50 °C. (a) Yield and ratio of 1,4-dihydropyridine to 1,2-dihydropyridine were determined via ¹H NMR analysis using tetraethylsilane as the internal standard. (b) Yield for diborylated product.

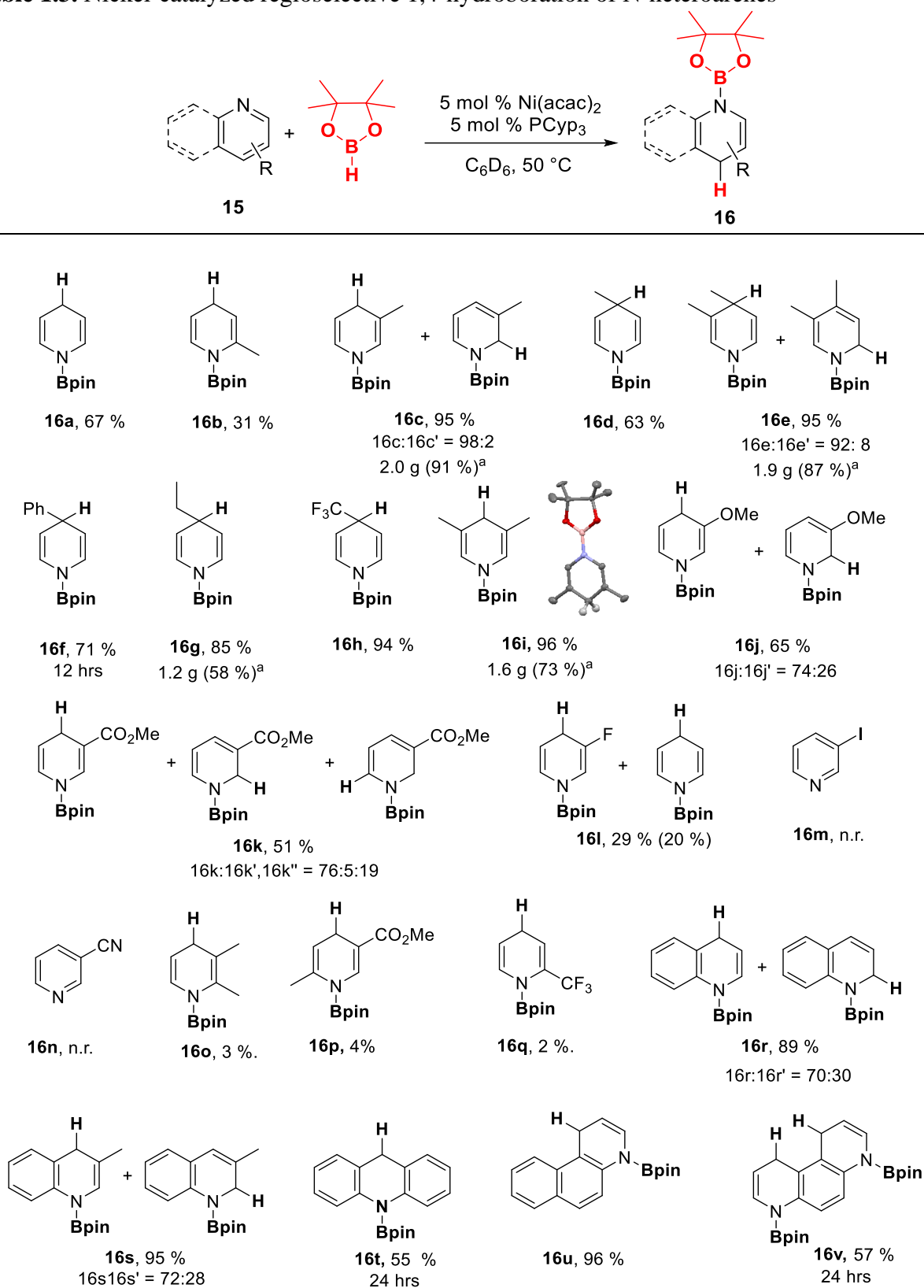
With these findings in hand, the hydroboration reactions of pyridine (**15a**) and picolines (**15b-d**) were used to screen metal/phosphine combinations: **14/L**₁, **14/L**₂, and **14/L**₃ (**Scheme 1.1**; **L**₁ = tricyclohexylphosphine, **L**₂ = dicyclohexylphenylphosphine, **L**₃ = tricyclopentylphosphine). In all combinations pyridine (**15a**) was converted quantitatively to the 1,4-DHP product (**16a**). In contrast, 2-picoline (**15b**) exhibited low conversions which likely arise from the presence of unfavorable steric interactions between the *o*-methyl group and Ni center (vide infra). Importantly, all **14/L**_x combinations afforded 1,4-DHPs regioselectively, moderate conversions (51-59 %) were observed in the case of the hydroboration of 4-picoline (**15d**). Significantly higher conversions (73-95 %) could be obtained using 3-picoline (**15c**) as substrate, although it should be noted that small amounts of 1,2-product (**16c'**) are formed in this case. Across these pyridine substrates, **L**₃ affords consistently higher conversion of substrates at lower reaction times. The combination of **14/L**₃ was used in all subsequent reactivity studies.



All conversions and product ratios were determined by ¹H NMR spectroscopy using tetraethylsilane as an internal standard. All reactions were monitored for 1 hr unless otherwise noted: (a) = 5.5 hrs; (b) = 18 hrs.

Scheme 1.1. Preliminary screening of pyridine (**15a**) and picoline substrates (**15b-d**) in hydroboration catalysis employing Ni(acac)₂ / PR₃.

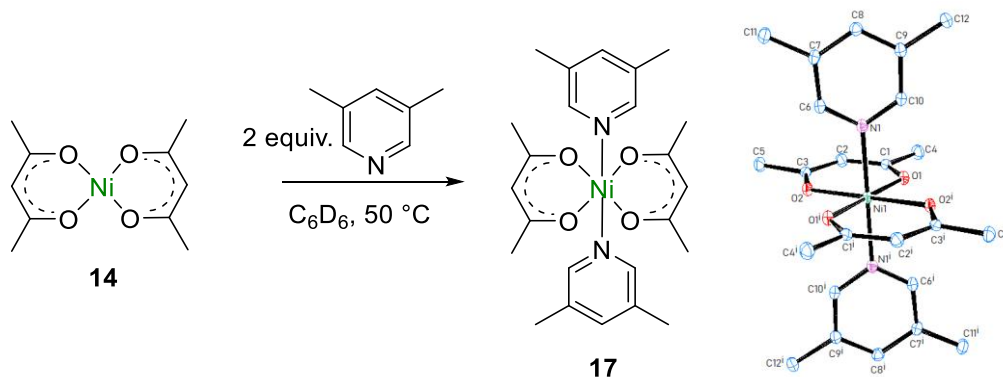
The scope of pyridines amenable to hydroboration using **14/L₃** (**Table 1.3**) was explored. Substrates bearing electron donating functional groups at the meta position showed high regioselectivity for 1,4-DHP products in good to excellent ¹H NMR yields (**16i** 96 %, **16j/16j'** 65 %, **16c/16c'** 95 %). In the case of 3-methoxypyridine (**16j**), only moderate conversion (65 %) was obtained. However, this substrate failed to react with the previously reported B(Me)ArF₂ catalyst,¹⁷ and in the case of a recently disclosed 1,3,2-diazaphosphonium triflate catalyst afforded the opposite (1,2-DHP) regioselectivity.²⁹ Thus, our system affords a high degree of complementarity to known hydroboration catalysts. Little to no reactivity was seen upon introduction of electron withdrawing groups at the meta position (**16k/16k'/16k''** 51%, **16n** n.r.); moreover, when the meta-substituent is a halide, dehalogenation chemistry was observed. Interestingly, we obtained products of complete 1,4-selectivity for para substituted pyridines in good to excellent yields. (**16d** 63%, **16e/16e'** 95 %, **16f** 71 %, **16g** 85 %, **16h** 94%). This is rather surprising, as para substituted pyridines are not known to be reactive for regioselective 1,4 hydroboration reactions; typically, these substrates are only capable of undergoing 1,2-hydroboration.

Table 1.3. Nickel-catalyzed regioselective 1,4-hydroboration of N-heteroarenes

Reaction conditions: pyridine substrates (0.5 mmol), HBpin (0.6 mmol), Ni(acac)₂ (5 mol %), PCyp₃ (5 mol %), C₆D₆ (0.7 mL). NMR yields and ratios of regioisomers (1,4-DHP: 1,2-DHP) were determined by ¹H NMR spectroscopy using tetraethylsilane as an internal standard; (a) 1 g of substrate, isolated yield in parenthesis.

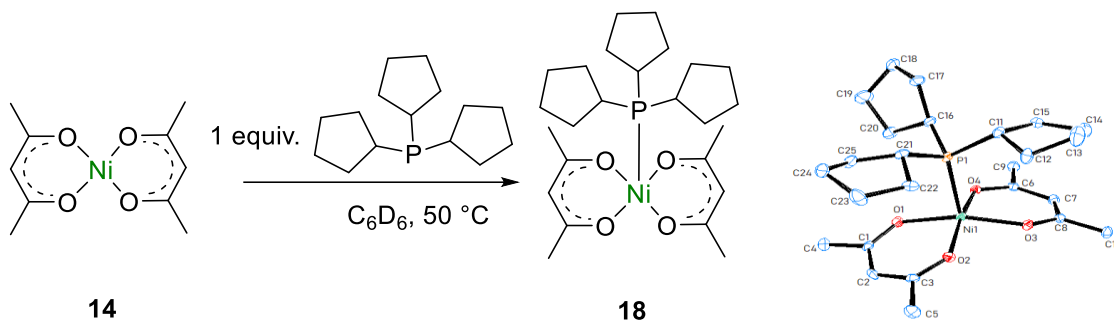
The substrate scope is not limited to just pyridines. The expansion to include other heteroarenes revealed quinoline, benzoquinoline, isoquinoline, acridine and phenanthrolines to be viable substrates for hydroboration. Until now, successful (regioselective) examples of 1,4-hydroboration of benzofused N-heteroarenes has been limited.^{19, 29-30} However, our results show good to excellent catalytic activity in 1,4-hydroboration of benzofused N-heterocycles (**16t** 55%) including quinolines (**16r/ 16r'** 89 %, **16s/ 16s'** 95 %), benzo[f]quinoline (**16u** 96 %), and phenanthroline (**16v** 57 %).

In the case of the hydroboration of pyridines catalyzed by Ru² formation of the 1,4-addition product was proposed to occur via intramolecular 1,5-hydride migration. However, **14** is stable toward HBPin, and under no experimental conditions have we been successful in detecting any signal attributable to “Ni-H” by ¹H NMR spectroscopic analysis. To gain further insight into the mechanism of the nickel-catalyzed hydroboration, several stoichiometric reactions were examined using 3,5-lutidine (**15i**) as the model heteroarene. We found that **14** reacted preferentially with **15i** rather than activating HBPin. Based upon NMR and X-ray crystallography, **14** is stable toward HBPin. The treatment of a green solution of **14**, in benzene, with two equivalents of **15i** leads to a rapid color change and precipitation of a purple solid. The resulting octahedral complex Ni(acac)₂(**15i**)₂ (**17**) (Scheme 1.2) was characterized by single crystal X-ray diffraction.



Scheme 1.2. Left: Preparation of **17**. Right: Solid-state structure of **17**.

Similarly, treatment of a benzene solution of **14** with an equimolar amount of PCyp₃ affords crystals of the 1:1 phosphine ligated complex, **18**, as a five-coordinate species (Scheme 1.3). This approach was also used to obtain the related complexes **19** and **20** arising from treatment of **14** with PCy₃ and PCy₂Ph, respectively (Figure 1.3).



Scheme 1.3. Left: Preparation of **18**. Right: Solid-state structure of **18**.

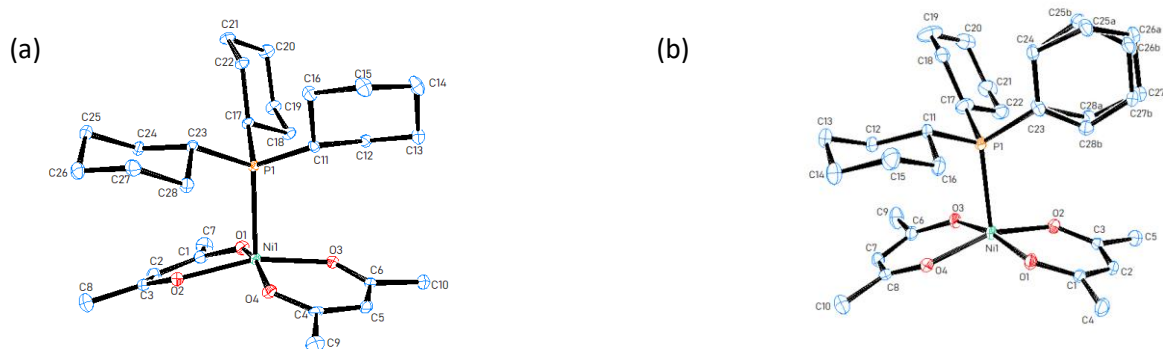
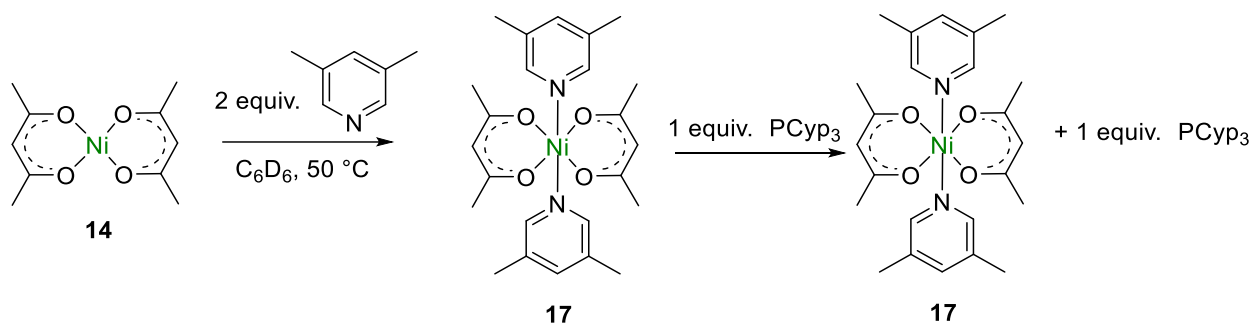


Figure 1.3. a) Structure of Ni(acac)₂·PCy₃ (**19**) b) Structure of Ni(acac)₂·PCy₂Ph (**20**)
Thermal ellipsoids are shown at 30% probability. Hydrogen atoms have been omitted for clarity.

Treatment of **14** with PCy₃ led to the formation of complex **18**. Exposure of **18** to 3,5-lutidine results in rapid phosphine displacement and the generation of complex **17** (**Figure 1.5**). Finally, no reaction was observed between HBpin and either PCy₃ or 3,5-lutidine (**Figures 1.11-1.13**).



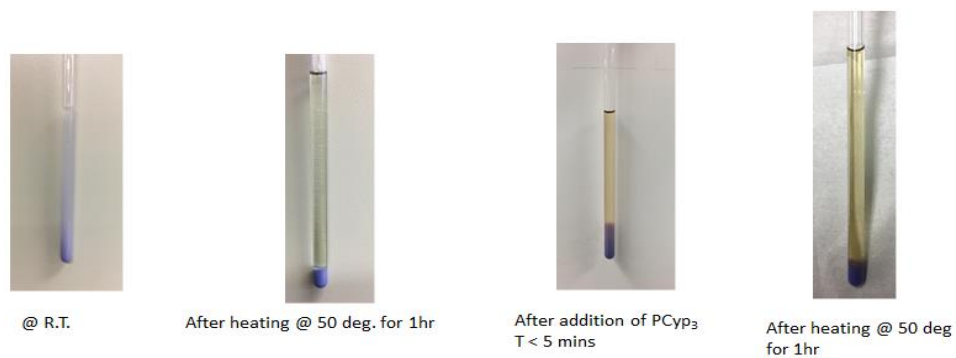


Figure 1.4. Reaction of **17** with Pcyp₃

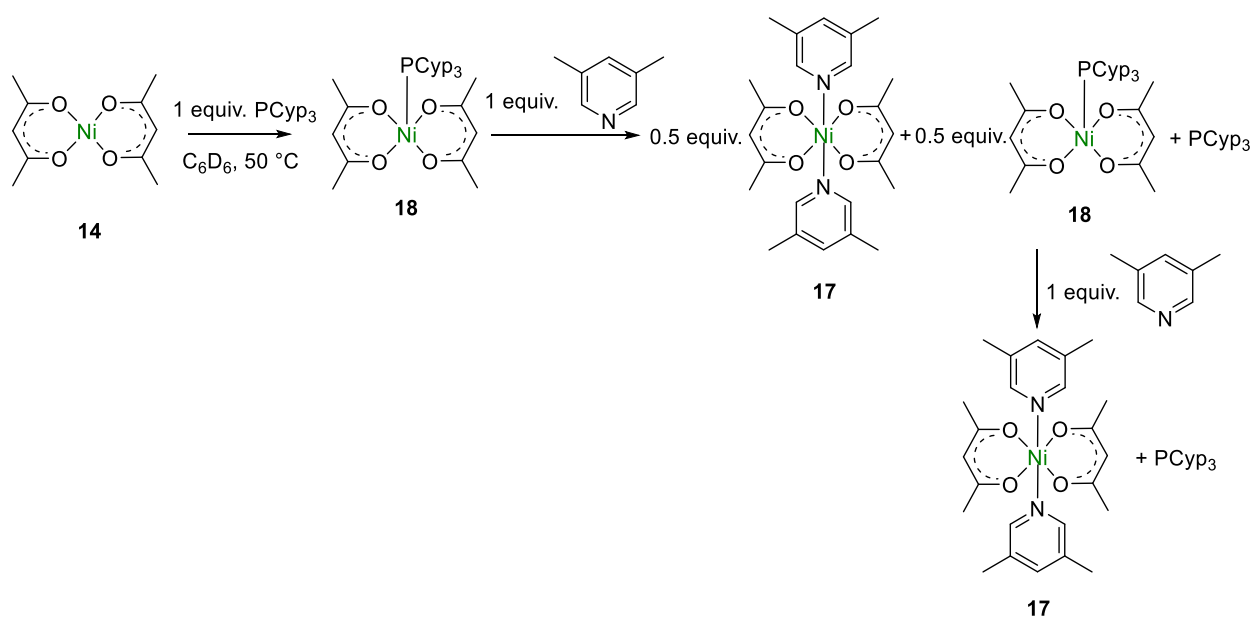


Figure 1.5. Displacement of PCyp₃ with 3,5-Lutidine from **18**

Preliminary kinetic analysis was performed for the catalytic hydroboration of 3,5-lutidine (**15i**). A plot of the initial rate for the formation of **15i** vs $[14/L_3]$ indicated the reaction was first-order in $[14/L_3]$, while the rate of formation was found to be independent of the concentration of **15i** (**Figures 1.15-1.16**). The zero order for **15i** suggests that the coordination of the substrate to the nickel center is not rate-limiting. Interestingly, varying the concentration of HBPIn appeared to reveal saturation kinetics, whereby the reaction is first-order in $[HBPIn]$ up to ~ 1.5 equiv. after which it becomes zero-order (**Figure 1.17**). Finally, analysis of the reaction profile (**Figure 1.6**) revealed the presence of an induction period.

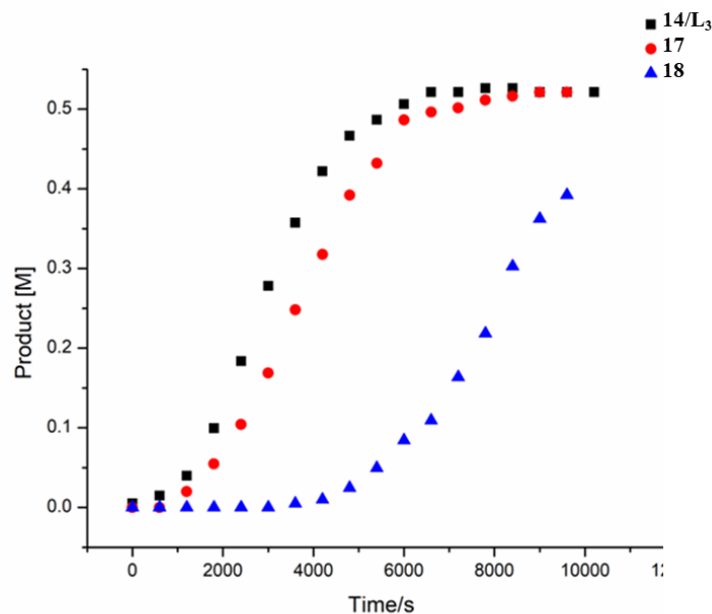


Figure 1.6. Reaction profile of reduction of 3,5-lutidine by HBPIn in the presence of **14/L₃** (■), **17** (●) and **18** (▲).

Interestingly, when isolated crystals of complex **17** were used to catalyze the hydroboration of 3,5-lutidine, a kinetic profile very similar to the in-situ catalysis (**14/L₃**) is observed (**Figure 1.6**). This supports the conclusion that the in-situ and well-defined precatalyst are able to access the same catalytic cycle. Subsequently, we probed the ability of isolated phosphine complex, **18**, to catalyze the hydroboration reaction. Complex **18** affords a completely different kinetic profile with a much longer induction period. Gunanathan and coworkers have proposed a hydroboration mechanism in which the active catalyst (Ru-based) contained both a bound heteroarene and a bound phosphine.² Unfortunately, all efforts to independently synthesize an analogous $Ni(acac)_2(PR_3)(heteroarene)$ complex failed. There are several potential mechanisms for the hydroboration catalyzed by **14**. Analogous nitrile hydroboration employing **14** proposes complete reduction of **14** from Ni(II) to Ni(0) by HBCat (Cat = catechol).³¹ We attempted to perform catalytic hydroboration of 3,5-lutidine employing a redox innocent catalyst, $Zn(acac)_2$ under otherwise identical reaction conditions. In this case, no reduced product was observed (**Figure 1.18**), implying that the role of nickel in the catalysis is not confined to that of a pure Lewis acid.

1.3. Conclusion

In summary, we have developed an efficient and regioselective 1,4-hydroboration of N-heteroarenes using a commercially available and air-stable nickel pre-catalyst. This catalysis exhibits excellent regioselectivity and broad functional group compatibility. Preliminary kinetic and mechanistic studies have also been reported. Future work will focus on a detailed mechanistic analysis and an expansion of catalytic reactions based upon Ni(acac)₂/PR₃.

1.4. Experimental Section

1.4.1. General considerations

All reactions were performed in oven dried apparatus under the atmosphere of Argon. Pyridines, quinolines were bought from commercial vendors and dried over activated molecular sieves (4Å) prior to usage; pyridine was distilled over CaH₂ and stored in the glovebox. Solid substrates were used without any purification or drying. ¹H, ¹³C, ³¹P, and ¹¹B spectra were recorded on a Jeol 400 MHz spectrometer. NMR Solvent (Benzene-d₆, was distilled over CaH₂ after refluxing under argon for 48 hrs. ¹H, ¹³C and ¹¹B NMR spectra were recorded on a Jeol 400 MHz spectrometer at 300K unless otherwise noted. ¹H NMR spectra were referenced to the solvent residual peak (C₆D₆, δ 7.16 ppm) and ¹³C{¹H} NMR spectra were referenced to the solvent residual peak (C₆D₆, δ 128.06 ppm). Coupling constants *J* are reported in Hz. NMR multiplicities are as follows: s = singlet, d = doublet, t = triplet, m = multiplet, br,s = broad singlet. Anhydrous Zn(acac)₂ was synthesized according to the literature.³² and confirmed by comparing unit cell with the reported structure in the database. Data for complexes **17**, **18**, **19**, **20** were collected on Bruker Smart Apex II CCD diffractometer. All data were collected at 100K using graphite-monochromated MoK α radiation ($\lambda = 0.71073 \text{ \AA}$). Intensity data were collected using ω -steps accumulating area detector images spanning at least a hemisphere of reciprocal space. All the data were corrected for Lorentz polarization effects. A multi-scan absorption correction was applied using SADABS.³³ Structures were solved by direct methods and refined by full- S2 matrix least-squares against F 2 (SHELXTL³⁴⁻³⁵). All hydrogen atoms were assigned riding isotropic displacement parameters and constrained to idealized geometries.

1.4.2. General procedure for the hydroboration of pyridines

An oven dried J-young tube was charged with Ni(acac)₂ (6.42mg, 0.025 mmol), PCyp₃ (5.95 mg, 6.08 μ L, 0.025 mmol), pyridines (39.55 mg, 40.27 μ L, 0.5 mmol), HBpin (76.78 mg, 87.06 μ L, 0.6 mmol), tetraethylsilane as internal standard (15.22 mg, 20 μ L, 0.105 mmol) and benzene-d₆ (0.7 mL). The reaction mixture was then placed on a preheated oil bath at 50 °C. The progress of the reaction was monitored by ¹H and ¹¹B NMR.

1.4.3. General procedure of Zn(acac)₂ with 3,5-lutidine and HBpin

An oven dried J-young tube was charged with Zn(acac)₂ (6.59mg, 0.025 mmol), PCyp₃ (5.95 mg, 6.08 μ L, 0.025 mmol), 3,5- lutidine (53.6 mg, 57.06 μ L, 0.5 mmol), HBpin (76.78 mg, 87.06 μ L, 0.6 mmol), tetraethylsilane as internal standard (15.22 mg, 20 μ L, 0.105 mmol) and benzene-d₆ (0.7 mL). The reaction mixture was then placed on a preheated oil bath at 50 °C. The progress of the reaction was monitored by ¹H NMR.

1.4.4. General procedure for ligand exchange reactions

An oven dried J-young tube was charged with Ni(acac)₂ (25.69 mg, 0.1 mmol), 3,5- lutidine (21.4 mg, 22.82 μ L, 0.2 mmol), and benzene (0.7 mL). Instantaneous precipitation of purple solid was observed upon shaking. The reaction mixture was then placed on a preheated oil bath at 50 °C for 1 hr. PCyp₃ (23.8 mg, 24.34 μ L, 0.1 mmol) was then added to the reaction mixture after it

cooled down to R.T. and the reaction mixture was then heated at 50 °C for 1 hr. The purple solid residue was separated from the supernatant by decantation, washed with copious amount (20 mL) of pentane and dried under vacuo to yield 74 % of the product, **17**.

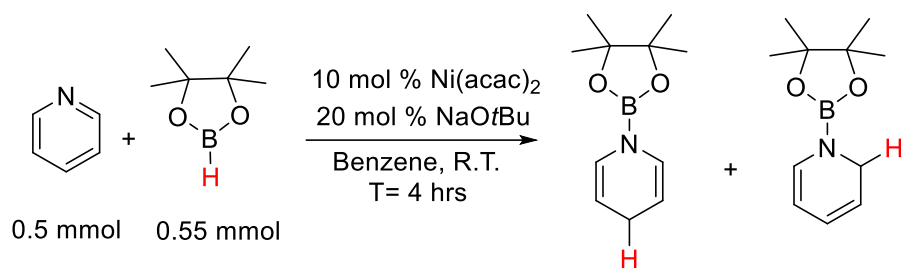
An oven dried J-young tube was charged with Ni(acac)₂ (25.69 mg, 0.1 mmol), PCyp₃ (23.8 mg, 24.34 μ L, 0.1 mmol), and benzene (0.7 mL). The reaction mixture was then placed on a preheated oil bath at bath at 50 °C for 1hr; a homogenous green solution was observed. One equivalent of 3,5-lutidine (10.7 mg, 11.41 μ L, 0.1 mmol) was added to the reaction mixture; instantaneous precipitation of purple solid was observed. The reaction mixture was then placed on a preheated oil bath at 50 °C for 1hr, and then another equivalent of 3,5-lutidine was added after the reaction mixture was cooled down. Complete discoloration of the green supernatant was observed upon addition, and the mixture was then heated at 50 °C for 1hr. The purple solid residue was separated from the supernatant by decantation, washed with copious amount of pentane and dried under vacuo to yield 73 % of the product, **17**.

1.4.5. Kinetics study and general procedure of kinetics experiments

Kinetic analysis of the NMR scale reactions was carried out by collecting multiple data points at intervals till the substrate concentrations were depleted. The temperature was ramped up stepwise, from R.T. to 35 °C (held for 3 minutes at 35 °C), and then increased from 35 °C to 50 °C, and held for 5 minutes before locking and shimming. The first reading at 50 °C was taken as 0 mins. Each data was taken at 10 minutes intervals and the reaction was monitored by ¹H NMR (400 MHz, C₆D₆) for 3 hrs at 50 °C. The kinetic data were obtained from the intensity increase of the C-H (s, 2H, δ = 6.41 ppm) integral of the dearomatized 1,4-dihydro-3,5-lutidine relative to the internal standard (tetraethylsilane). K_{max} was determined by taking the maximum rate of reaction.

A J-young tube was charged with Ni(acac)₂ (6.42 mg, 0.025 mmol), PCyp₃ (5.95 mg, 6.08 μ L, 0.025 mmol), and benzene-d₆ (0.5 mL). The reaction mixture was heated at 50 °C. On a preheated oil bath for ~ 30 minutes till a homogeneous green solution was obtained. Then, the reaction mixture was allowed to cool down to R.T. and moved inside the glove box. 3,5-lutidine (53.57 mg, 57.07 μ L, 0.5 mmol), HBpin (0.5 mmol, 72.55 μ L, 63.99 mg), benzene-d₆ (0.2 mL) and tetraethylsilane as internal standard (20 μ L) were then added. The reaction mixture was then analyzed by ¹H NMR at 50 °C. The temperature was ramped up stepwise, from R.T. to 35 °C (held for 3 minutes at 35 °C), and then increased from 35 °C to 50 °C, and held for 5 minutes before locking and shimming. The first reading at 50 °C was taken as 0 minutes. Each data was taken at 10 minutes intervals for 3 hrs.

1.5. Appendix



Ratio 40 : 60

% Pyridine converted = 63 %

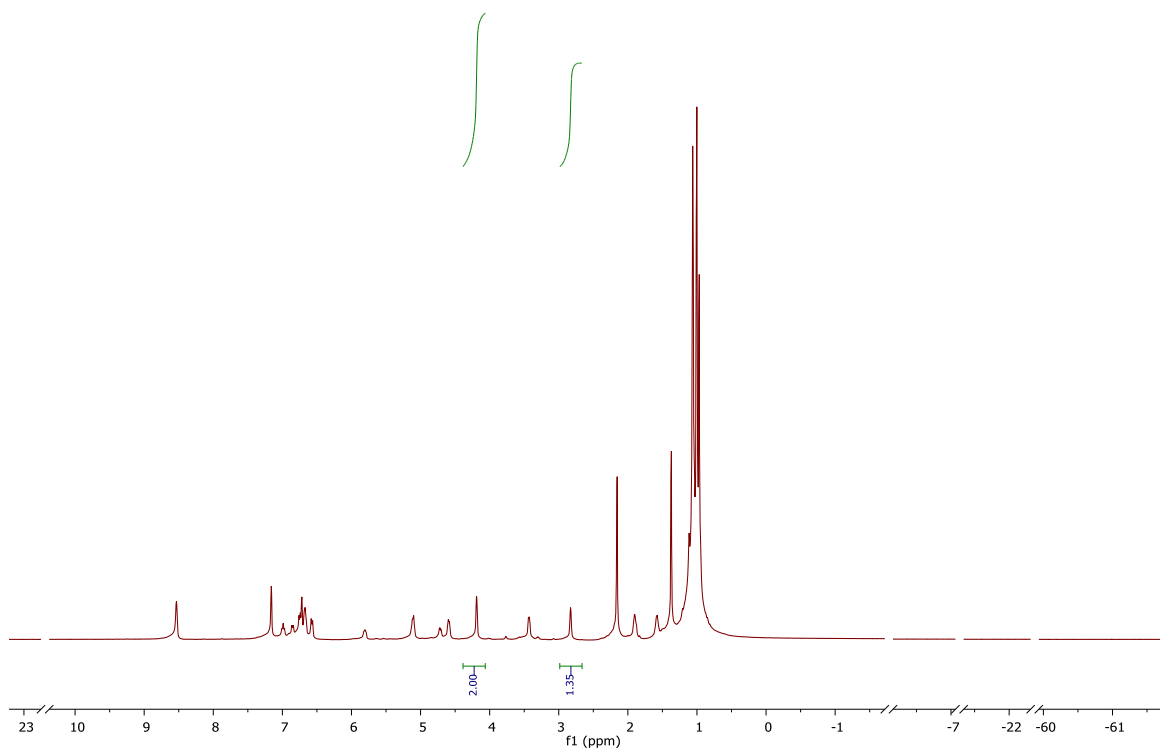


Figure 1.7. ¹H NMR for Initial hydroboration of pyridine in the presence of Ni(acac)₂ and NaOtBu at R.T.

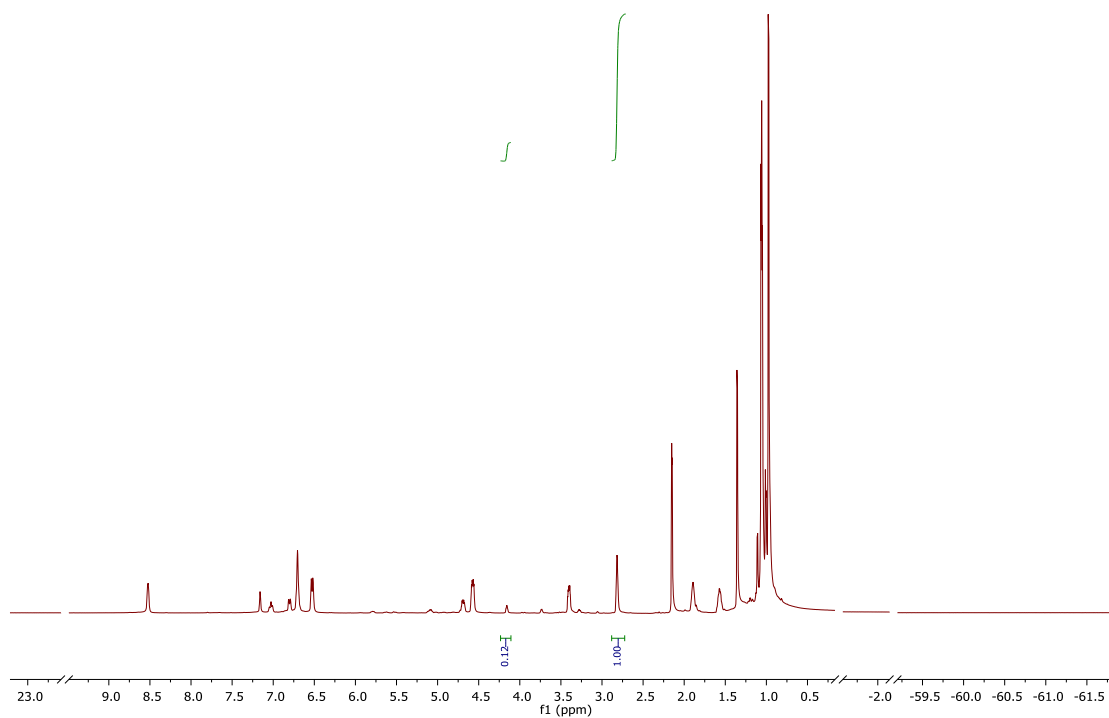
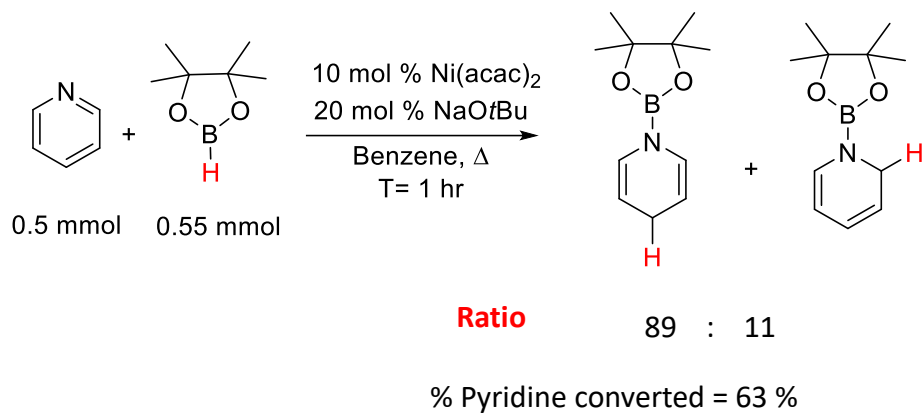


Figure 1.8. ¹H NMR for Initial hydroboration of pyridine in the presence of Ni(acac)₂ and NaOtBu at 50 °C

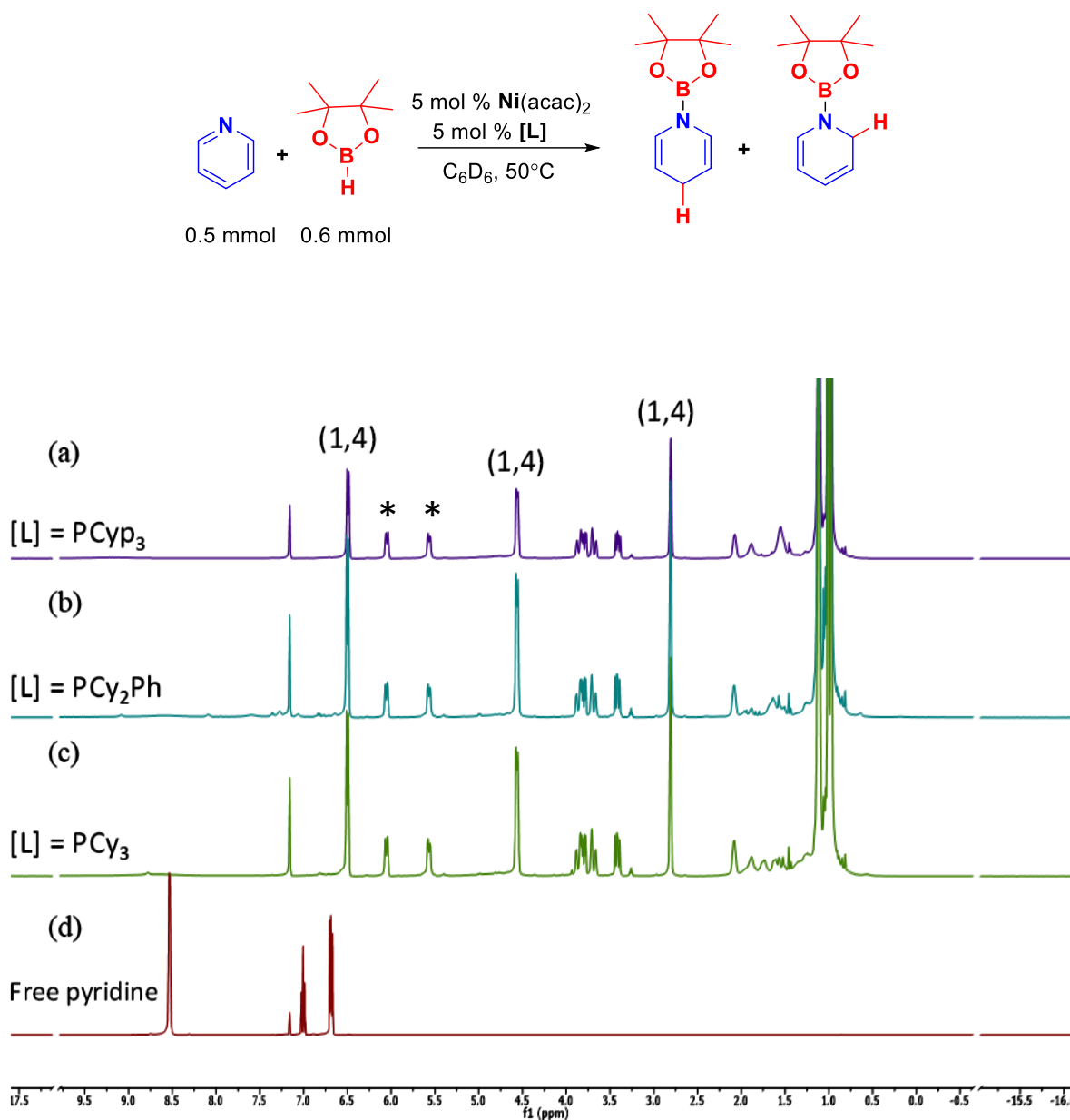


Figure 1.9. ¹H NMR of reaction mixture for hydroboration of pyridine at T= 1hr. (a) Ni(acac)₂/PCyp₃; (b) Ni(acac)₂/PCy₂Ph; (c) Ni(acac)₂/PCy₃; and (d) free pyridine. The (*) represents the peak for diborylated 1,4- DHP.

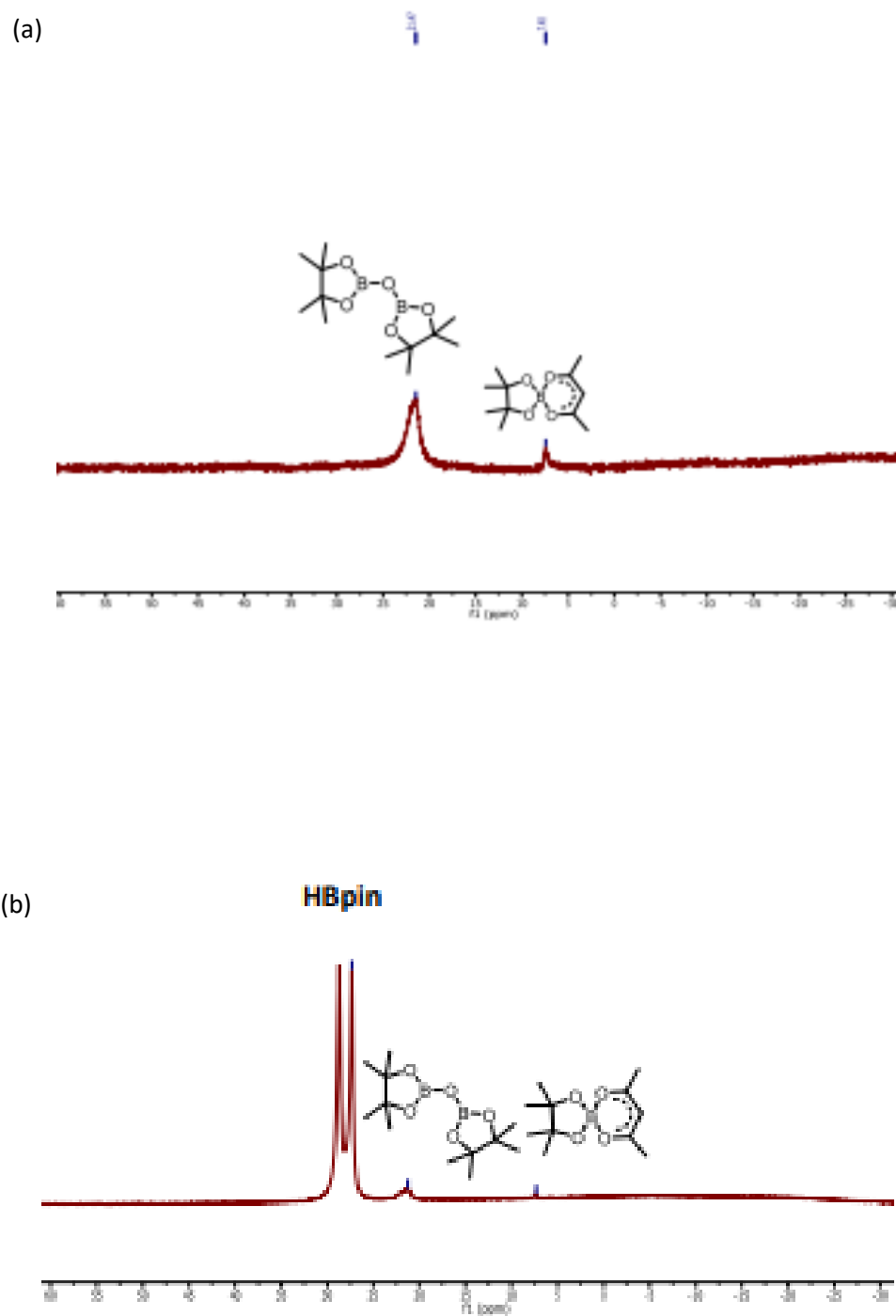


Figure 1.10. (a) ^{11}B NMR of stoichiometric reaction of $\text{Ni}(\text{acac})_2$ (25.69 mg, 0.1 mmol), and HBpin (12.80 mg, 14.51 μL , 0.1 mmol) in benzene- d_6 ; (b) ^{11}B NMR of reaction of $\text{Ni}(\text{acac})_2$ (25.69 mg, 0.1 mmol), and HBpin (76.79 mg, 87.06 μL , 0.6 mmol) under standard catalytic condition in benzene- d_6

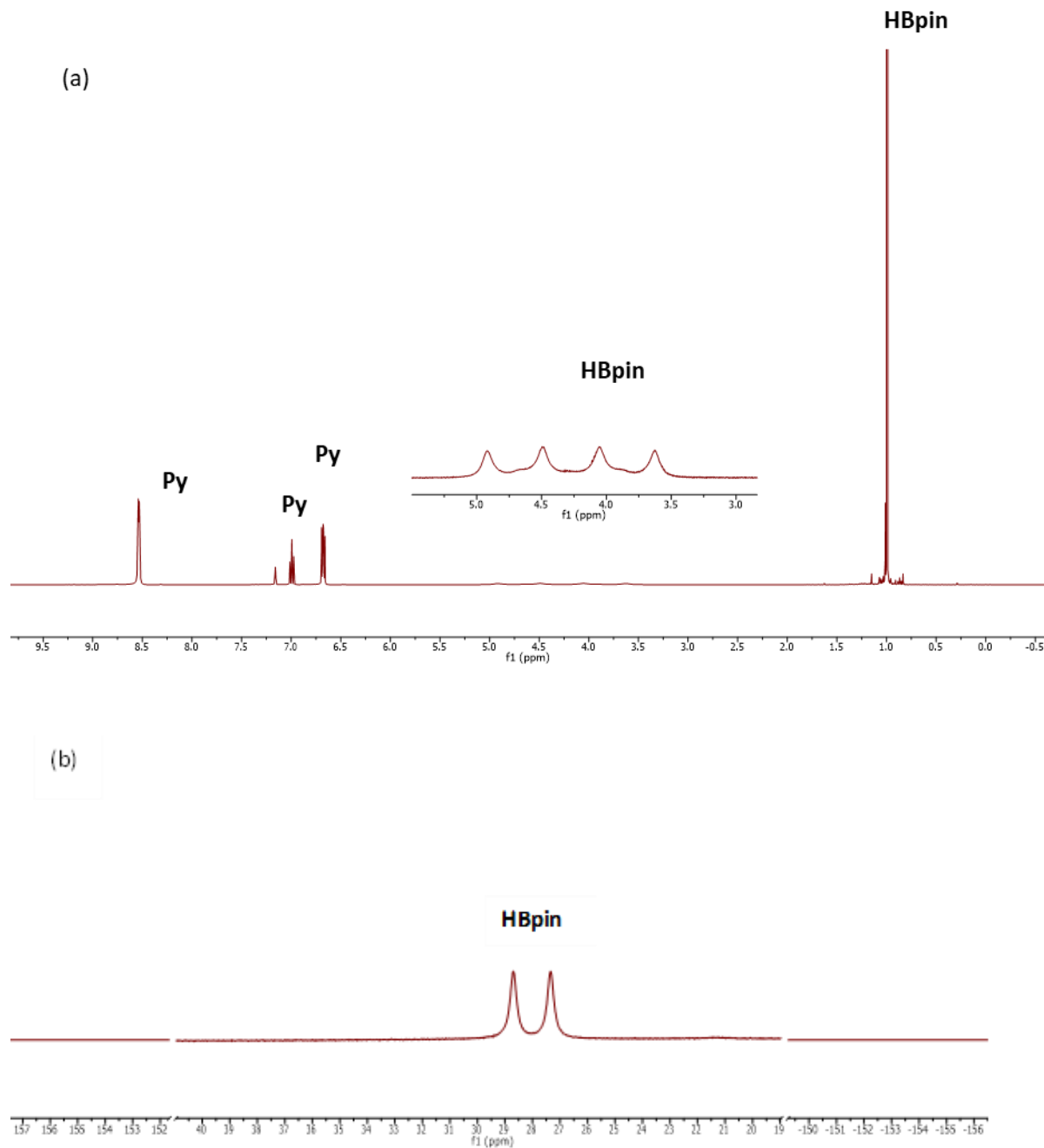
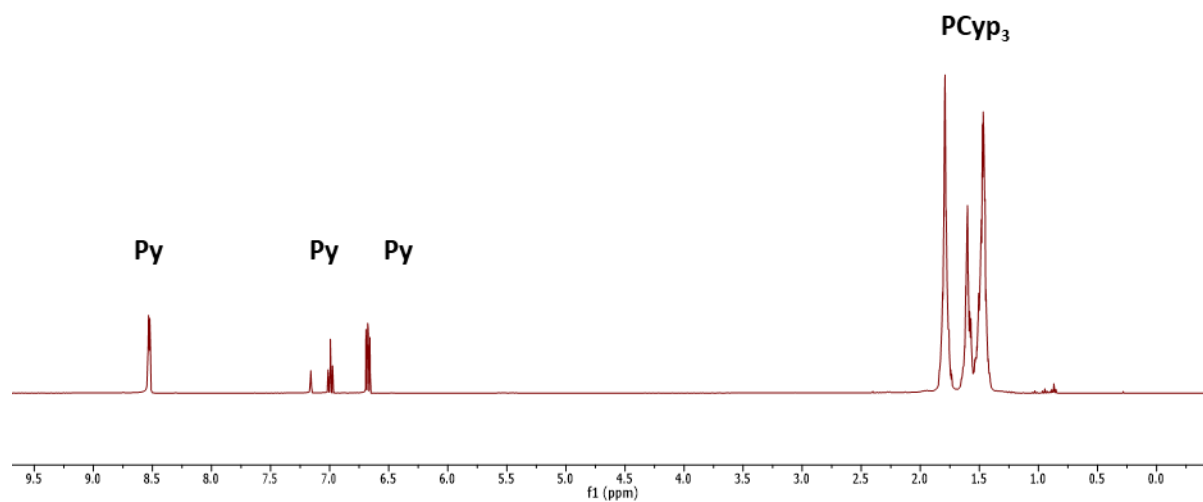


Figure 1.11. Stoichiometric reaction of pyridine (7.91 mg, 8.08 μL , 0.1 mmol), and HBpin (12.80 mg, 14.51 μL , 0.1 mmol) in benzene- d_6 . (a) ^1H NMR at $T=1$ hr; (b) ^{11}B NMR at $T=1$ hr.

Stoichiometric reaction of pyridine and PCyp₃

(a)



(b)

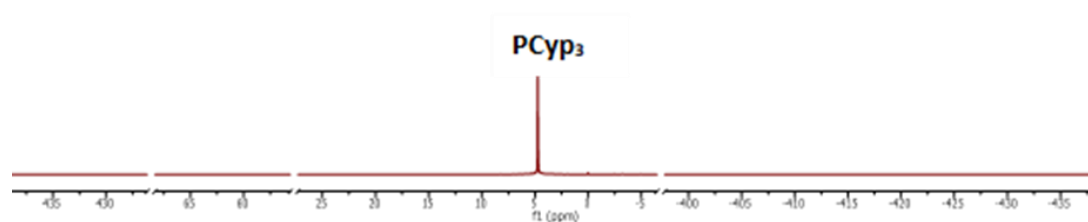


Figure 1.12. Stoichiometric reaction of pyridine (7.91 mg, 8.08 uL, 0.1 mmol), and PCyp₃ (23.83 mg, 24.34 uL, 0.1 mmol) in benzene-d₆. (a) ¹H NMR at T= 1 hr; (b) ³¹P NMR at T= 1hr.

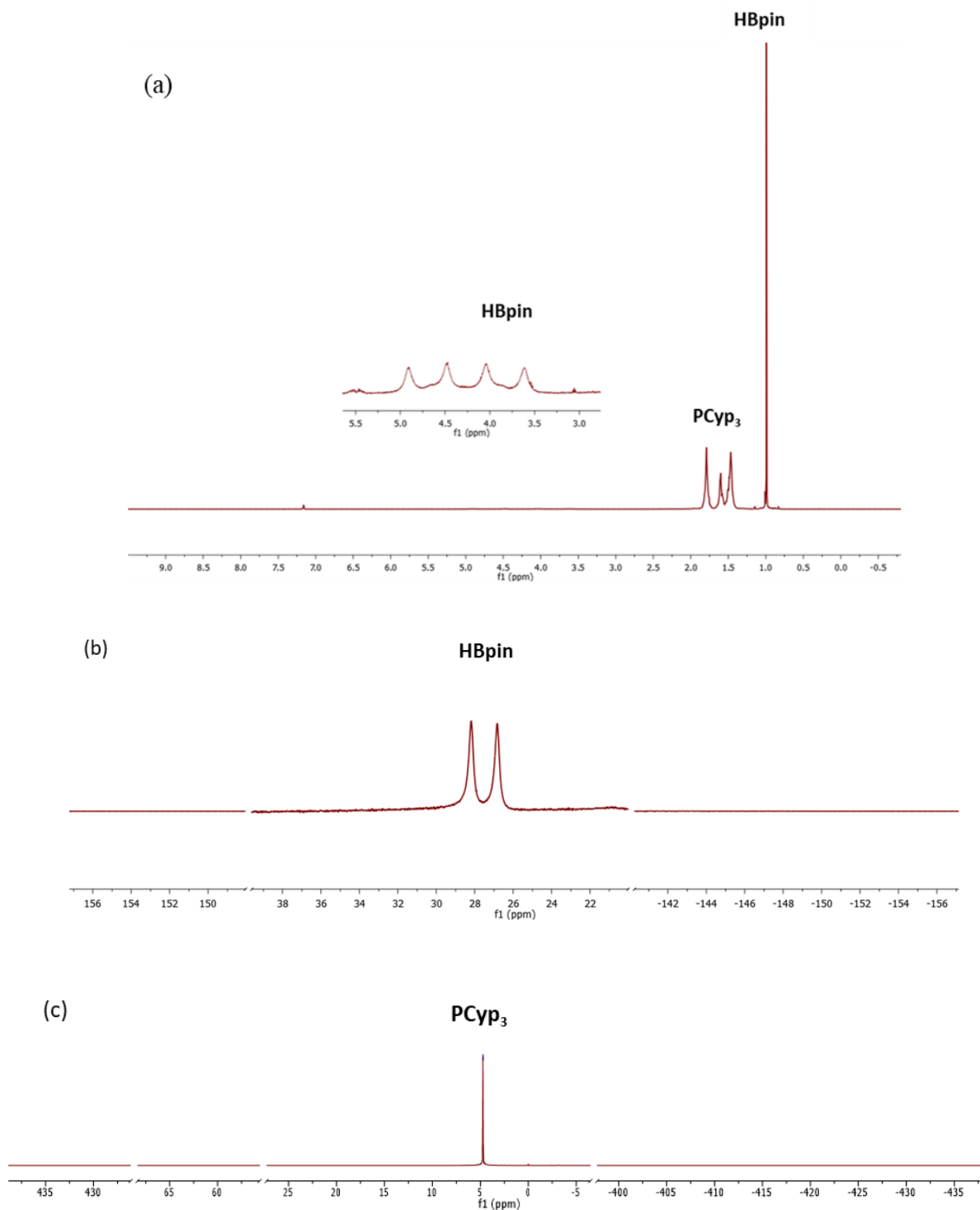
Stoichiometric reaction of PCyp₃ with HBpin

Figure 1.13. Stoichiometric reaction of HBpin (12.80 mg, 14.51 μ L, 0.1 mmol), and PCyp₃ (23.83 mg, 24.34 μ L, 0.1 mmol) in benzene-d₆. (a) ¹H NMR at T= 1 hr; (b) ¹¹B NMR at T= 1 hr; (c) ³¹P NMR at T= 1 hr.

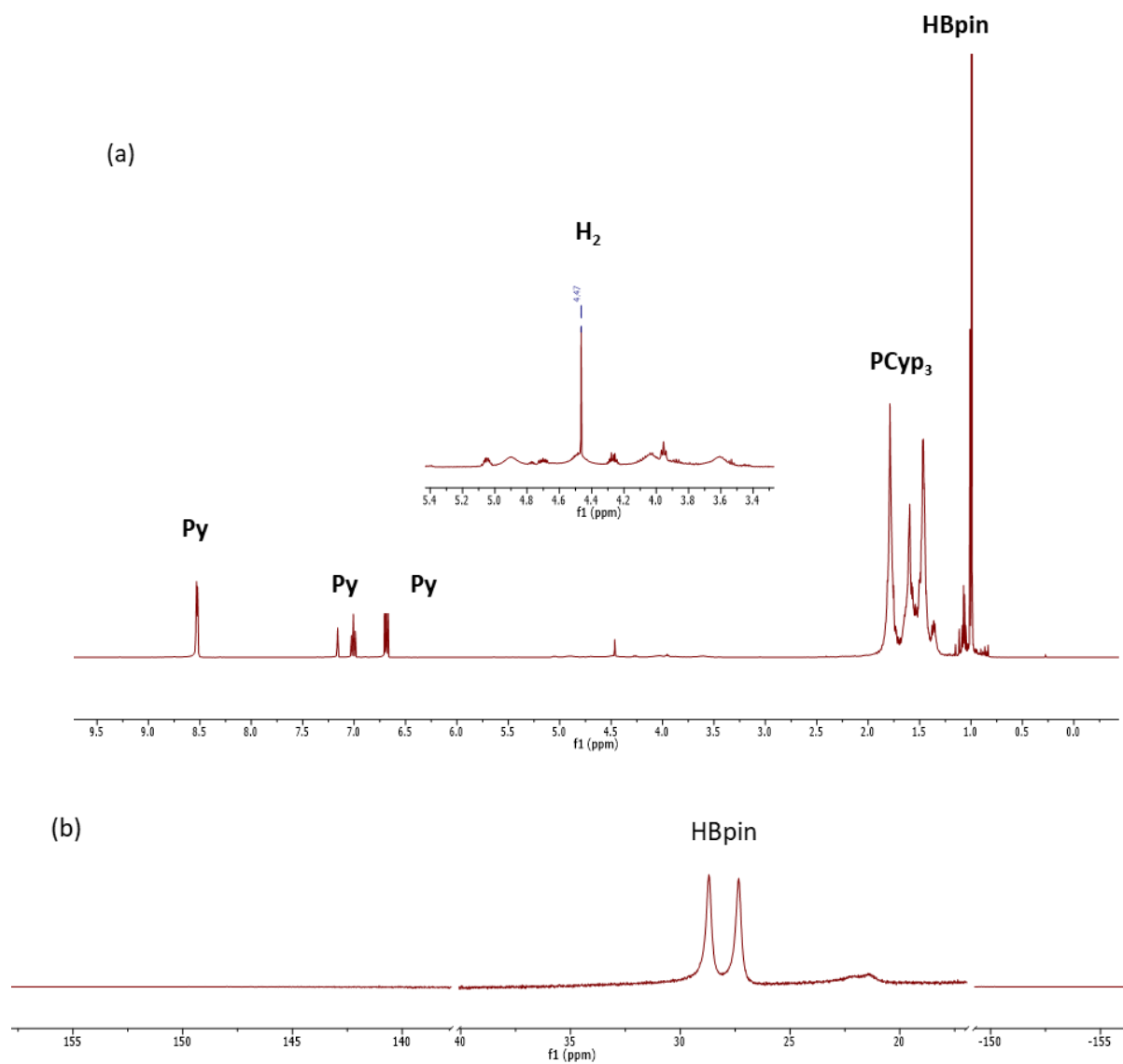
Stoichiometric reaction of PCyp₃, HBpin, and pyridine

Figure 1.14. Stoichiometric reaction of pyridine (7.91 mg, 8.08 μ L, 0.1 mmol), HBpin (12.80 mg, 14.51 μ L, 0.1 mmol), and PCyp₃ (23.83 mg, 24.34 μ L, 0.1 mmol) in Benzene-d₆. (a) ¹H NMR at T= 1 hr; (b) ¹¹B NMR at T= 1 hr.

[Ni] rate order assessment

Varying concentration of [Ni] while keeping concentration of HBpin and 3,5-lutidine constant

$C_{\text{cat}}(\text{M})$	$C_{\text{HBpin}}(\text{M})$	$C_{3,5\text{-lutidine}}(\text{M})$	$k(\text{M/s})$	R^2
0.035	0.59	0.59	9.45E-05	0.997
0.029	0.59	0.59	8.59E-05	0.997
0.024	0.59	0.59	7.93E-05	0.993
0.018	0.59	0.59	7.30E-05	0.991
0.012	0.59	0.59	6.52E-05	0.994

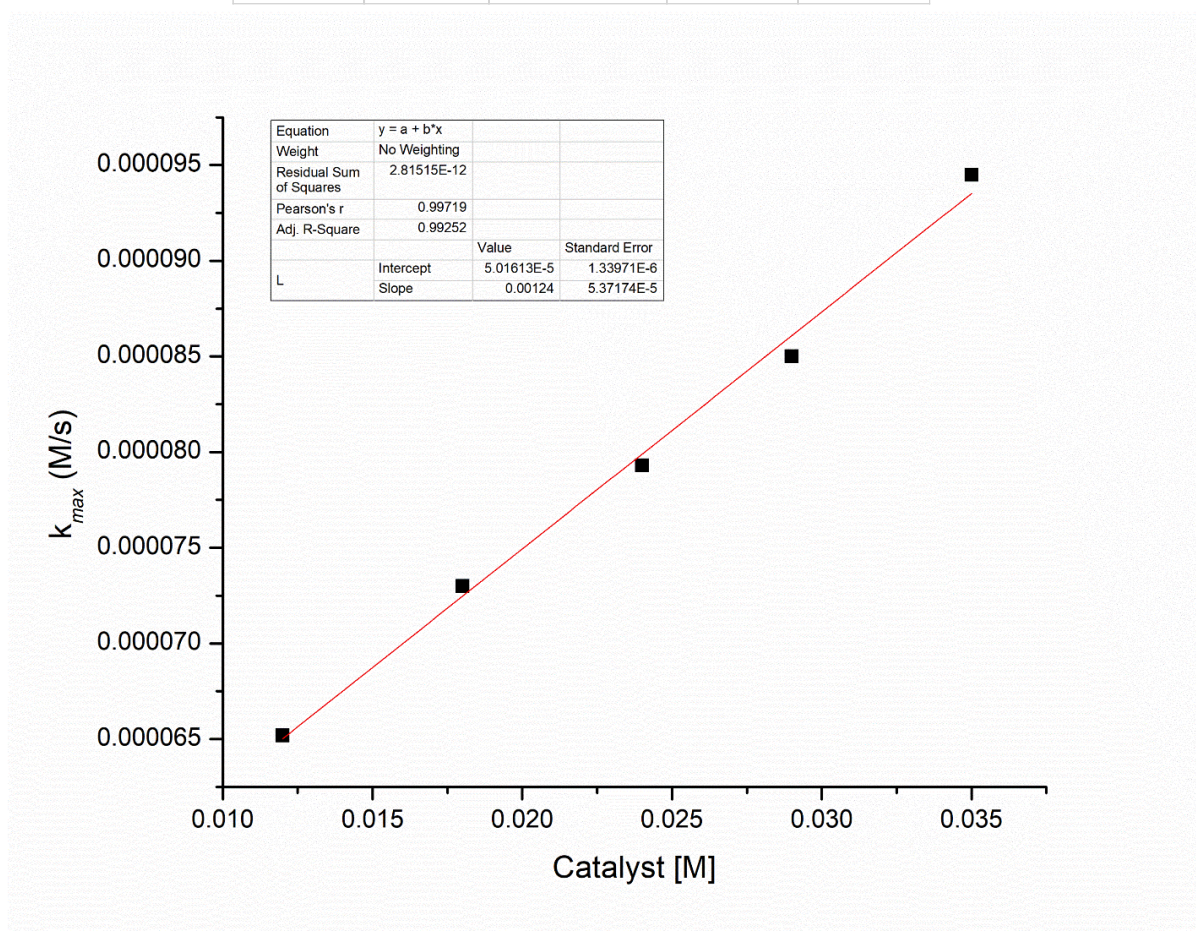


Figure 1.15. Plot of [Ni] vs. reaction rate (K_{max}), the reaction follows 1st order dependence on [Ni].

3,5-lutidine rate order assessment

Varying concentration of 3,5-lutidine while keeping concentration of HBpin and [Ni] constant

$C_{\text{cat}}(\text{M})$	$C_{\text{HBpin}}(\text{M})$	$C_{\text{3,5-lutidine}}(\text{M})$	$k(\text{M/s})$	R^2
0.029	0.59	0.59	8.59E-05	0.997
0.029	0.59	0.71	8.84E-05	0.999
0.029	0.59	1.06	1.03E-04	0.988
0.029	0.59	1.41	8.88E-05	0.997

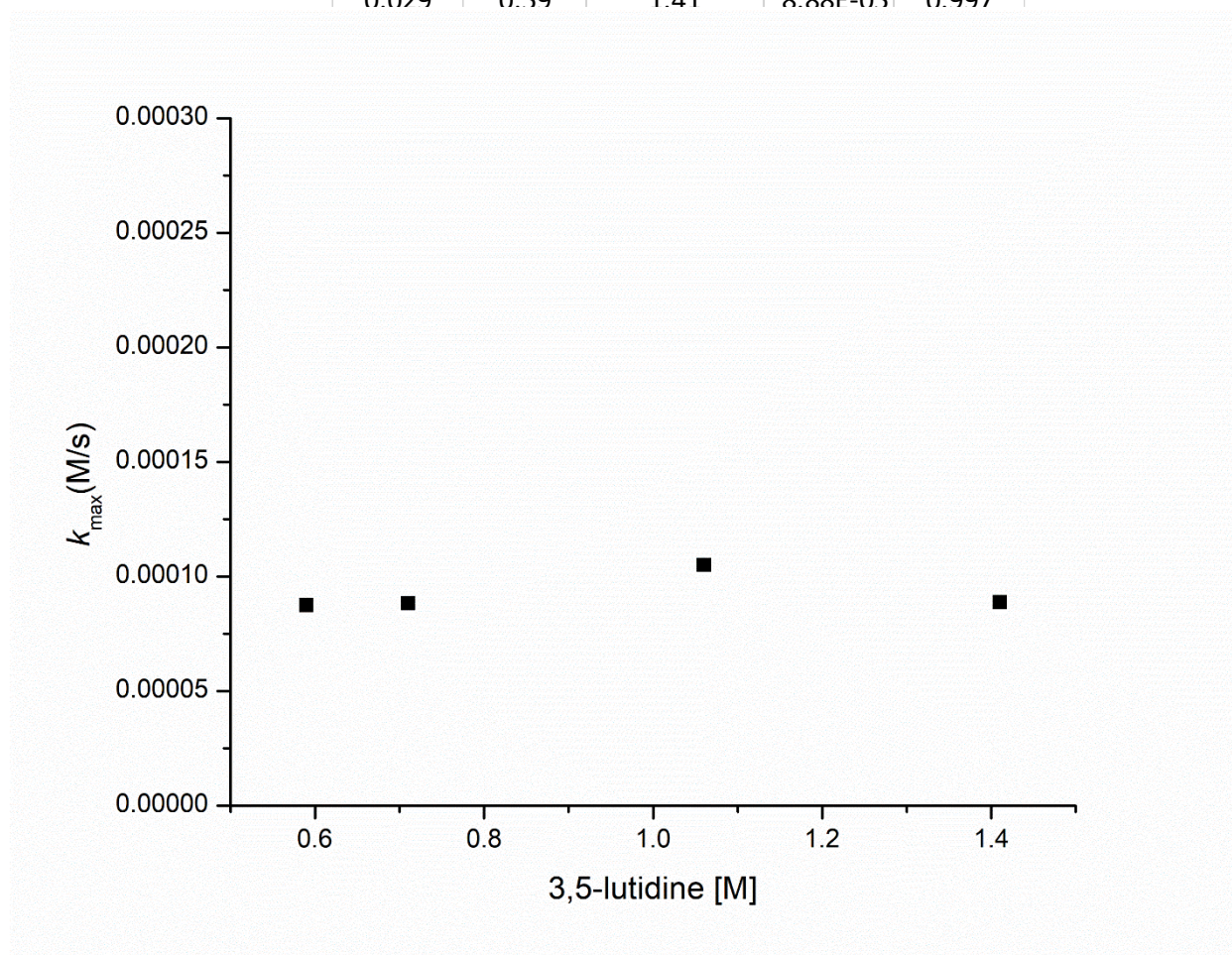


Figure 1.16. Plot of [3,5-lutidine] vs. reaction rate (K_{max}), the reaction follows 0th order dependence on [3,5-lutidine].

HBpin rate order assessment

Varying concentration of HBpin while keeping concentration of 3,5-lutidine and [Ni] constant

$C_{\text{cat}}(\text{M})$	$C_{\text{HBpin}}(\text{M})$	$C_{3,5\text{-lutidine}}(\text{M})$	$k(\text{M/s})$	R^2
0.029	0.35	0.59	4.16E-05	0.997
0.029	0.59	0.59	9.72E-05	0.993
0.029	0.71	0.59	1.20E-04	0.996
0.029	0.88	0.59	1.79E-04	0.991
0.029	1.18	0.59	1.96E-04	0.994
0.029	1.77	0.59	1.80E-04	0.973

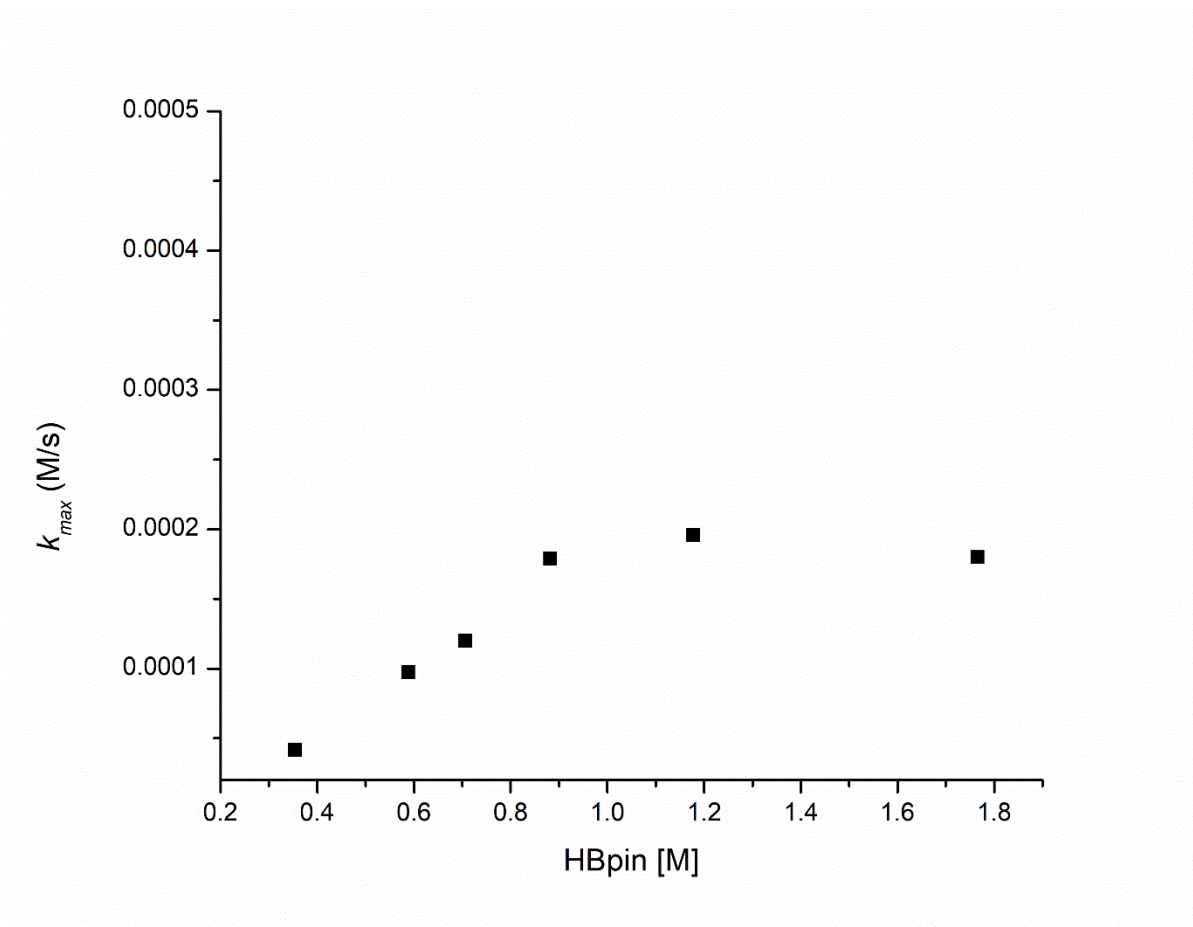


Figure 1.17. Plot of [HBpin] vs. reaction rate (κ_{max}), the reaction follows first order dependence on HBpin till 1.5 equiv. [HBpin], and then 0th order at higher concentration.

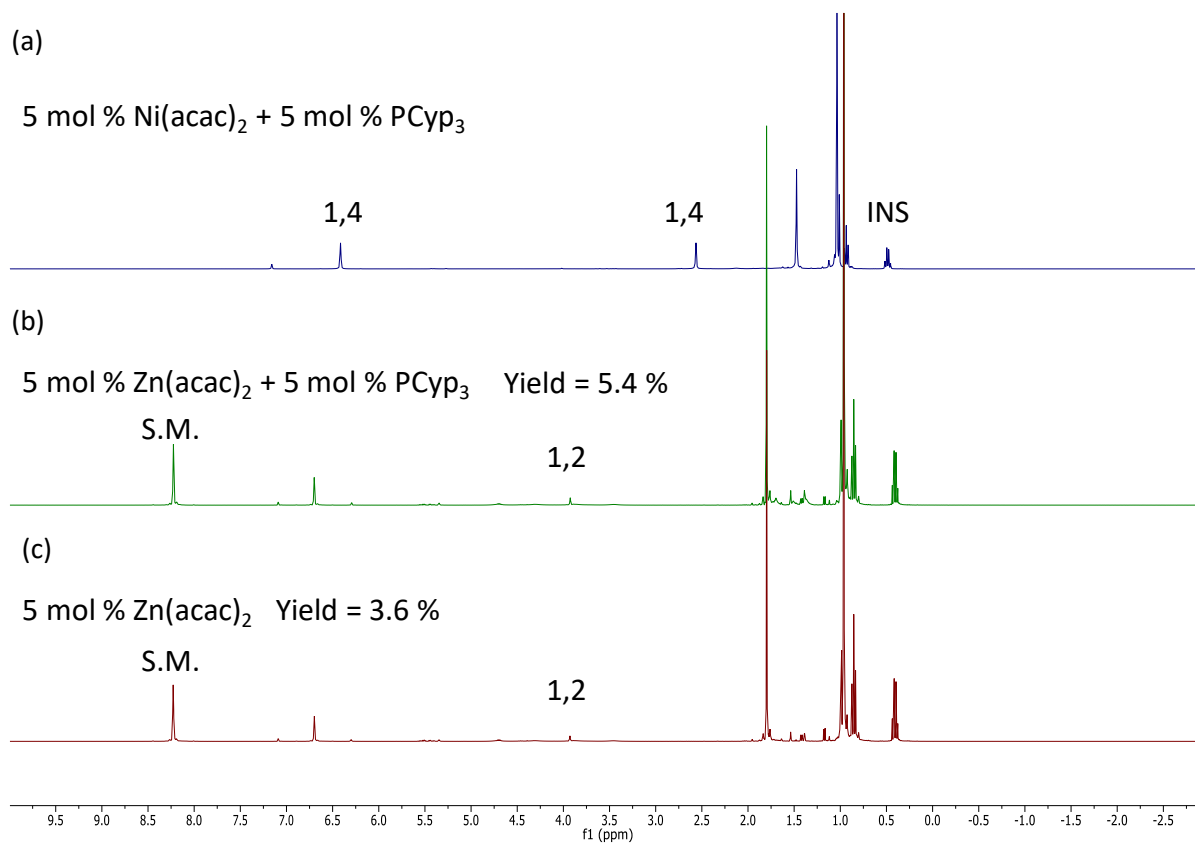
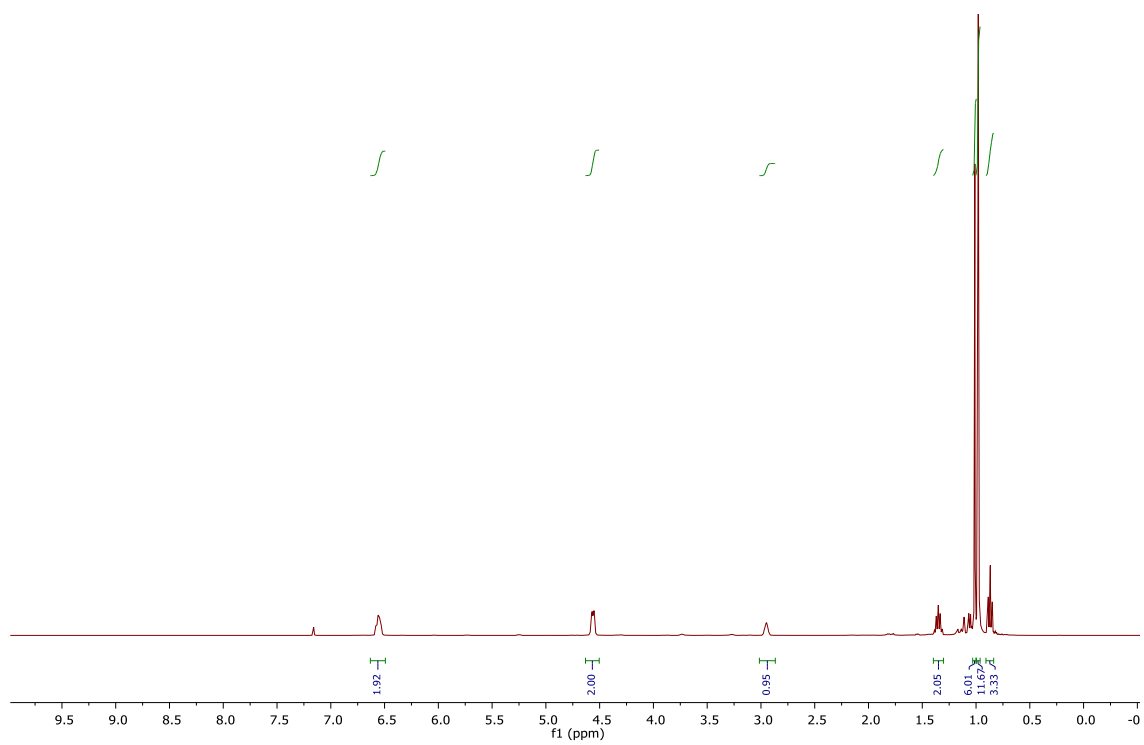


Figure 1.18. ¹H NMR comparison for hydroboration of 3,5-lutidine. (a) Ni(acac)₂/ PCyp₃; (b) Zn(acac)₂/ PCyp₃; (c) Zn(acac)₂.

(a)



(b)

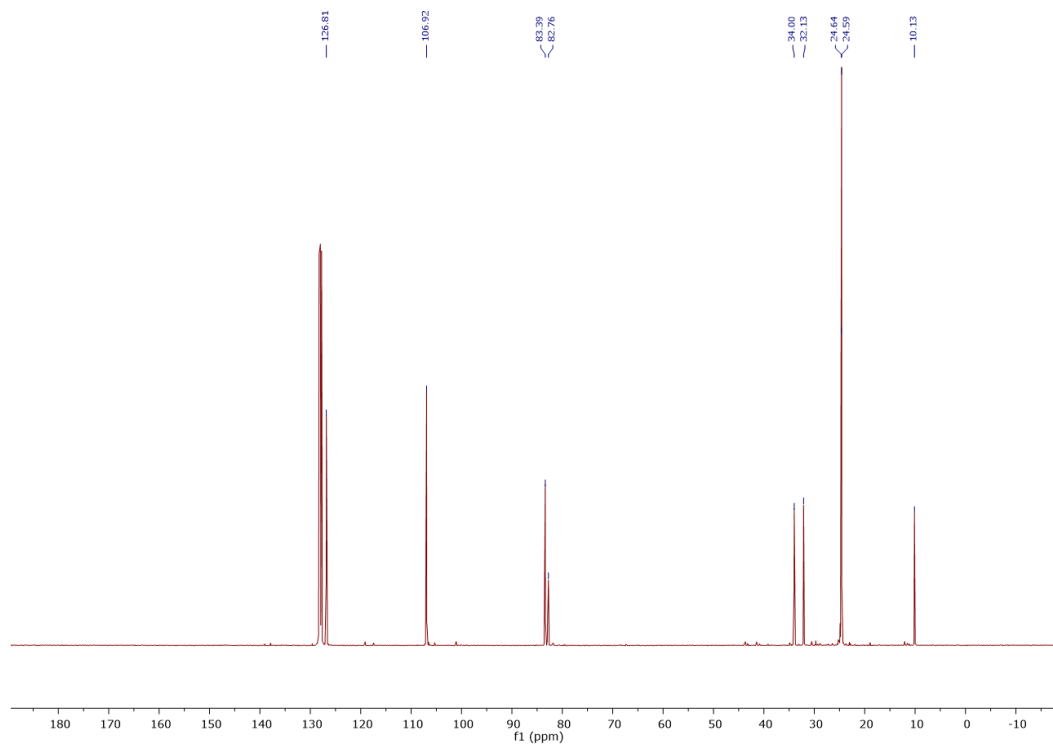


Figure 1.19. (a) ^1H NMR of **16g**; (b) ^{13}C NMR of **16g**

1.6. References

1. Pollak, N.; Dölle, C.; Ziegler, M., The power to reduce: pyridine nucleotides–small molecules with a multitude of functions. *Biochemical Journal* **2007**, *402* (2), 205-218.
2. Kaithal, A.; Chatterjee, B.; Gunanathan, C., Ruthenium-catalyzed regioselective 1, 4-hydroboration of pyridines. *Organic letters* **2016**, *18* (14), 3402-3405.
3. Richter, D.; Mayr, H., Hydride-Donor Abilities of 1, 4-Dihydropyridines: A Comparison with π Nucleophiles and Borohydride Anions. *Angewandte Chemie International Edition* **2009**, *48* (11), 1958-1961.
4. Ouellet, S. G.; Walji, A. M.; Macmillan, D. W., Enantioselective organocatalytic transfer hydrogenation reactions using Hantzsch esters. *Accounts of chemical research* **2007**, *40* (12), 1327-1339.
5. Stout, D. M.; Meyers, A., Recent advances in the chemistry of dihydropyridines. *Chemical Reviews* **1982**, *82* (2), 223-243.
6. Wan, J.-P.; Liu, Y., Recent advances in new multicomponent synthesis of structurally diversified 1, 4-dihydropyridines. *RSC advances* **2012**, *2* (26), 9763-9777.
7. Bull, J. A.; Mousseau, J. J.; Pelletier, G.; Charette, A. B., Synthesis of pyridine and dihydropyridine derivatives by regio- and stereoselective addition to N-activated pyridines. *chemical reviews* **2012**, *112* (5), 2642-2713.
8. Donohoe, T. J.; McRiner, A. J.; Sheldrake, P., Partial reduction of electron-deficient pyridines. *Organic letters* **2000**, *2* (24), 3861-3863.
9. Sundberg, R. J.; Hamilton, G.; Trindle, C., Synthesis and Diels-Alder reactions of N-carbalkoxydihydropyridines. Substituent effects on the regiochemistry of reduction of N-carbalkoxy pyridinium ions. *The Journal of Organic Chemistry* **1986**, *51* (19), 3672-3679.
10. Glorius, F., Asymmetric hydrogenation of aromatic compounds. *Organic & biomolecular chemistry* **2005**, *3* (23), 4171-4175.
11. Liu, Y.; Du, H., Metal-free borane-catalyzed highly stereoselective hydrogenation of pyridines. *Journal of the American Chemical Society* **2013**, *135* (35), 12968-12971.
12. Park, S.; Chang, S., Catalytic Dearomatization of N-Heteroarenes with Silicon and Boron Compounds. *Angewandte Chemie International Edition* **2017**, *56* (27), 7720-7738.
13. Arrowsmith, M.; Hill, M. S.; Hadlington, T.; Kociok-Köhn, G.; Weetman, C., Magnesium-catalyzed hydroboration of pyridines. *Organometallics* **2011**, *30* (21), 5556-5559.
14. Oshima, K.; Ohmura, T.; Suginome, M., Regioselective synthesis of 1, 2-dihydropyridines by rhodium-catalyzed hydroboration of pyridines. *Journal of the American Chemical Society* **2012**, *134* (8), 3699-3702.
15. Dudnik, A. S.; Weidner, V. L.; Motta, A.; Delferro, M.; Marks, T. J., Atom-efficient regioselective 1, 2-dearomatization of functionalized pyridines by an earth-abundant organolanthanide catalyst. *Nature chemistry* **2014**, *6* (12), 1100-1107.
16. Eisenberger, P.; Bailey, A. M.; Crudden, C. M., Taking the F out of FLP: simple Lewis acid–base pairs for mild reductions with neutral boranes via borenium ion catalysis. *Journal of the American Chemical Society* **2012**, *134* (42), 17384-17387.
17. Fan, X.; Zheng, J.; Li, Z. H.; Wang, H., Organoborane catalyzed regioselective 1, 4-hydroboration of pyridines. *Journal of the American Chemical Society* **2015**, *137* (15), 4916-4919.
18. Lortie, J. L.; Dudding, T.; Gabidullin, B. M.; Nikonov, G. I., Zinc-catalyzed hydrosilylation and hydroboration of N-heterocycles. *ACS Catalysis* **2017**, *7* (12), 8454-8459.
19. Zhang, F.; Song, H.; Zhuang, X.; Tung, C.-H.; Wang, W., Iron-catalyzed 1, 2-selective hydroboration of N-heteroarenes. *Journal of the American Chemical Society* **2017**, *139* (49), 17775-17778.

20. Liu, J.; Chen, J.-Y.; Jia, M.; Ming, B.; Jia, J.; Liao, R.-Z.; Tung, C.-H.; Wang, W., Ni–O Cooperation versus nickel (II) hydride in catalytic hydroboration of N-heteroarenes. *ACS Catalysis* **2019**, *9* (5), 3849-3857.
21. Jeong, E.; Heo, J.; Park, S.; Chang, S., Alkoxide-Promoted Selective Hydroboration of N-Heteroarenes: Pivotal Roles of in situ Generated BH₃ in the Dearomatization Process. *Chemistry–A European Journal* **2019**, *25* (25), 6320-6325.
22. Liu, T.; He, J.; Zhang, Y., Regioselective 1, 2-hydroboration of N-heteroarenes using a potassium-based catalyst. *Organic Chemistry Frontiers* **2019**, *6* (15), 2749-2755.
23. Chirik, P. J.; Gunnoe, T. B., A Meeting of Metals □ A Joint Virtual Issue between Organometallics and ACS Catalysis on First-Row Transition Metal Complexes. ACS Publications: 2015; Vol. 5, pp 5584-5585.
24. Tasker, S. Z.; Standley, E. A.; Jamison, T. F., Recent advances in homogeneous nickel catalysis. *Nature* **2014**, *509* (7500), 299-309.
25. Li, Y.-Y.; Yu, S.-L.; Shen, W.-Y.; Gao, J.-X., Iron-, cobalt-, and nickel-catalyzed asymmetric transfer hydrogenation and asymmetric hydrogenation of ketones. *Accounts of chemical research* **2015**, *48* (9), 2587-2598.
26. Yue, H.; Guo, L.; Lee, S. C.; Liu, X.; Rueping, M., Selective Reductive Removal of Ester and Amide Groups from Arenes and Heteroarenes through Nickel-Catalyzed C–O and C–N Bond Activation. *Angewandte Chemie* **2017**, *129* (14), 4030-4034.
27. Simmons, B. J.; Hoffmann, M.; Hwang, J.; Jackl, M. K.; Garg, N. K., Nickel-catalyzed reduction of secondary and tertiary amides. *Organic letters* **2017**, *19* (7), 1910-1913.
28. Caddick, S.; Judd, D. B.; de K Lewis, A. K.; Reich, M. T.; Williams, M. R., A generic approach for the catalytic reduction of nitriles. *Tetrahedron* **2003**, *59* (29), 5417-5423.
29. Rao, B.; Chong, C. C.; Kinjo, R., Metal-free regio- and chemoselective hydroboration of pyridines catalyzed by 1, 3, 2-diazaphosphenium triflate. *Journal of the American Chemical Society* **2018**, *140* (2), 652-656.
30. Keyzer, E. N.; Kang, S. S.; Hanf, S.; Wright, D. S., Regioselective 1, 4-hydroboration of pyridines catalyzed by an acid-initiated boronium cation. *Chemical Communications* **2017**, *53* (68), 9434-9437.
31. Nakamura, G.; Nakajima, Y.; Matsumoto, K.; Srinivas, V.; Shimada, S., Nitrile hydroboration reactions catalysed by simple nickel salts, bis (acetylacetonato) nickel (II) and its derivatives. *Catalysis Science & Technology* **2017**, *7* (15), 3196-3199.
32. Coates, P. D. A study of the preparation and pyrolysis of β-diketonate and carboxylate precursors to semiconducting zinc oxide films., Durham University, 1994.
33. Sheldrick, G. M., SADABS v2008/1. *SADABS v2008/1* **2008**.
34. Sheldrick, G. M., Crystal structure refinement with SHELXL. *Acta Crystallogr. C* **2015**, *71* (Pt 1), 3-8.
35. Sheldrick, G., A short history of SHELX. *Acta Crystallogr. A* **2008**, *64* (1), 112-122.

II. METAL-CATALYZED HYDROBORATION OF ALKENES AND AMIDES

Modified with permission from *Polyhedron* **2019**, *159*, 365-374.

Patrick J Larson, Francis S Wekesa, Arpita Singh, Cecilia R Smith, Amit Rajput, Gregory P McGovern, Daniel K Unruh, Anthony F Cozzolino, Michael Findlater*

(<https://doi.org/10.1016/j.poly.2018.11.060>)

Modified with permission from *Asian J. Org. Chem.* **2020**, *9*, 416-420.

Arpita Singh, Sara Shafiei-Haghighi, Cecilia R. Smith, Dr. Daniel K. Unruh, Prof. Dr. Michael Findlater*

(<https://onlinelibrary.wiley.com/doi/abs/10.1002/ajoc.201900615>)

Modified with permission from *Nat. Catal.* **2020**, *3*, 154-162.

Sem Raj Tamang, Arpita Singh, Deepika Bedi, Adineh Rezaei Bazkiaei, Audrey A. Warner, Keeley Glogau, Corey McDonald, Daniel K. Unruh, Michael Findlater*

(<https://www.nature.com/articles/s41929-019-0405-5>)

2.1. Introduction

Hydroboration is an effective method for the reduction of alkenes, alkynes, amides etc. Precious metal-catalyzed hydroboration has been well-explored in the past. The sustainability, toxicity and the cost of the first-row transition metals and rare-earth elements are the motivating factors driving the use of these metals in catalysis. We have been continuously developing catalytic systems based on first-row transition metals and rare-earth metals for the hydrofunctionalization of C=C and C=O bond. Herein, we report the hydroboration of alkenes and amides with iron and lanthanum based catalytic systems respectively. This chapter is divided into two sub-parts:¹⁻²

2.2. Iron-catalyzed hydroboration of alkenes

Metal-catalyzed hydroboration of unsaturated C–C bonds (e. g. alkynes and alkenes) provides access to boron-containing organic synthons that can be used as intermediates in a number of important transformations including Suzuki-Miyaura coupling reactions.³⁻⁵ Non-catalyzed hydroboration was a significant advance in the development of organoboron chemistry, but one which requires highly reactive boranes like 9-BBN or BH₃–THF (extremely air- and moisture-sensitive species) to afford alkylborane products.⁶⁻⁸ Metal-catalyzed hydroboration employing boronic esters is an attractive alternative because of the relative stability of the products formed while still retaining subsequent reactivity. Excellent regio- and chemoselectivity have been achieved using precious metal catalysts based on Ir,⁹ Rh,¹⁰⁻¹¹ Ru,¹²⁻¹³ and Pd¹⁴ and even main group metals like Al¹⁵ in the hydroboration of alkenes and alkynes. The limited availability, high and volatile cost of precious metal catalysts, and their toxicity has shifted the focus more recently towards the development of cheap, sustainable, and environmentally benign first row metal alternatives.

Iron is the most abundant transition metal and is the fourth most abundant element in the earth's crust, it has a low cost, long-term commercial availability and is environmentally benign.¹⁶ The replacement of precious metal elements in homogeneous catalysis using iron is often hampered due to the fact that iron prefers to undergo single electron transfer (SET) processes in preference to the, more typical, two-electron processes (involved in oxidative addition and reductive elimination steps) associated with precious metals. So, clearly, there is a need to design ligands which can interact with the metal such that the metal can undergo two electron changes. These types of ligands are classified as 'redox non-innocent' and can play a crucial role in modifying the reactivity of the metal catalyst.¹⁷ These ligands are not mere spectator ligands, instead they actively participate in the redox process; they function as electron reservoirs by temporarily storing, and subsequently releasing electrons whenever required in a multi-electron transformation. One of the most prominent classes of redox non-innocent ligands are the diimines; several classes of complexes and catalysts have been reported (**Figure 2.1**) and α -diimine complexes of iron using the simple diazabutadiene (DAB) (**21**) have been known for nearly four decades.¹⁸ Most notably, the groups of Brookhart and Gibson applied bis(imino)pyridine (PDI) (**22**) complexes of iron as successful olefin polymerization catalysts.¹⁹ The ability of the PDI ligand to reversibly exchange electrons with a coordinated iron center is a key characteristic of this ligand architecture. Thus, the elementary steps of the catalytic cycle are facilitated by the participation of the ligand in electron exchange and uncommon oxidation states at the iron center may be avoided.

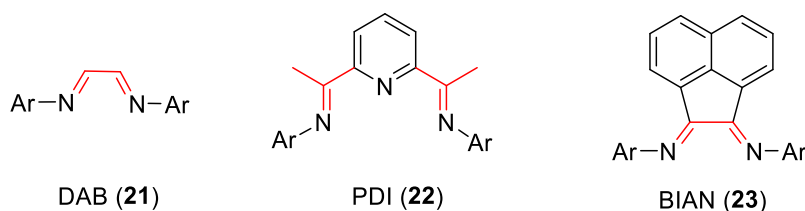


Figure 2.1. Prominent examples of redox non-innocent ligands

For example the stepwise reduction of (**24**) to (**26**) is illustrative of this approach (**Figure 2.2**).²⁰ Electron-counting assigns an Fe(0) center in the complex (**26B**), theoretical and spectroscopic studies reveal that the system is Fe(II) species (d^6) supported by a diradical ligand (**26A**; the spin singlet ground state state ($S = 0$) is due to antiferromagnetic coupling of iron and ligand triplet state). In other terms, the redox non-innocent ligands allow the base metals to mimic the precious metals in some of the catalytic applications.

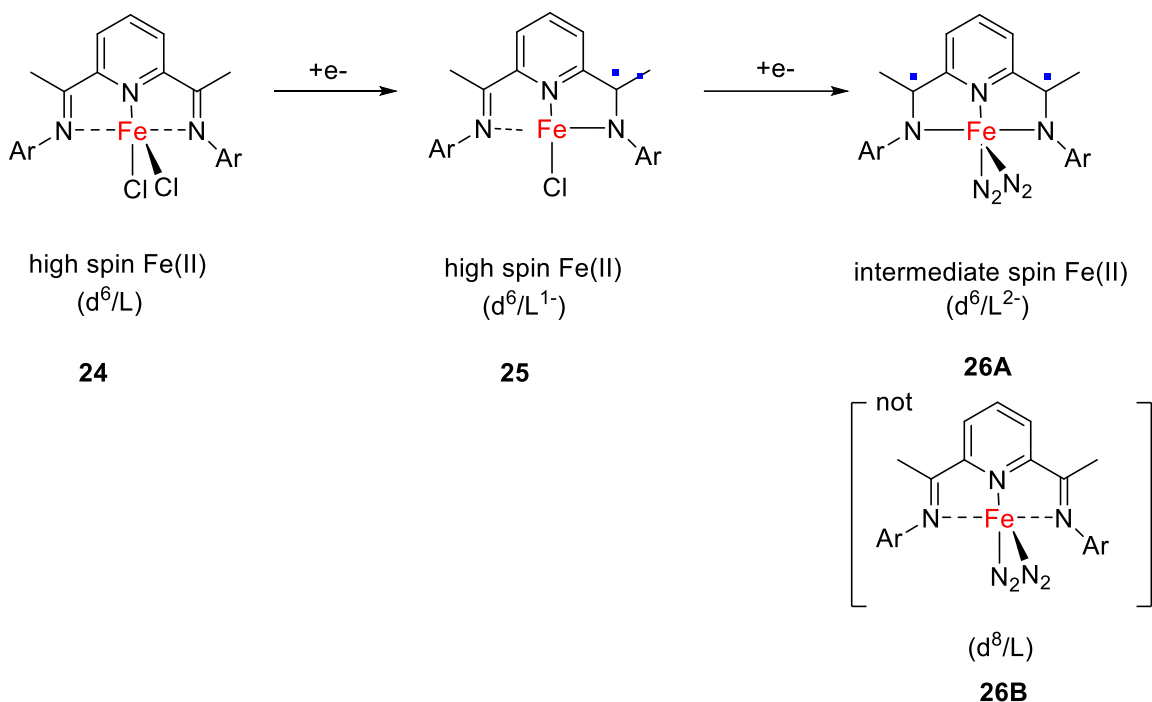


Figure 2.2. A well understood example serving to illustrate the concept of redox non-innocence.

Bis(arylimino)-acenaphthene (BIAN) ligands are one class of redox non-innocent diimine ligand which may be considered as the fusion of diazabutadiene with naphthalene; the rigid ligand backbone provides a robust support for transition metal complexes. Although BIAN ligands are well-known in the literature for their coordination chemistry with transition metals²⁰⁻²¹ there are only few reports of iron complexes of BIAN.²²⁻²⁶

The seminal work on hydroboration was reported by utilizing the Wilkinson's catalyst $[(\text{Ph}_3\text{P})_3\text{RhCl}]$ for hydroboration of alkenes.²⁷ This opened new platform towards catalyst designing and employing metals in the hydroboration of alkenes. In 2013, Huang and co-workers developed an electron rich iron complex (**27**) using a pyridyl-based phosphine ligand (PNN) which was used as a precatalyst to afford anti-Markovnikov products in good yields.²⁸ Also the catalytic system could tolerate various functional groups like tosylate, amine, ether and acetal. A little later, Chirik and co-workers employed bis(imino)pyridine iron dinitrogen (${}^{\text{iPr}}\text{PDI}(\text{N}_2)_2$) (${}^{\text{iPr}}\text{PDI} = 2,6-(2,6\text{-}^{\text{iPr}}_2\text{-C}_6\text{H}_3\text{-N}=\text{CMe})_2\text{C}_5\text{H}_3\text{N}$) complex (**28**) to successfully carry out anti-Markovnikov hydroboration of alkenes and styrene. The precatalyst was highly selective to afford linear boronate esters (>95%).²⁹ In 2016, Webster and co-workers reported an iron based pre-catalyst (**29**, 5mol%) to afford Markovnikov:anti-Markovnikov selective products with selectivity ranging from 60:40 to 70:30 for styrene derivatives.³⁰ The catalytic system was also active towards the hydroboration of alkynes and nitriles. In 2016, Thomas and co-workers employed NHC based iron precatalyst (**30a**, 2.5mol%) in presence of HBpin to carry out Markovnikov selective hydroboration of the styrenes in moderate to good yields and selectivity ranging from 37:1 to 5:1.³¹ Also when catalyst (**30b**, 2.5 mol%) was used in conjunction with HBCat, anti-Markovnikov hydroboration products were obtained in yields ranging from 39% to 71%. By careful design of catalyst, and with the use of appropriate borylating agent, selectivity of the hydroboration product can be tuned. In 2017, Lu and coworkers utilized commercially available FeCl_2 (2.5mol%) salt in presence of ligand OPPA

(**31**, 3mol%) to afford products in good to moderate yields (35-81%) and excellent selectivity (37:1 to 50:1).³² The catalytic system had tolerance to wide variety of functional groups such as ether, silyl ether, ketal and also showed promising reactivity even with difficult substrates such as indene and β -methylstyrene. Liu and co-workers exploited simple iron salts for the hydroboration of alkenes. FeBr₃ used in conjunction with LiOtBu in MeOtBu as a solvent afforded the hydroborated product with anti-Markovnikov regioselectivity, whereas Fe(OTf)₃ with LiOtBu in NMP as solvent gave the Markovnikov selective product.³³

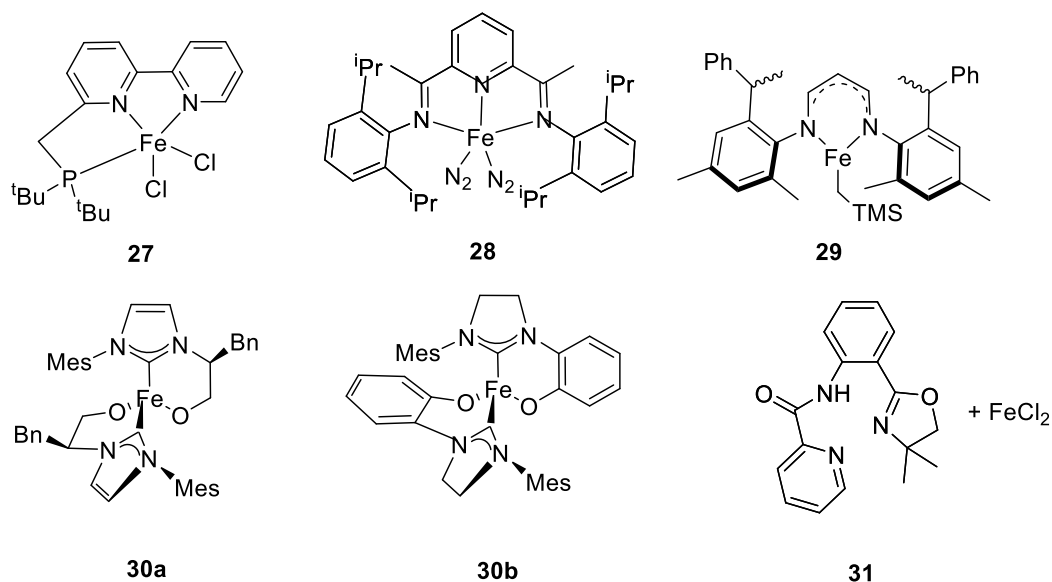


Figure 2.3. Representative examples of iron complexes utilized for hydroboration of alkenes.

Catalytic hydroboration of alkenes leads to the formation of organoboron species, building blocks in organic synthesis. Transition-metal catalyzed hydroboration of alkenes affords alkylboronate ester products, that are air-stable and bench-stable and can be purified with column chromatography. Due to the wide applicability of the alkylboronate esters in synthetic chemistry, we explored the hydroboration of alkenes with iron-based catalyst.

Our group has previously shown the catalytic activity of [BIAN]Fe(η^6 -toluene) (**M1**) towards the hydrosilylation of carbonyls.²⁵ We further developed the catalytic applications of [BIAN]-Fe complexes to include both imine and ester hydrosilylation and ring-opening polymerization of lactide.^{22, 34-35} Recently, van Wangelin reported similar complexes to be capable of catalytic hydrogenation of alkenes.²⁴ With this broad range of reactivity in mind, we explored the ability of [BIAN]-Fe complexes to catalyze the hydroboration of unsaturated hydrocarbon substrates.

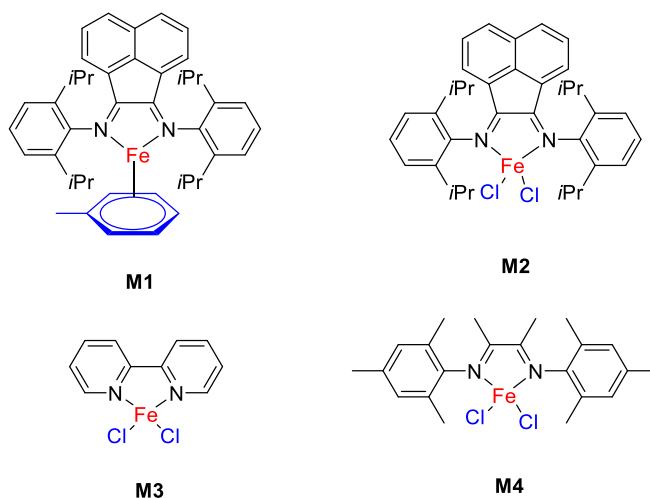
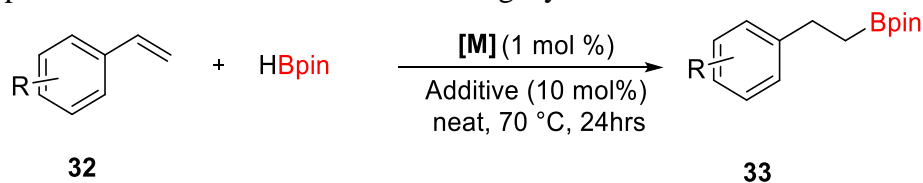


Figure 2.4. Iron pre-catalysts used for hydroboration of alkenes

Table 2.1. Optimization of reaction conditions using styrene as the model substrate

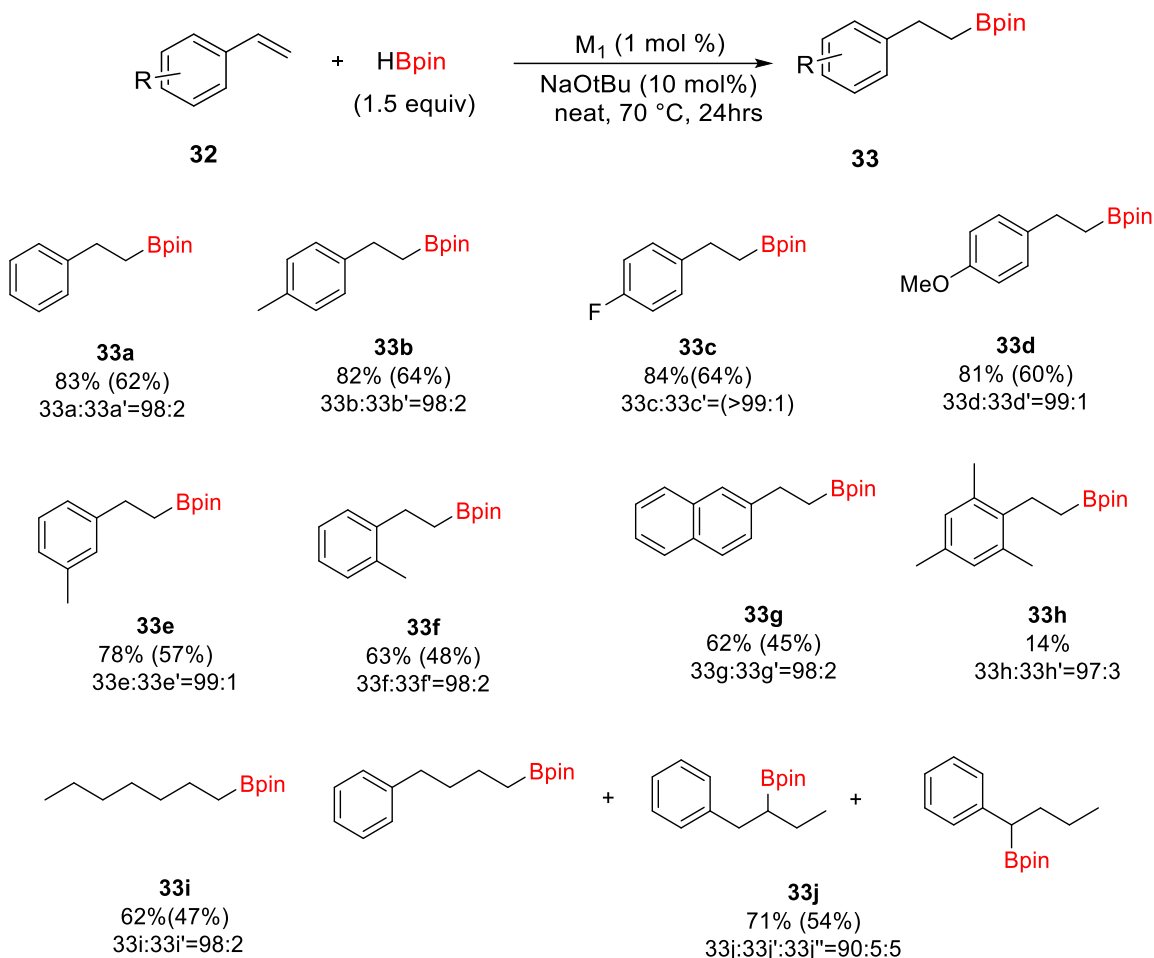


Entry	[M]/[ADDITIVE]	T (hrs)	Conversion of 32a (%)	Ratio (33a: 33b)
1	M1	24	16	n.d.
2	M1/NaBHET ₃	24	73	84:16
3	M1/NaOtBu	24	75	97:3
4	M1/LiOMe	24	68	92:8
5	M1/Cs ₂ CO ₃	24	80	45:55
6	M1/K ₂ CO ₃	24	52	95:5
7 ^a	M1/NaOtBu	24	100	97:3
8 ^a	M2/NaOtBu	24	75	66:34
9 ^a	M3/NaOtBu	24	56	63:37
10 ^a	M4/NaOtBu	24	85	76:24

Reaction conditions: Styrene (0.5 mmol), **M** (0.005 mmol), NaOtBu (0.05 mmol), HBpin (0.55 mmol). Conversions and regioselectivity determined by GC-MS (a) HBpin (0.75 mmol) was used.

Using styrene as a model substrate in the presence of 1.1 equiv. of HBPin, a mixture of unreacted substrate, hydroboration product and hydrogenated product were observed by GC-MS (when employing **M1** at 70 °C). However, upon increasing the HBpin loading to 1.5 equiv. and adding NaOtBu., an improved yield of hydroboration product (83% by NMR, 62% isolated) was obtained. Using these optimized conditions, a wide range of substrates was explored. Styrenes with electron withdrawing and releasing group (**32b-32d**) gave good yields for hydroboration with excellent anti-Markovnikov regioselectivity (1:b > 98:2). The catalytic system also afforded good yield with *meta*-

substituted styrenes (**32e** 78%). 2-methylstyrene (**32f**) and vinylnaphthalene (**32g**) gave moderate yields, 48 and 45% isolated, respectively, while retaining excellent regioselectivity (>98%). Mesitylstyrene (**32h**) was low-yielding presumably due to the presence of sterically encumbering groups at the *ortho* and *para*-positions. Surprisingly, 1-hexene (**32i**) afforded only a moderate yield with anti-Markovnikov selectivity (>98%). A mixture of products (**32j**, **32j'**, **32j''** = 90:5:5) was observed for 4-phenyl-1-butene as a result of hydroboration at the 1-, 2-, and 4- positions, possibly a result of alkene isomerization prior to hydroboration. (**Scheme 2.1**)

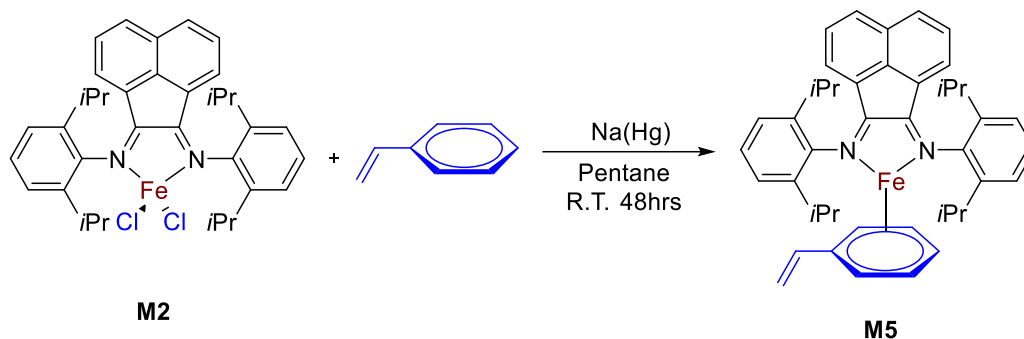


Scheme 2.1. Substrate scope for hydroboration of alkenes

Reaction conditions: Styrene (0.5 mmol), **M1** (0.005 mmol), NaOtBu (0.05 mmol), HBpin (0.75 mmol). NMR yields were determined by ^1H NMR spectroscopy using mesitylene as an internal standard and ratio of regioisomers were determined by GC-MS. Isolated yield in parenthesis.

To gain further insight into the hydroboration mechanism, we attempted to synthesize plausible intermediates along the proposed catalytic cycle, which in turn, we would examine for catalytic competence. Reduction of [BIAN]FeCl₂ (**M2**) with sodium amalgam in pentane in the presence of

styrene led to the formation of substrate bound complex **M5** (Scheme 2.2), ORTEP diagrams of the complex is shown in **Figure 2.5**. Interestingly, in the case of **M5**, the substrate is not bound through the anticipated η^2 -alkene interaction, but rather in an η^6 -arene manner.



Scheme 2.2. Method for the preparation of **M5**

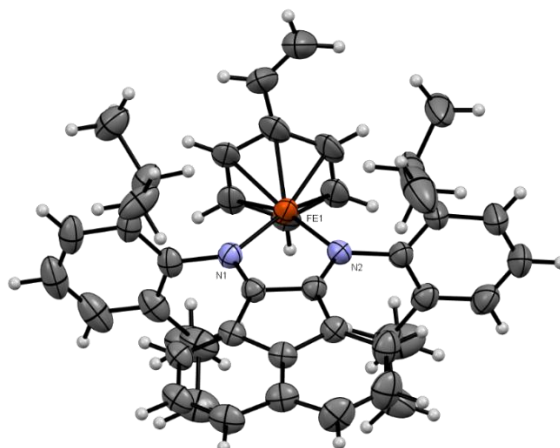


Figure 2.5. Crystal structure of **M5**.

A mechanism for hydroboration of alkenes was proposed and we believe that the toluene cap of **M1** is liberated at elevated temperature to afford a coordinatively unsaturated iron center which is rapidly coordinated by substrate. In the case of those substrates with an arene component, further reaction may occur from the η^2 or η^6 coordination mode. Based upon the report of Thomas and coworkers, reaction between HBPin and NaOtBu produces the reducing agent shown (**Figure 2.6**). It is this borate species which is proposed to react with the unsaturated, iron-bound, substrate to afford a reduced species. Upon further addition of HBpin the borate ion is regenerated, rejoining the catalytic cycle. Subsequently, incoming substrate then binds to the iron centre and product is liberated (**Figure 2.6**).

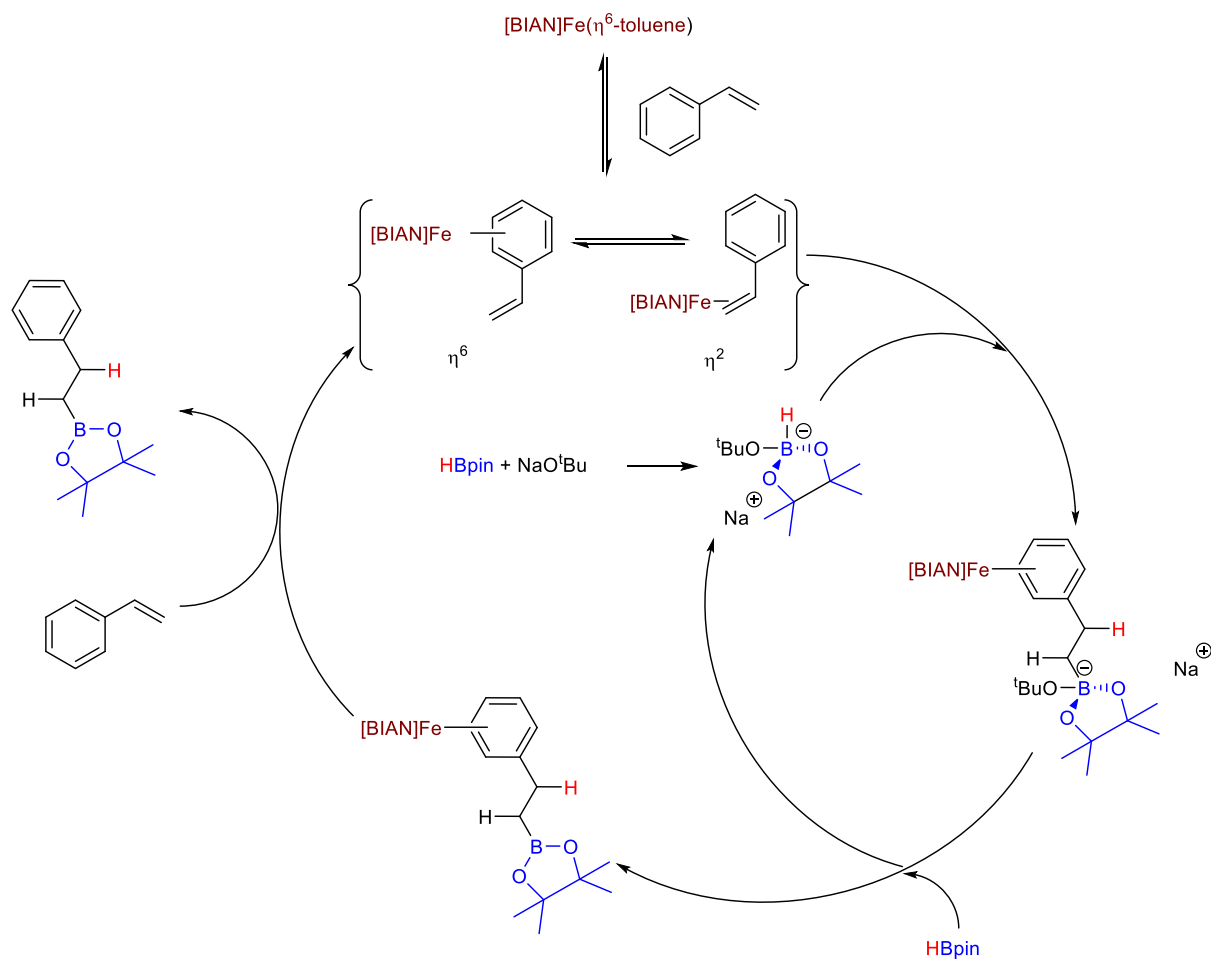


Figure 2.6. Mechanism for the hydroboration of alkenes

Based upon GC-MS analysis, treatment of 1 equivalent of complex of **M5** with 4 equivalents of HBPin in the presence of NaOtBu (10 mol%) under solvent-free conditions at 70 °C, affords the corresponding hydroborated organic product. Formation of hydrogenated products was also observed along with the hydroborated product. These data suggested that the arene cap needs to be removed from the iron center in **M5** to form a catalytically active species that can initiate hydroboration (**Figure 2.6**). We carried out experiments to determine what, if any, kinetic isotope effects were present; deuterium labelling experiments were performed using styrene as substrate and DBPin (**Figure 2.24-2.25**), which was synthesized according to the procedure reported by Chavant and co-workers.³⁶ An inverse kinetic isotopic effect (0.76) was observed for alkene substrate (styrene) suggesting that C-D bond breaks faster than C-H bond in the substrate. (**Figure 2.12-2.13**)

2.3. Lanthanum-catalyzed hydroboration of amides

Reduction of amides to amines is one of the most useful transformations that provides access to amines.³⁷⁻³⁸ Amines are utilized in pharmaceutical industry, crop protection, natural product chemistry, and in advanced materials.³⁹ Amides are least reactive substrates among the carboxylic acid derivatives; the lone pair on nitrogen atom is in conjugation with the C=O bond which leads to resonance structures I and II. Due to the orbital overlap, the electrophilicity on the carbonyl carbon is diminished, making amides least reactive (**Figure 2.7**).

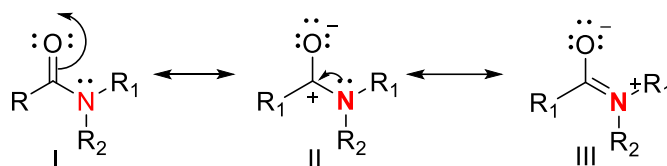


Figure 2.7. Resonance structures of amides

Traditional methods to access amines involve the alkylation of N-H bond with alkyl halides and alcohols, reduction of imines and amides and reductive amination of the carbonyl group. The reduction of carboxamides into amines can now be accomplished via a number of catalytic strategies:⁴⁰⁻⁴¹ deoxygenation,⁴²⁻⁴⁸ hydrogenation⁴⁹ and C-N bond cleavage.⁵⁰⁻⁵⁴ All these transformations require the use of stoichiometric reagents and harsh conditions⁵⁵ such as high temperature and pressure, usage of precious metals. Also, there is no control on regio-, stereo and chemo selectivity and they often lead to a huge number of byproducts.

Interestingly, the majority of the deoxygenation of amides to amines via hydrofunctionalization methodology is achieved via hydrosilylation; most catalytic systems report reduction of tertiary and secondary amines with a very limited number being successfully applied to primary amides. In 2013, Beller and co-workers utilized benzophenone derived boronic acids (**34**) to carry out the hydrosilylation of amides; only 6 examples of 2° and 4 examples of 1° amides were reported.⁵⁶ Cantat and co-workers reported B(C₆F₅)₃ catalyzed hydrosilylation of primary amides in which the silylation of one N-H bond with chlorotrimethylsilane was essential to obtaining primary amine as the final product; secondary amine was formed as the predominant product in the absence of a previous silylation step.⁵⁷ A similar observation was reported by Darcel and co-workers when primary amides were subjected to hydrosilylation in the presence of a ruthenium catalyst.⁵⁸ Szostak and co-workers reported the only known example of an *f*-block element effecting reduction of an amide.⁵³ In this case, the combination of SmI₂/Et₃N/H₂O results in the conversion of amides into alcohols under non-catalytic conditions, although it is noteworthy that 1°, 2° and 3° amides were tolerated. In contrast, application of a hydroboration strategy has been surprisingly limited. In 2015, Sadow and co-workers reported the first example of amide reduction via hydroboration in the presence of a Mg catalyst (**35**).⁴⁶ Tertiary amides and secondary amides were effectively reduced to their corresponding amines, although it should be noted that longer reaction times (24-48 h) were required to obtain quantitative conversion of secondary amides. Khalimon and co-workers reported the first example of a base metal, in this case a Ni(II) pincer complex (**36**), in reduction of tertiary (two examples), secondary (one example) and primary (one example) amides.⁴⁴ Mandal and co-workers developed a catalytic system involving NHC based potassium complex (**37**) for the deoxygenation of amides; the system worked well for chiral amides.⁵⁹ Shao and co-workers utilized KOtBu/BEt₃ as a catalyst and HBpin as a hydrogen source for the hydroboration of 3°, 2° and 1° amides.⁶⁰ In 2021, Sen and co-workers employed 2,6-di-tert-butyl phenolate lithium·THF (**38**)

along with HBpin as a borylating agent to carry out the deoxygenative hydroboration of 1°, 2° and 3° amides.⁶¹ In the same year, another approach was reported by Sen and co-workers where they carried out the solvent and catalyst free hydroboration of amides; 18 examples of 1° amides and 5 examples of 2° were reported. The system was incapable of reducing 3° amides.⁶²

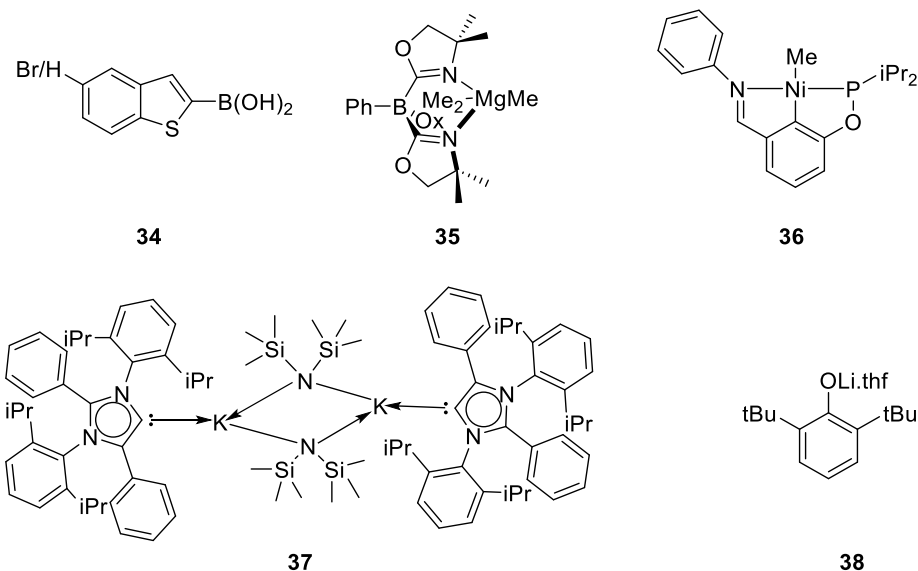


Figure 2.8. Selected examples of catalysts for hydrofunctionalization of amides

Given the paucity of reports of f-block elements in hydroboration catalysis and in the reduction of amides in particular, we decided to explore simple diketonate complexes of the lanthanides as potential catalysts. In our attempt to remove water from the commercially available lanthanide salts prior to catalysis, we were surprised to observe the formation of polynuclear diketonato clusters (or polyoxometalates (POMs)) upon heating the lanthanide acetylacetonate salts under dynamic vacuum. For example, heating $\text{La}(\text{acac})_3 \cdot n\text{H}_2\text{O}$ hydrate (acac = acetylacetonate) under dynamic vacuum resulted in the formation of $\text{La}_4(\text{O})(\text{acac})_{10}$ (**39**) with a polynuclear tetrahedral $\text{La}_4(\mu_4\text{-O})$ core (**Figure 2.9**).

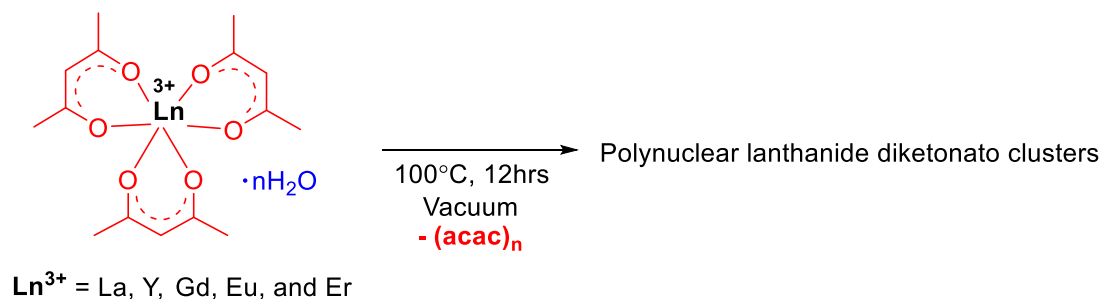


Figure 2.9. Synthesis of polynuclear lanthanide-diketonato clusters

This has been previously observed and proposed to arise from the loss of 2,4-pentadione and a water molecule by mild heating. Moreover, these complexes exhibit enhanced solubility in non-

polar solvents such as benzene and pentane. Single crystal X-ray crystallography revealed a series of POMs based on lanthanide acetylacetonate salts (La (**39**), Y (**40**), Gd (**41**), Eu (**42**), and Er (**43**)) (Figure 2.10a-e). This is rather surprising as this simple approach differs from some of the more common synthetic strategies that have been employed in synthesis of lanthanide POMs (Er,⁶³ Nd,⁶⁴ Gd,⁶⁵ Eu⁶⁶ etc.)⁶⁷ Single crystal diffraction experiments revealed that the Eu-POM was isostructural to the Gd-POM (Figure 2.10c and 2.10d); each of these structures is comprised of 4 metal centers with bridging μ -OH groups. In contrast, Er-POM was isostructural to Y-POMs (Figure 2.10b and 2.10e); each of these structures is comprised of 6 metal centers and bridged by μ_3 -OH.

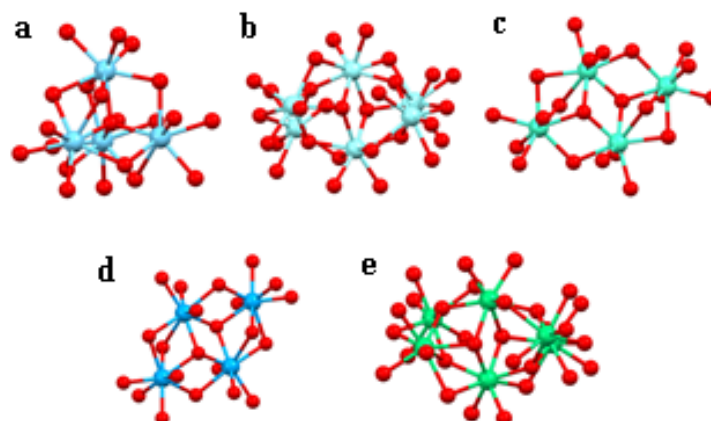
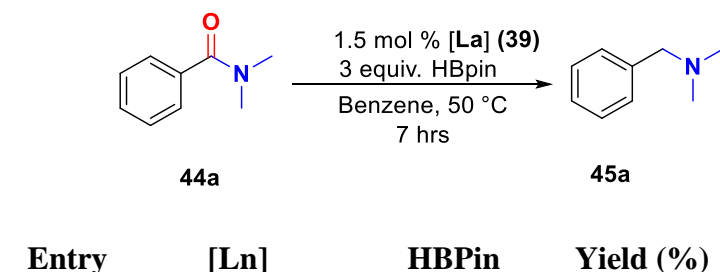


Figure 2.10. POMs with various lanthanide elements. (a) La (**39**); (b) Y (**40**); (c) Gd (**41**); (d) Eu (**42**); (e) Er (**43**). All hydrogen and carbon atoms have been omitted for clarity.

Initially, we chose N,N-dimethylbenzamide (**44a**) as our model substrate and undertook catalytic hydroboration reactions employing 1 equiv. of HBpin with La₄(O)acac₁₀ (**39**). The progress of the reaction was conveniently monitored using ¹H NMR, and a product yield (N,N-dimethylbenzylamine, **45a**) of 27 % was obtained. Upon increasing to 3 equiv. of HBpin, relative to amide, deoxygenated product **45a** was obtained in 95 % yield. Screening of alternative commercially available lanthanum (III) complexes, La(OTf)₃ and LaCp₃ resulted in no detected reaction product. Furthermore, a moderate yield of 78% was observed when the untreated hydrate salt, La(acac)₃·nH₂O was used as the catalyst. Further screening with POMs based on Y (**40**), Gd (**41**), Eu (**42**) and Er (**43**) revealed that La₄(O)(acac)₁₀ (**39**) was the most effective (Table 2.3). As a control, catalytic experiments carried out in the absence of La₄(O)acac₁₀ (**39**) showed little to no activity (Table 2.2).

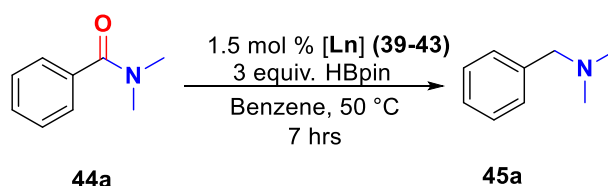
Table 2.2. Optimization of hydroboration of amides using various lanthanum salts



1	La ₄ O(acac) ₁₀	1	27
2	La ₄ O(acac) ₁₀	2	80
3	La ₄ O(acac) ₁₀	3	95
4	-	3	0
5	La(OTf) ₃	3	0
6	LaCp ₃	3	0
7	La(acac) ₃ ·nH ₂ O	3	78

Yield determined by ¹H NMR using tetraethylsilane as the internal standard.

Table 2.3. Optimization of reaction with various polynuclear lanthanide-diketonato clusters



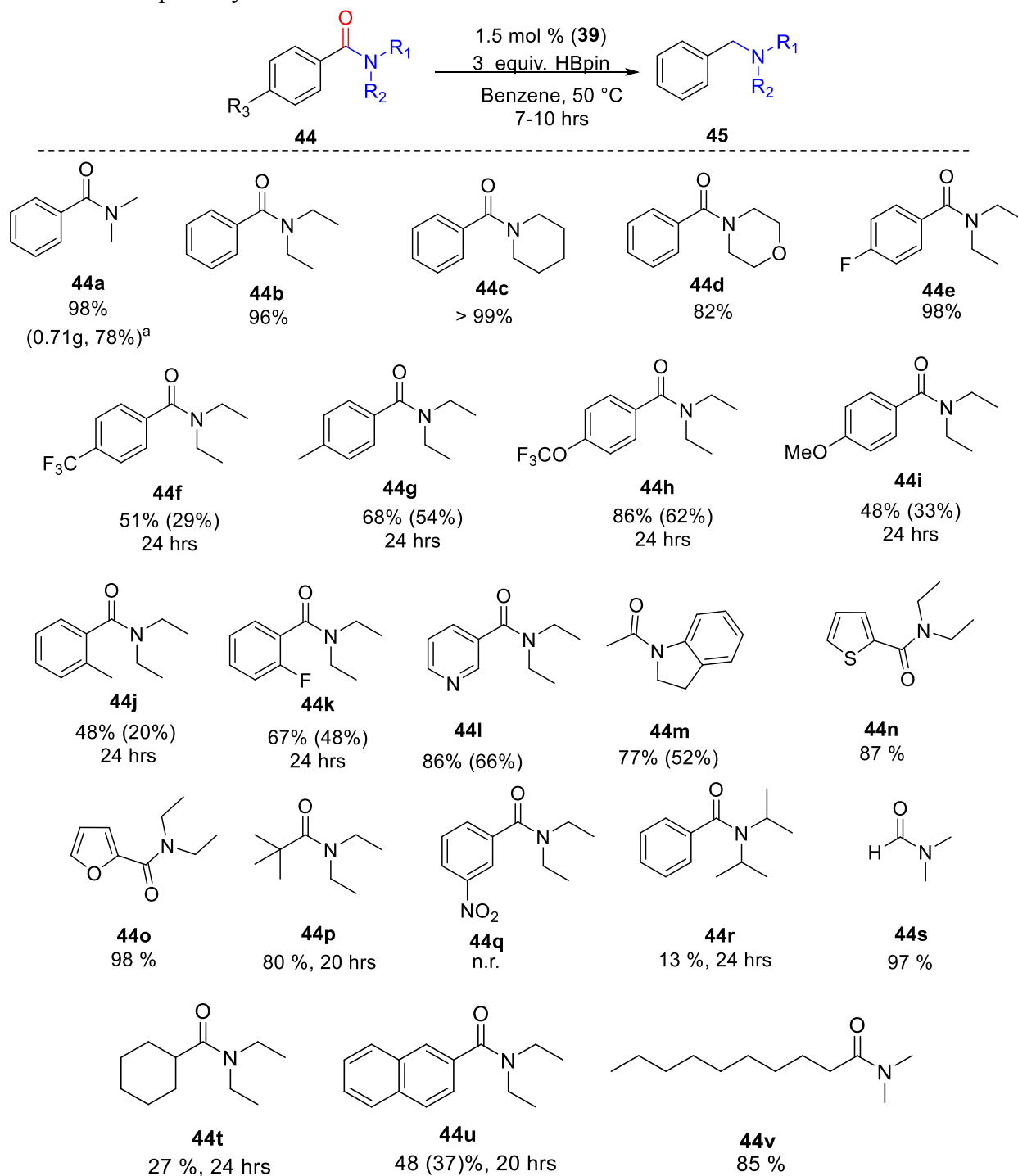
Entry	[Ln]	Yield (%)
1	La	95
2 ^a	Er	87
3	Eu	70
4	Gd	66
5	Y	84

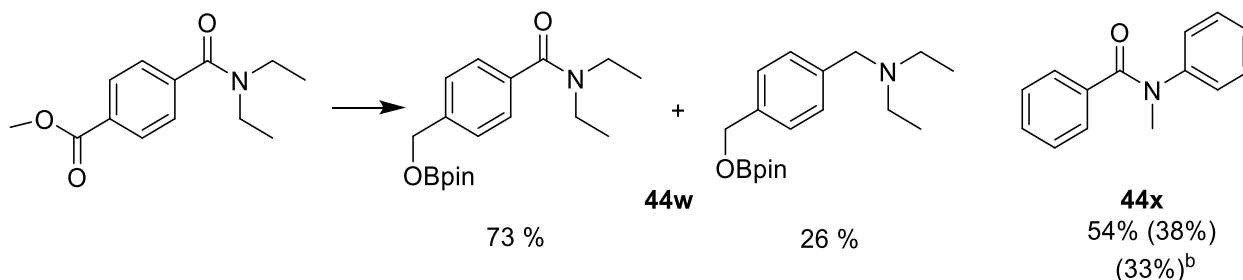
Yields based on ¹H NMR spectroscopy using tetraethylsilane as the internal standard; (a) Yield based on GC-MS.

We were excited to explore the scope of substrate amenable to our optimized conditions; a wide range of tertiary amides bearing a variety of functional groups and heteroatoms (**Table 2.4**) was tested. Good to excellent yields were observed for aliphatic amides (**44v**), and aromatic amides bearing electron-withdrawing substituents (**44e**, **44f**, and **44h**); moderate yields were obtained for those aromatic amides which incorporate electron-donating substituents (**44g**, **44i**). Longer reaction time was needed for aromatic amides, which bear ortho-substituents, presumably a result of unfavorable steric interactions (**44j**, **44k**). A mixture of products was observed for the substrate (**44w**), which bears an ester group, which is a reducible functional group. Upon increasing the amount of HBpin to 5 equiv., the ratio of the product formed changed to 85:15. This observation is not surprising as esters are, relatively, an easier functional group to reduce compared to amides. Significantly, substrates bearing N (**44l**), O (**44o**) and S (**44n**) heteroatoms were not only tolerated, but catalytic reactions proceeded in excellent yield. To our knowledge, this is the first such system in hydroboration catalysis that has tolerated a variety of heteroatoms. It should also be noted that the R groups on N play an important role as reactions tended to be sluggish when R₁ and R₂ =

isopropyl (**44r**), and evidence of competing C-N bond cleavage alongside deoxygenation was observed when $R_1 = \text{Ph}$, and $R_2 = \text{Me}$ (**44x**). GC-MS of the reaction mixture showed the formation of benzyl alcohol, and *N*-methylaniline alongside the deoxygenated product. This result proved rather interesting as it suggested that the selectivity for bond activation (C-O vs C-N) is tuned by *N*-substituent identity.

Table 2.4. Scope of hydroboration of amides

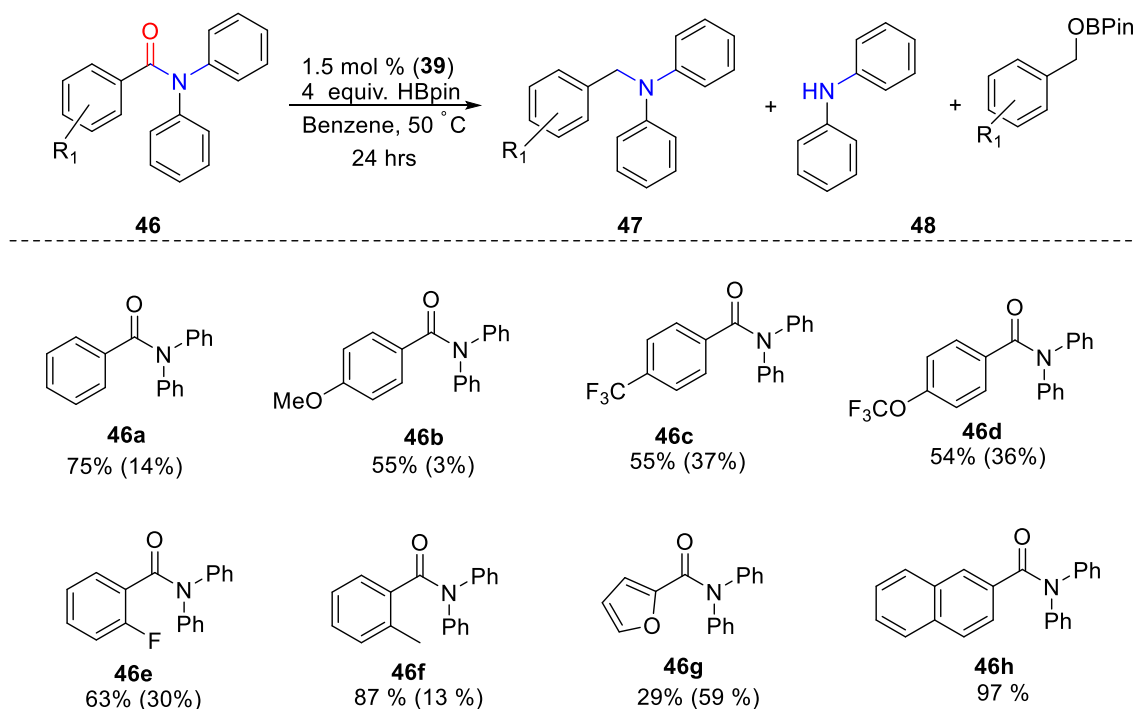




Yields determined by ¹H NMR using tetraethylsilane as the internal standard. Yields in parenthesis represents isolated yields after column chromatography; (a) 1g of **44a** was used, isolated yield in parenthesis; (b) Yield in parenthesis for **44x** represents benzyl alcohol which was formed via C-N bond activation.

We were intrigued by the observation of both C-N and C-O bond cleavage when *N*-methyl-*N*-phenyl benzamide (**44x**) was used as the substrate. This suggested that the mode of bond activation could be tuned by changing the identity of the *N*-substituents; the introduction of aromatic groups directly at nitrogen could be the key to switching selectivity (**Table 2.4**). Thus, we screened a number of *N,N*-diphenylbenzamide derivatives to probe this feature. We were pleased to observe that selectivity for C-N bond activation was observed when the R groups around nitrogen were substituted with phenyl groups (**Table 2.5**). The reaction was monitored by ¹H NMR and conversion to the desired products was further confirmed by GC-MS. In all substrates studied, a mixture of products (both **47** and **48**) were observed with the reaction favoring C-N activation except for **46g** whereby the deoxygenation product was favored more.

Table 2.5. Modulating bond activation by changing the R group



Yields determined by ¹H NMR using mesitylene as the internal standard; Yields in parenthesis represents the yield for deoxygenated products (obtained after C-O bond cleavage).

In a recent study, Bao and co-workers showed that binding of an electrophilic lanthanide center with aldehyde was favored over binding with HBpin.⁶⁸ Furthermore, it was also proposed that HBpin could attack the oxygen of the aryloxy ligand to form an intermediate which could undergo hydride migration to the electrophilic carbon of the carbonyl group of the aldehyde.⁶⁹ However, the current mechanistic understanding of catalytic reduction of amides via hydroboration remains limited. Sadow and co-workers proposed the formation of a formimidate species and revealed that the rate of addition of HBpin to the amide was fast and the C-O bond cleavage was the turnover-limiting step for the reduction of both tertiary and secondary amides.

In our effort to explain the reaction mechanism, preliminary kinetic analysis was performed for the hydroboration of *N,N*-dimethylbenzamide (**44a**). A plot of the initial rates for the formation of **45a** indicated that it was first order with respect to **39** until a catalyst loading of 3 mol %. It was observed that at higher loading (i.e., 4.5 mol % and 6 mol %), the initial rates were found to be lower. This could possibly arise due to formation of catalytically inactive lanthanide clusters, which occurs as the concentration of lanthanide is increased (**Figure 2.20**). Increasing the equivalence of HBpin from 1 to 3 equiv. showed that the catalytic activity and initial rates at higher catalyst loading was faster as expected compared to the initial rates for our optimized condition of 1.5 mol % catalyst and 3 equiv. HBpin. Subsequently, the formation of product was found to be independent of the substrate loading. The zero order for **39** suggests that the binding of the substrate to the lanthanum center is not rate-determining (**Figure 2.21**). Varying the [HBpin] revealed a first order dependence until 3 equivalents, after which it becomes zero order in [HBpin] (**Figure 2.22**). Stoichiometric reactions of **39** with **44a** showed shifts in ¹H NMR (**Figure 2.28**) suggesting an association of the substrate to the metal center to be part of the catalytic cycle.

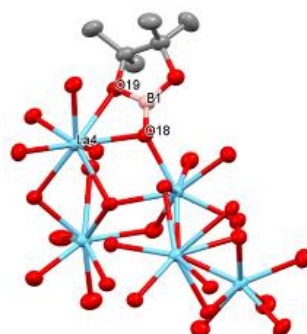


Figure 2.11. Reaction intermediate presumed to be catalytically inactive species **49**

An interesting lanthanum cluster (**49**) was characterized crystallography when equimolar amounts of **39** and HBpin were combined (**Figure 2.11**); ¹¹B NMR of the isolated species, (**49**), revealed three peaks at 21.53 ppm, 4.96 ppm and 4.43 ppm (**Figure 2.30**). The formation of a B-O bond was observed which is very similar to the intermediate for the hydroboration of aldehydes which was suggested by Bao and co-workers.⁶⁹ However, in our study, stoichiometric reaction of the isolated species with an equivalent of **44a** did not show the formation of product. Therefore, suggesting that this might be an “inactive” or off-cycle species; ¹¹B NMR showed an increase in

the intensity of peak at 21.53 ppm suggesting the formation of pinBOBpin (**Figure 2.30**). Further studies are ongoing in our group and will be reported in due time.

2.4. Conclusion

In conclusion, we have developed catalysts based on metals that are present in plentiful supply i.e iron and lanthanum. The products obtained after the hydroboration of alkenes are used as coupling partners for a well-studied Suzuki coupling whereas amines obtained by reduction of amides are synthons in some medicines and agricultural products. Preliminary mechanistic studies entailing plausible intermediates formed during the reaction and kinetics have also been reported. Future work will focus on detailed mechanistic studies to elucidate reaction pathways and expand more on further catalytic reactions based on iron and lanthanum based catalytic systems.

2.5. Experimental Section

2.5.1. General considerations

All reactions were performed in oven dried apparatus under an inert argon atmosphere unless indicated otherwise. All lanthanide salts were purchased from commercial vendors (Strem and Sigma Aldrich). The identity of the commercial salts were confirmed by single crystal X-ray diffraction. All alkenes were purchased from commercial vendors and were used without any purification or drying. All tertiary amides were synthesized according to reported procedures.⁷⁰⁻⁷³ THF was distilled using sodium and benzophenone and stored over activated molecular sieves (4 Å) prior to usage. DBPin was synthesized according to the reported procedure.⁷⁴ ¹H, ¹³C, ¹¹B spectra were recorded on a Jeol 400 MHz spectrometer at 300K unless otherwise noted. NMR Solvent (Benzene-d₆ and Toluene-d₈) were dried over activated molecular sieves prior to usage. ¹H NMR spectra were referenced to the solvent residual peak [(C₆D₆, δ 7.16 ppm), (CDCl₃, δ 7.26 ppm)], and ¹³C{¹H} NMR spectra were referenced to the solvent residual peak (C₆D₆, δ 128.06 ppm and CDCl₃, δ 77.16 ppm). Coupling constants *J* are reported in Hz. NMR multiplicities are as follows: s = singlet, d = doublet, t = triplet, m = multiplet, br,s = broad singlet.

2.5.2. General procedure for hydroboration of terminal alkenes

To an oven-dried vial a stir bar, [BIAN]Fe(η⁶-toluene) (**M1**) (3.24 mg, 0.005 mmol), NaOtBu (4.8 mg, 0.05 mmol), styrene (52 mg, 57 μL, 0.5 mmol) and HBpin (96 mg, 108 μL, 0.75 mmol) were added and the reaction mixture was stirred at 70 °C for 24 hrs. The reaction was quenched by addition of water (5 mL) and ether (1 mL). The organic layer was separated, and the solvent was removed under reduced pressure. The crude NMR yield was determined using mesitylene as an internal standard. For those reactions in which products were isolated, the reaction was scaled to 1 mmol and the crude product was purified using flash column chromatography with silica as a stationary phase and hexanes/ethyl acetate (98/2) as the eluent.

2.5.3. General procedure for synthesis of [BIAN]Fe-Styrene complex (**M5**)

In a glove box, an oven dried schlenk flask was charged with mercury (5.5 g, 27.51 mmol) and anhydrous pentane (5 mL). Sodium (27.5 mg, 1.195 mmol) was cut into small pieces which were added to the flask (the flask contents warmed). The mixture was stirred for 30 min and then [BIAN]FeCl₂ (150 mg, 0.239 mmol), styrene (24.9 mg, 27.47 μL, 0.239 mmol) and more anhydrous pentane (10 mL) were added. The colour of the mixture gradually changed from green to reddish-brown. The mixture was stirred for 48hrs and the reaction mixture was decanted away from the amalgam and filtered through a pad of celite. The solvent was removed under vacuum, [BIAN]Fe(C₈H₈) was isolated as a reddish brown solid, (76 mg, 48 % yield).

2.5.4. Kinetic isotope effect experiment for hydroboration of styrene

An oven dried scintillation vial was charged with [BIAN]Fe(η^6 -toluene) (6.48mg, 0.01 mmol), NaO*t*Bu (9.6 mg, 0.1 mmol), styrene (104mg, 114 μ L, 1 mmol). HBpin (64 mg, 72.5 μ L, 0.5 mmol) and DBpin (515 μ L, 0.5 mmol, 0.97 M in THF) was added. The mixture was stirred for 24 hrs. The reaction was quenched by cooling to room temperature and adding diethyl ether. The reaction mixture was filtered over celite and a sample taken for GC-MS analysis.

2.5.5. General procedure for the formation of lanthanum polyoxometalate (POM)

A scintillation vial (20 mL) was charged with Ln(acac)₃·nH₂O. The sample was then put under vacuo at 100 °C for 12 hrs, and then transferred into the glove box. Single crystals of the polynuclear lanthanide diketonato clusters were grown by slow evaporation of pentane. (*It should be noted that the clusters have enhanced solubility in non-polar solvents such as hexane, pentane).

2.5.6. General procedure for deoxygenation of 3° amides

An oven dried J-young tube was charged with **39** (11.72 mg, 0.0075 mmol), *N,N*-dimethylbenzamide (75 mg, 0.5 mmol), HBpin (192 mg, 218 μ L, 1.5 mmol), tetraethylsilane as internal standard (15.22 mg, 20 μ L, 0.105 mmol) and benzene-*d*₆ (0.7 ml). The reaction mixture was then placed on a preheated oil bath at 50 °C. The progress of the reaction was monitored by ¹H NMR, and ¹H NMR yield was determined based on the internal standard, tetraethylsilane. In all cases, the product peaks were integrated with respect to the -CH₂- peak of the internal standard which was normalized to 1.

For substrates (**44f**, **44g**, **44h**, **44i**, **44j**, **44k**, **44l**, **44m**, **44u**, **44x**) where assignment of peaks was difficult, isolation of the pure product from the crude reaction mixture was performed. For the isolation of deoxygenated products, the reactions were performed using 1 mmol of 3° amides. The crude product was purified by flash column chromatography using basic alumina as a stationary phase and hexanes / ethyl acetate (98/2) as eluent to afford desired products (3° amines). For substrate **44w**, the product was isolated using flash column chromatography using silica as stationary phase and hexanes / ethyl acetate (50 / 50) with 1% triethylamine as eluent to afford the product **45w**. The ¹H and ¹³C NMRs of the isolated tertiary amines are reported in CDCl₃.

2.5.7. Gram scale reaction for hydroboration of 3° amide

An oven dried 20mL scintillation vial was charged with **39** (157.05 mg, 0.101 mmol), *N,N*-dimethylbenzamide (1.0g, 6.70 mmol), HBpin (2.57 g, 2.92 mL, 20.1 mmol), anhydrous benzene (2 ml), and a stir bar. The reaction mixture was then placed on a preheated oil bath at 50 °C. After 24 hrs of heating, the reaction was quenched by opening the reaction mixture to air. The solvent was then removed under vacuo and the crude product was purified by flash column chromatography over basic alumina using hexane/ ethyl acetate (98: 2) as the eluent to afford the desired deoxygenated product. Isolated yield = 706 mg (78 %).

2.5.8. General procedure for C-N bond activation reactions

An oven dried scintillation vial (20 mL) was charged with **39** (11.72 mg, 0.0075 mmol), *N,N*-diphenylbenzamide (136.67 mg, 0.5 mmol), HBpin (256 mg, 290 μ L, 2.0 mmol), anhydrous benzene (1 mL) and a stir bar. The reaction mixture was then placed on a preheated oil bath at 50 °C for 24 hrs. The reaction was quenched by opening the reaction mixture to air and the solvent was evaporated. The ¹H NMR of the crude reaction mixture was taken in CDCl₃ using mesitylene (17.28 mg, 20 μ L) as the internal standard. The peaks in the aromatic region are not assigned because of the overlap of the peaks of diphenylamine, borylated alcohol and deoxygenated product formed after the reaction. The yields were calculated based on the CH₂ of borylated alcohol formed

after the C-N bond cleavage and amine formed after deoxygenation of the amide using ^1H NMR. To further confirm the product formation, GC-MS was used after working up the reaction with 2 M NaOH (10 mL).

Kinetics data

Kinetic analysis of the NMR scale reactions was carried out by collecting multiple data points at intervals till the substrate concentrations were depleted. The temperature was ramped up stepwise, from R.T. to 35 °C (held for 3 minutes at 35 °C), and then increased from 35 °C to 50 °C, and held for 5 minutes before locking and shimming. The first reading at 50 °C was taken as 0 mins. Each data was taken at 10 minutes intervals and the reaction was monitored by ^1H NMR (400 MHz, C_6D_6) for 7 hrs at 50 °C (VT NMR). The kinetic data were obtained from the intensity increase of the $-\text{CH}_2-$ (s, 2H, $\delta = 3.24$ ppm) integral of *N,N*-dimethyl-1-phenylmethanamine (**45a**) relative to the internal standard (tetraethylsilane). K_{max} was determined by taking the maximum rate of reaction.⁷⁵

2.5.9. General procedure for kinetic studies

An oven dried J-young tube was charged with **39** (5.45 mg, 0.0125 mmol), *N,N*-dimethylbenzamide (37.29 mg, 0.25 mmol) and 0.7 mL of benzene- d_6 . HBpin (0.25 mmol, 31.99mg, 36.27 μL) and tetraethylsilane as Internal standard (20 μL) were then added. The reaction mixture was then analyzed by ^1H NMR at 50 °C. The temperature was ramped up stepwise, from R.T. to 35 °C (held for 3 minutes at 35 °C), and then increased from 35 °C to 50 °C, and held for 5 minutes before locking and shimming. The first reading at 50 °C was taken as 0 minutes. Each data was taken at 10 minutes intervals for 7 hrs.

2.6. Appendix

Kinetic Isotope effect experiment for hydroboration of styrene

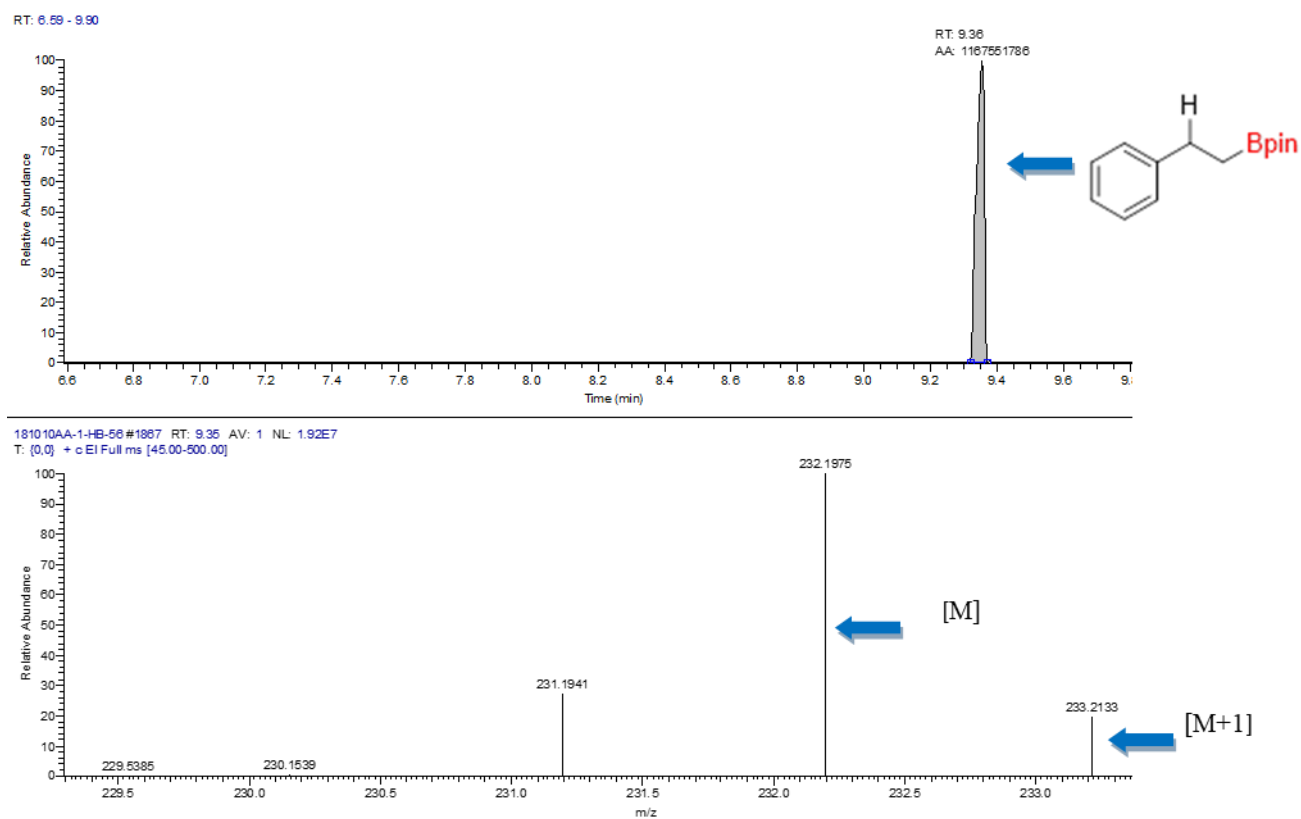
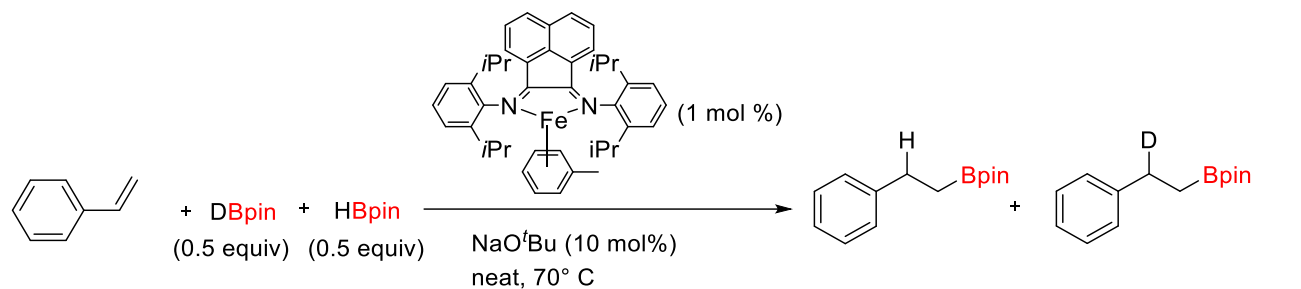


Figure 2.12. Top diagram shows the GC-Mass of ion mass of alkyl boronate, as a function of time. Bottom diagram is mass spectrum taken at RT = 9.36 min.

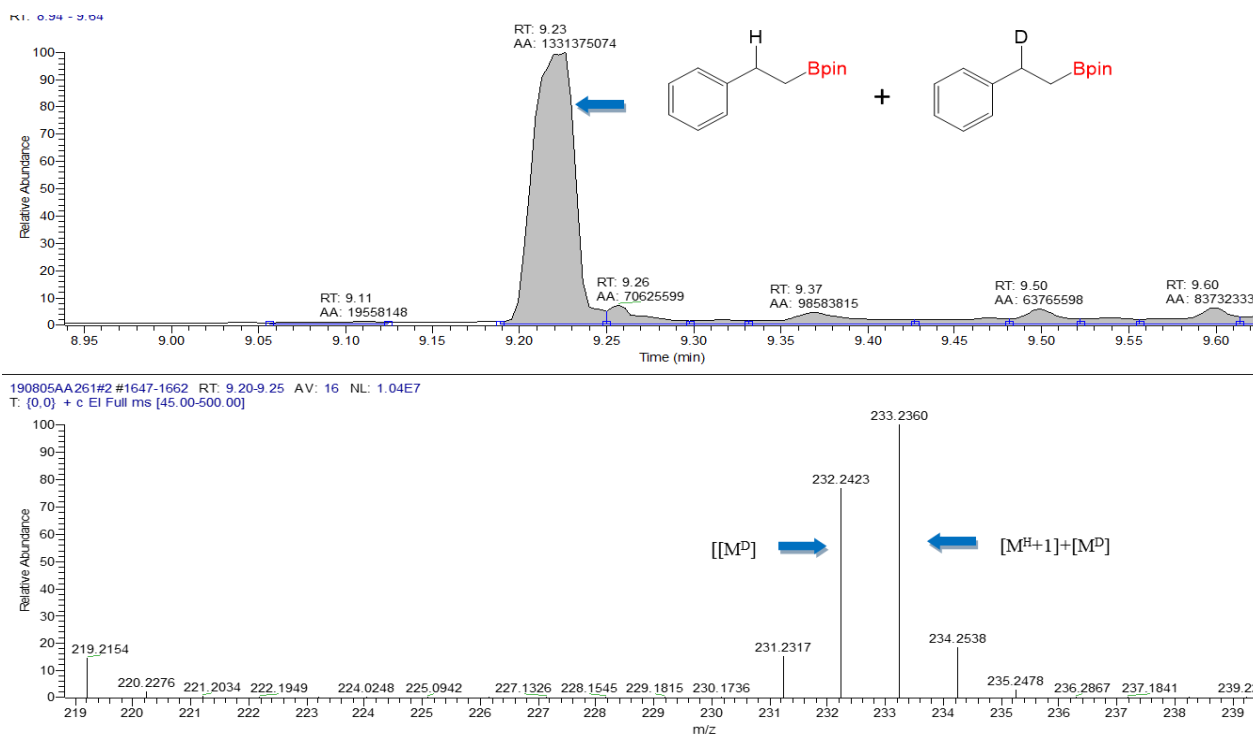


Figure 2.13. The GC-Mass of reaction mixture. Top diagram shows ion mass of product as a function of time. Bottom diagram is mass spectrum taken at RT = 9.23 min.

As can be seen from the GC-Mass of alkyl boronate, the relative abundance for $[M+1]$ is 20% (**Fig 2.12**). The GC-Mass for the product of KIE experiment shows $[M]:[M+1] = 66:100$ or can be written as 100:151. 151 % is the percentage for $[M^H+1]+[M^D]$ (**Fig 2.13**). Therefore, if we expected the same relative abundance for $[M^H+1]$ of hydroborated product as for the starting material, we can attribute 20% to $[M^H+1]$ and 131% to $[M^D]$ (Deuterated product). With these results in hand, the ratio of nondeuterated product to deuterated product is equal to $1/1.31 = 0.76$, showing an inverse kinetic isotope effect

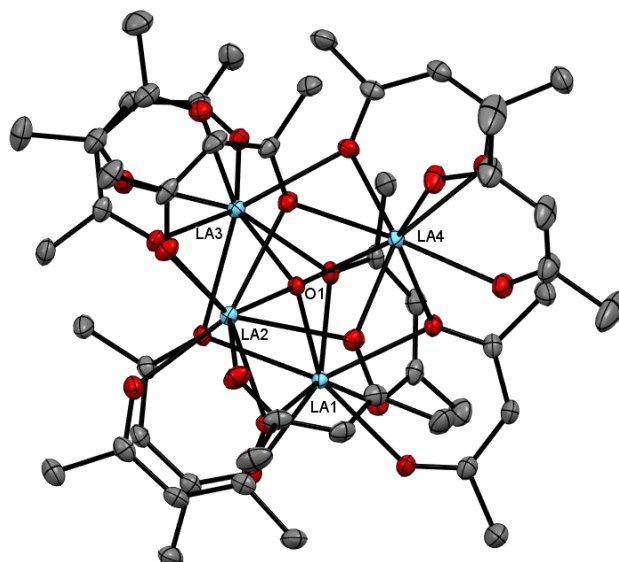


Figure 2.14. Crystal data and structure refinement for [La] (39).

The thermal ellipsoids are represented at 50% probability. Carbon, hydrogen, oxygen, and lanthanum atoms are represented by gray, white, red, and light blue ellipsoids, respectively. Hydrogen atoms were omitted for clarity.

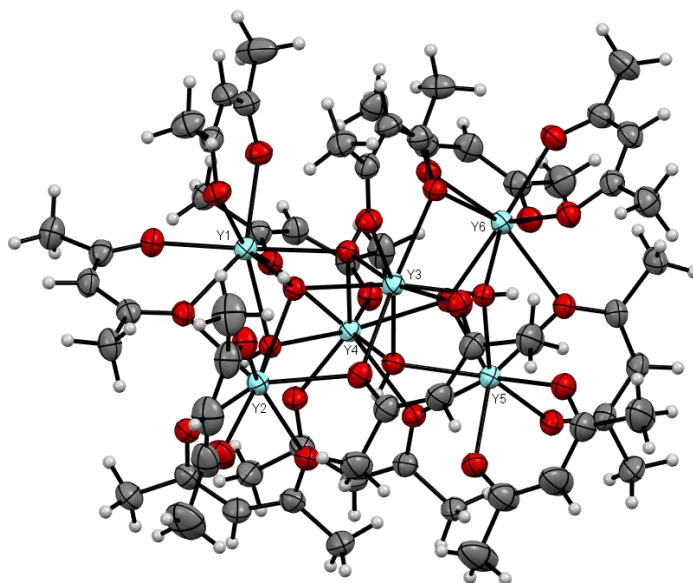


Figure 2.15. Crystal data and structure refinement for [Y] (40).

The thermal ellipsoids are represented at 50% probability. Carbon, hydrogen, oxygen, and yttrium atoms are represented by gray, white, red and light blue ellipsoids, respectively.

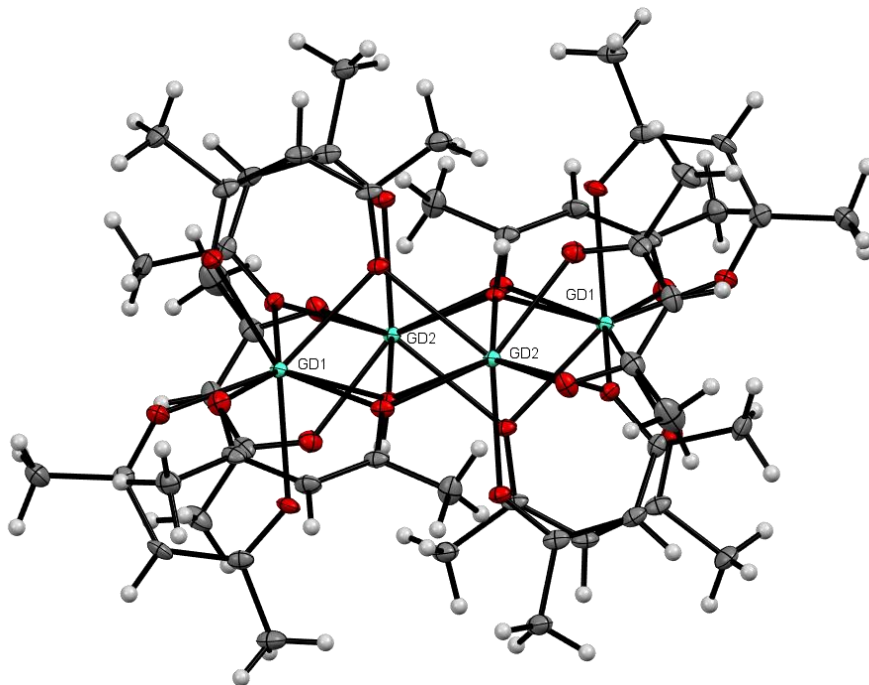


Figure 2.16. Crystal data and structure refinement for [Gd] (41).

The thermal ellipsoids are represented at 50% probability. Carbon, hydrogen, oxygen, and gadolinium atoms are represented by gray, white, red and aquamarine ellipsoids, respectively.

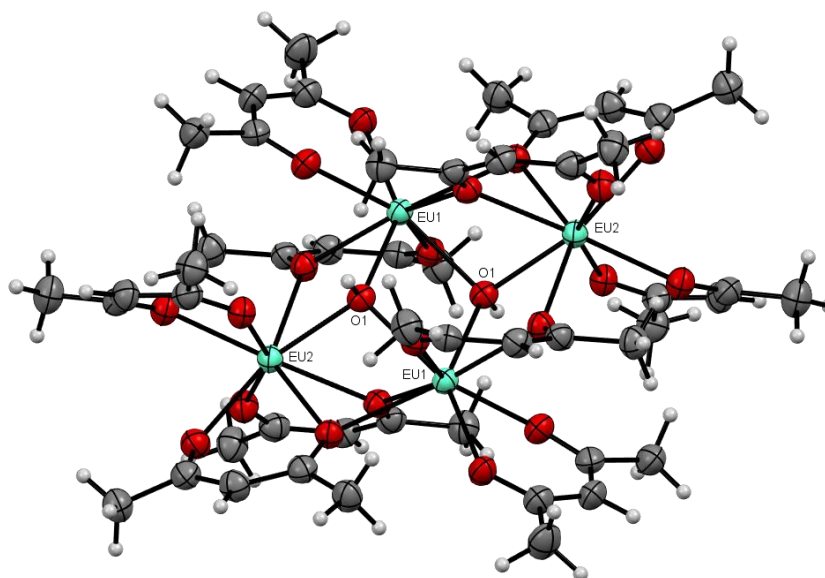


Figure 2.17. Crystal data and structure refinement for [Eu] (42).

The thermal ellipsoids are represented at 50% probability. Carbon, hydrogen, oxygen, and europium atoms are represented by gray, white, red and light tan ellipsoids, respectively.

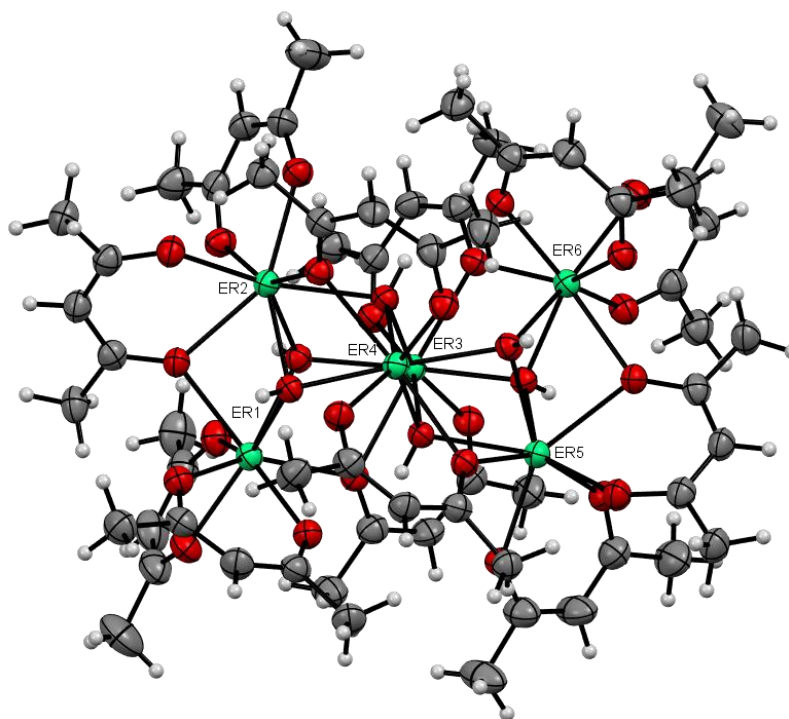


Figure 2.18. Crystal data and structure refinement for [Er] (**43**).

The thermal ellipsoids are represented at 50% probability. Carbon, hydrogen, oxygen, and erbium atoms are represented by gray, white, red and light green ellipsoids, respectively. The interstitial pentane molecule was omitted for clarity.

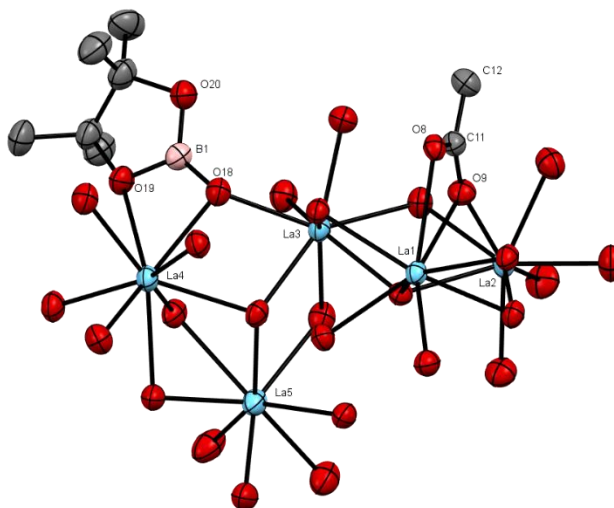


Figure 2.19. Crystal data and structure refinement for (**49**).

The thermal ellipsoids are represented at 50% probability. Carbon, hydrogen, oxygen, boron and lanthanum atoms are represented by gray, white, red, light pink and light blue ellipsoids, respectively. The interstitial pentane molecule, carbon and hydrogen atoms around the La center were omitted for clarity.

[Catalyst] rate order assessment

Varying concentration of Catalyst while keeping HBpin and Substrate constant

$C_{\text{substrate}}$ [M]	C_{HBpin} [M]	C_{cat} [M]	k_{max} (M/min)	R^2
0.33	0.33	0.0033	0.0852	0.9976
0.33	0.33	0.0099	0.156	0.9938
0.33	0.33	0.0165	0.1894	0.9928
0.33	0.33	0.033	0.2884	0.9891
0.33	0.33	0.0495	0.2064	0.9844
0.33	0.33	0.066	0.150	0.9766

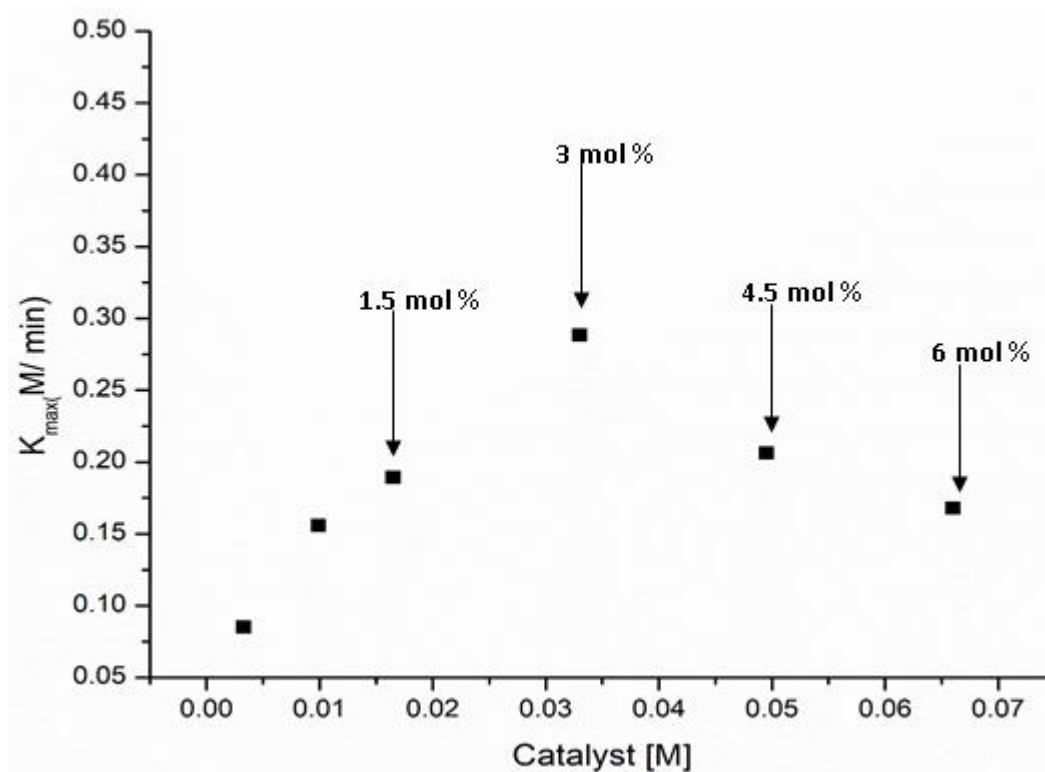


Figure 2.20. Plot of [Catalyst] Vs. reaction rate (K_{max}), the reaction follows 1st order till 3 mol % catalyst loading.

[Substrate] rate order assessment

Varying concentration of Substrate while keeping Catalyst and HBpin constant.

C_{HBpin} [M]	C_{cat} [M]	$C_{\text{substrate}}$ [M]	k_{max} (M/min)	R^2
0.33	0.0165	0.33	0.1894	0.9928
0.33	0.0165	0.66	0.1924	0.994
0.33	0.0165	0.99	0.238	0.9931
0.33	0.0165	1.32	0.168	1

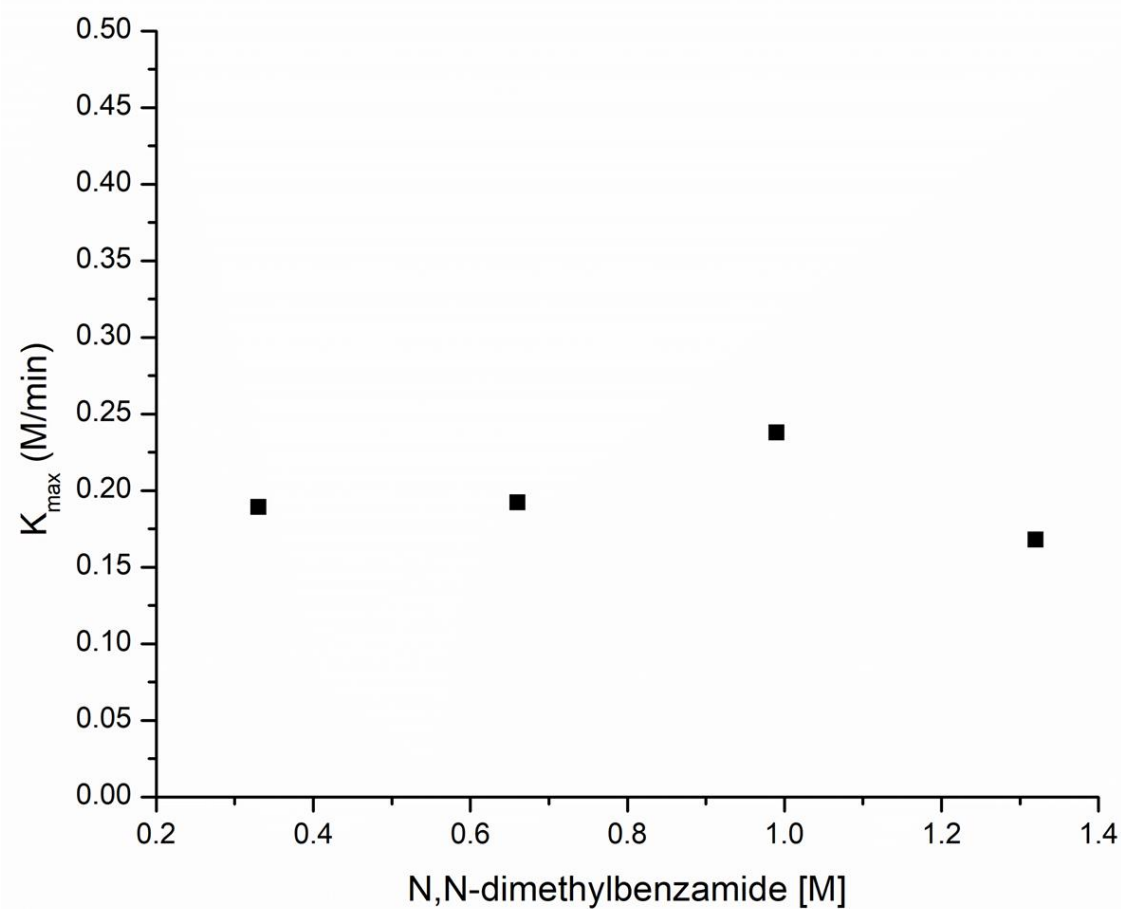


Figure 2.21. Plot of [Substrate] Vs. reaction rate (K_{max}), the reaction follows 0th order dependence on the substrate.

[HBpin] rate order assessment

Varying concentration of HBpin while keeping Catalyst and Substrate constant

C_{cat} [M]	$C_{\text{substrate}}$ [M]	C_{HBpin} [M]	k_{max} (M/min)	R^2
0.0165	0.33	0.33	0.1894	0.9928
0.0165	0.33	0.66	0.4928	0.992
0.0165	0.33	0.99	0.5375	0.9942
0.0165	0.33	1.32	0.52	0.9905
0.0165	0.33	1.65	0.528	0.9925

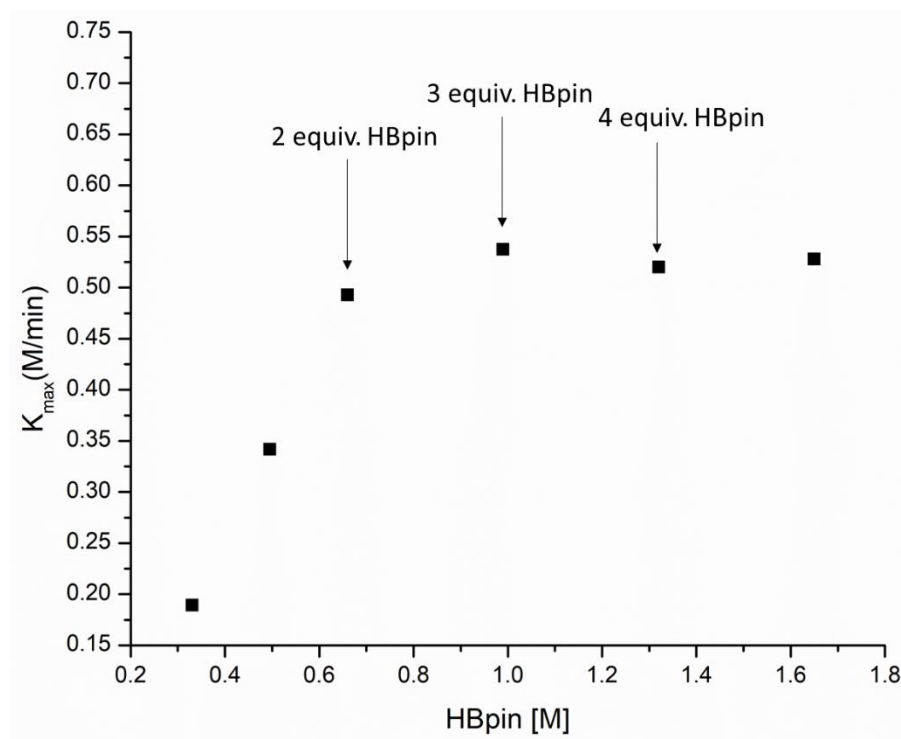


Figure 2.22. Plot of [HBpin] Vs. reaction rate (K_{max}), the reaction follows 1st order dependence on HBpin till 2 equiv. [HBpin], and then 0th order at higher concentration.

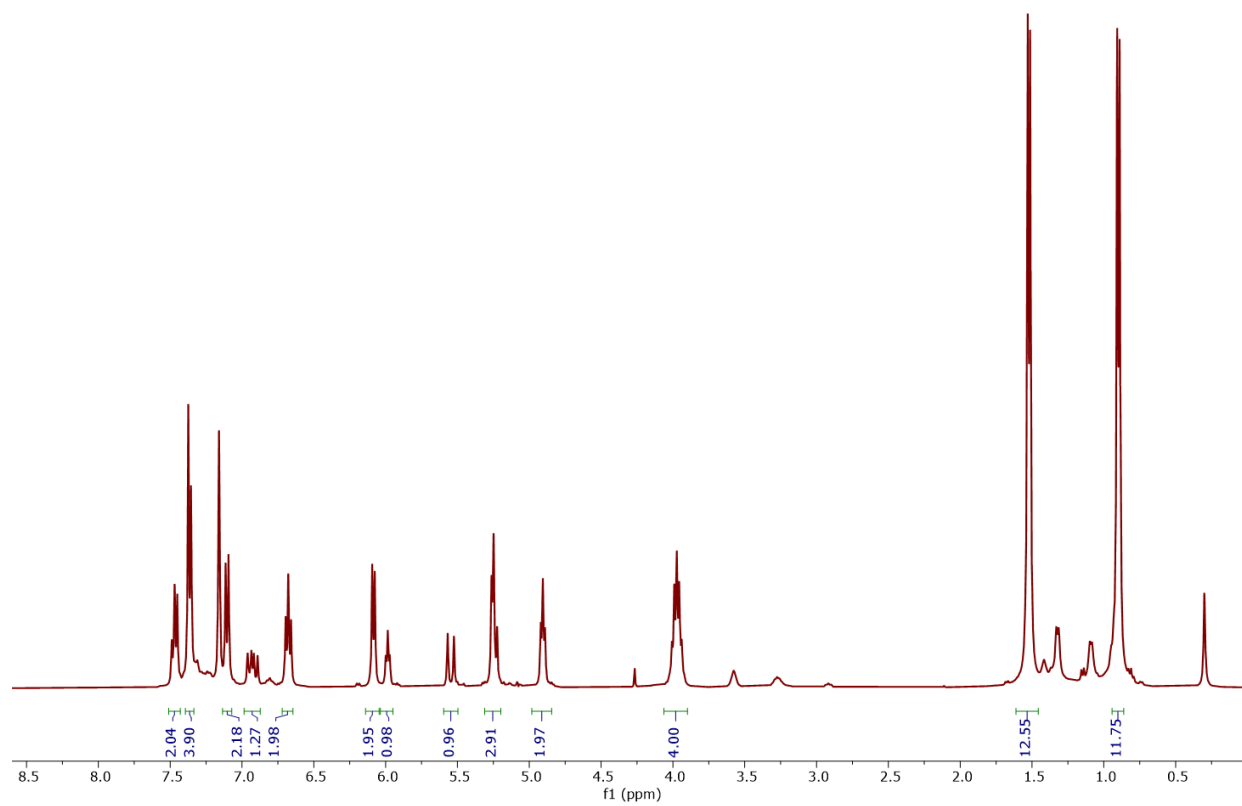


Figure 2.23. ^1H NMR of [BIAN]Fe-Styrene complex (M5).

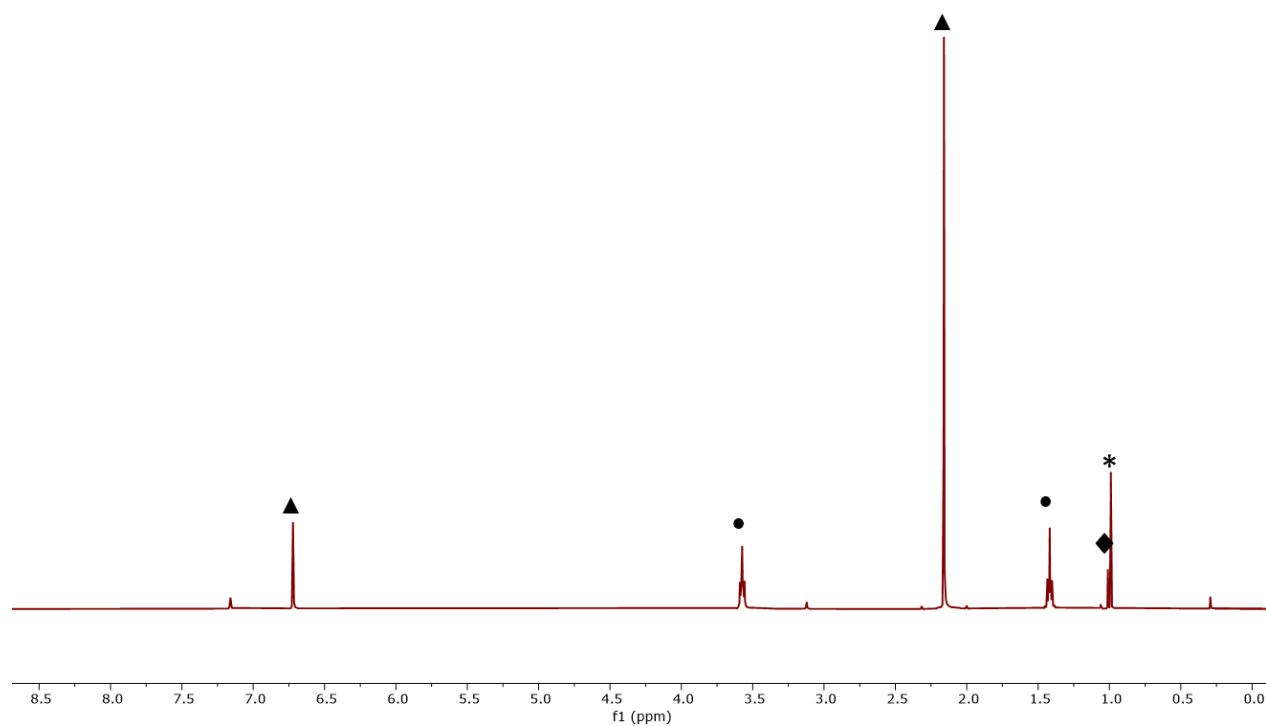


Figure 2.24. ^1H NMR of DBpin, * represents product, (▲) represents mesitylene, (●) represents THF and (◆) represents pinacol

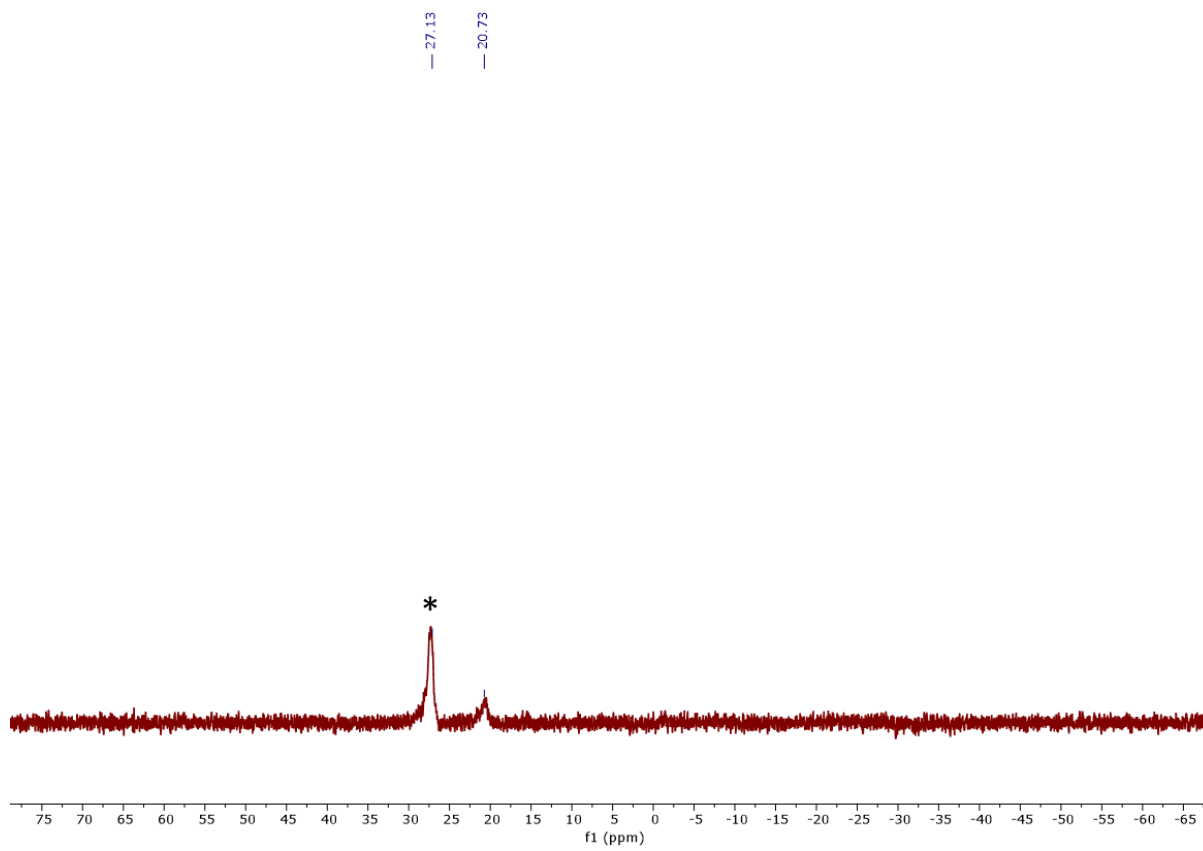


Figure 2.25. ^{11}B NMR of DBpin

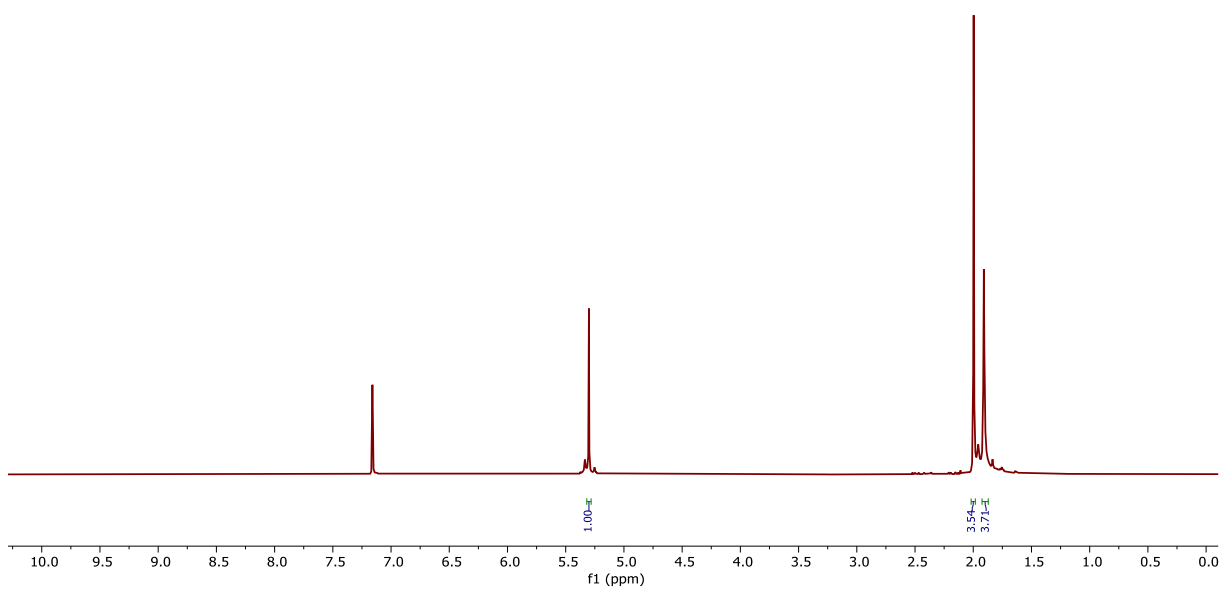


Figure 2.26. ^1H NMR of **39**

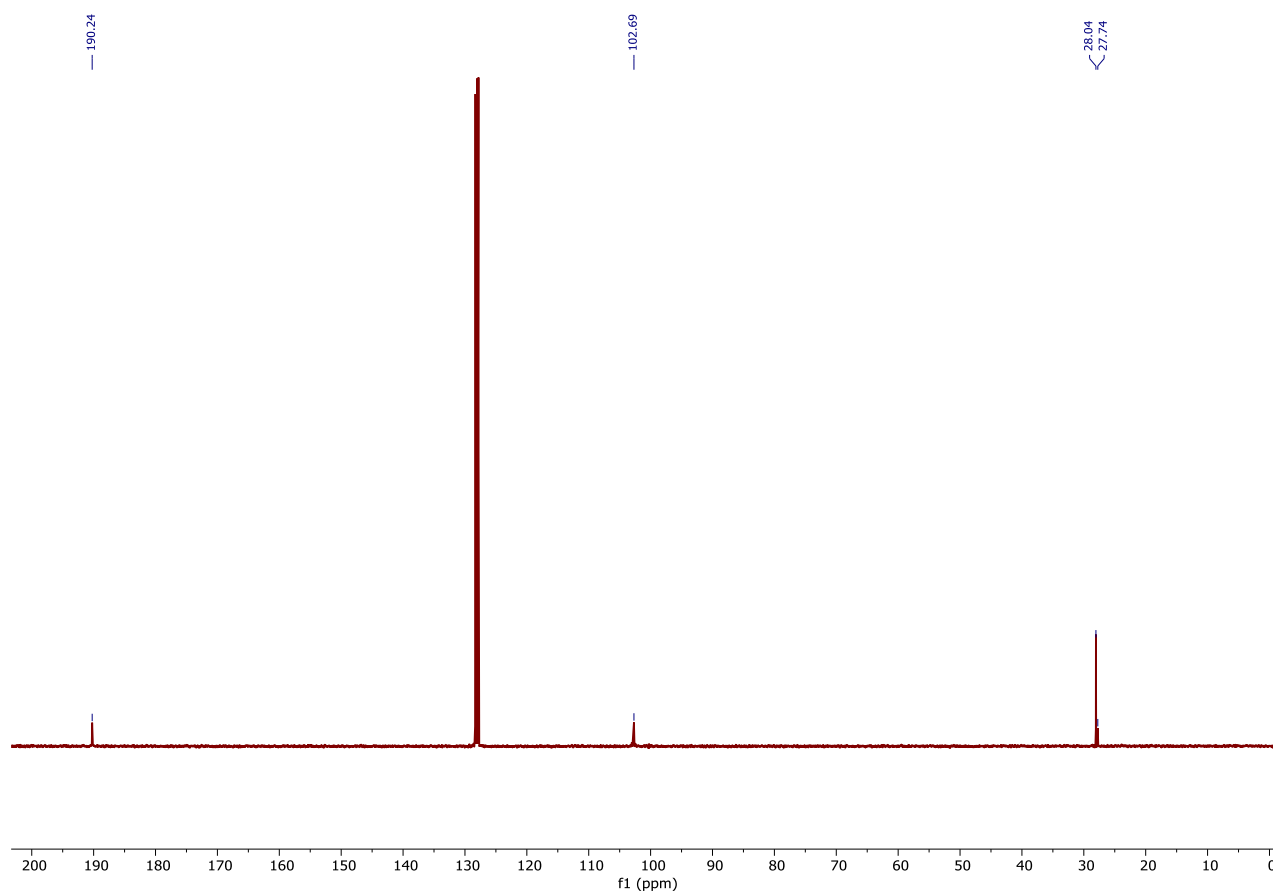


Figure 2.27. ^{13}C NMR of **39**

Stoichiometric reactions

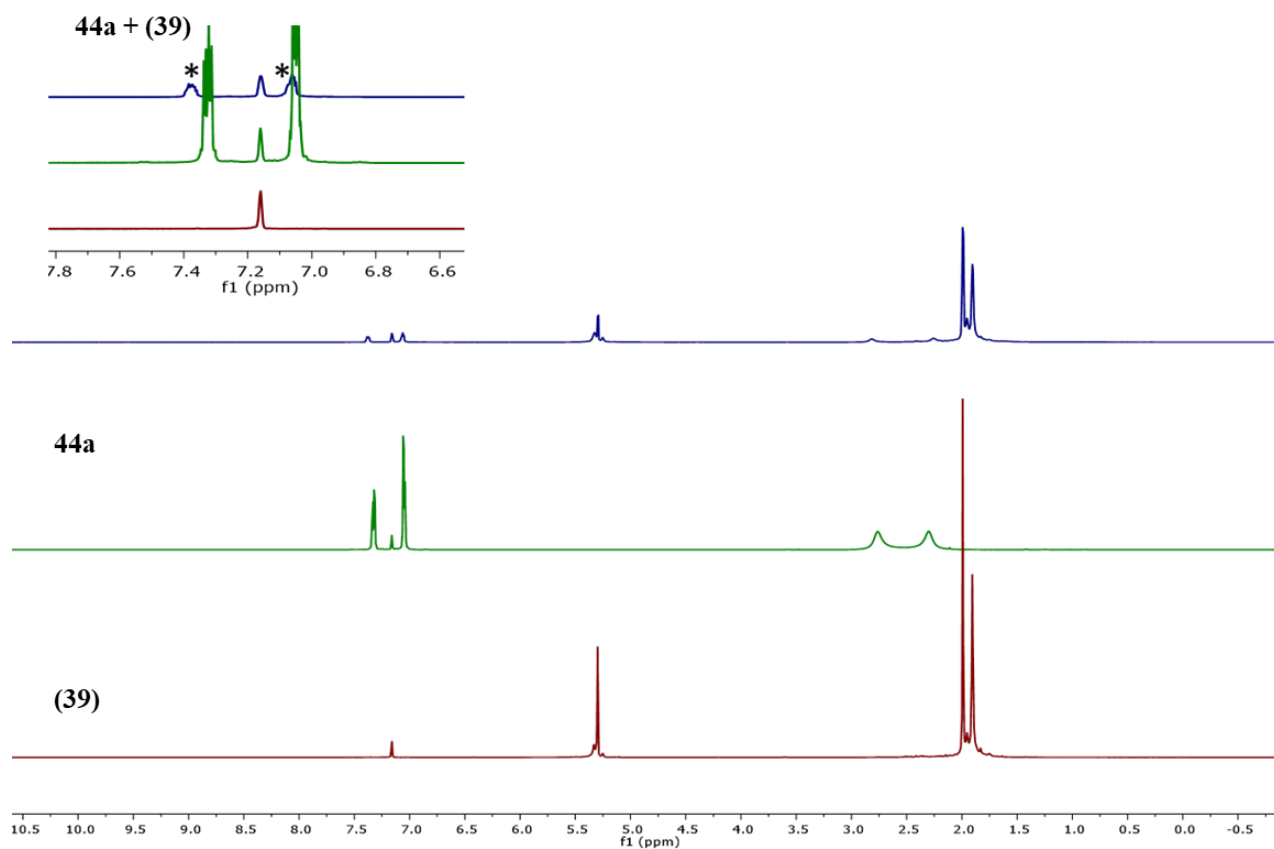


Figure 2.28. ^1H NMR of stoichiometric reaction. (Top): ^1H NMR of **39** + **44a** heated at 50 °C for 1hr; (Middle): ^1H NMR of **44a**; (Bottom): ^1H NMR of **39**. The (*) in the inset shows the shifts in the peak of **44a** after heating with **39**.

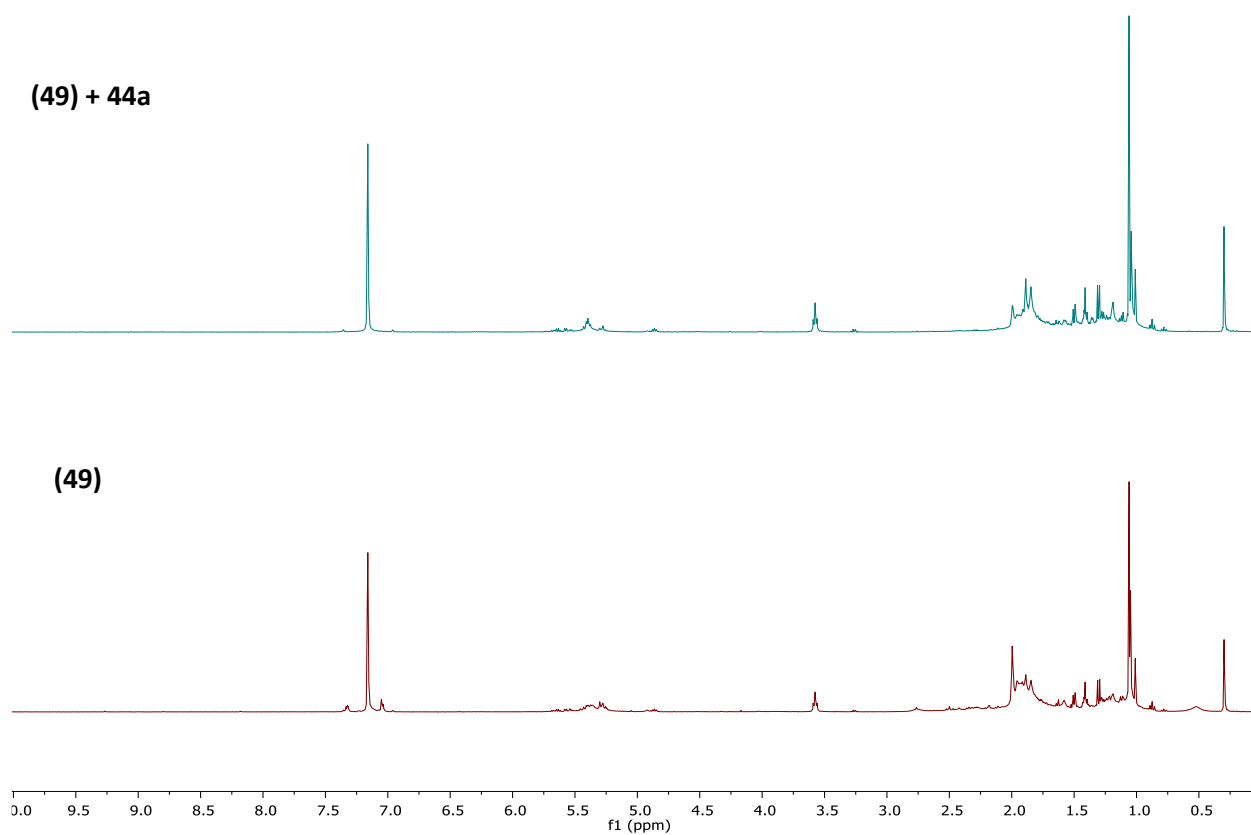


Figure 2.29. ^1H NMR of stoichiometric reaction. (**Top**): ^1H NMR after heating (49) + 44a at 50°C for 2 hrs; (**Bottom**): ^1H NMR of (49).

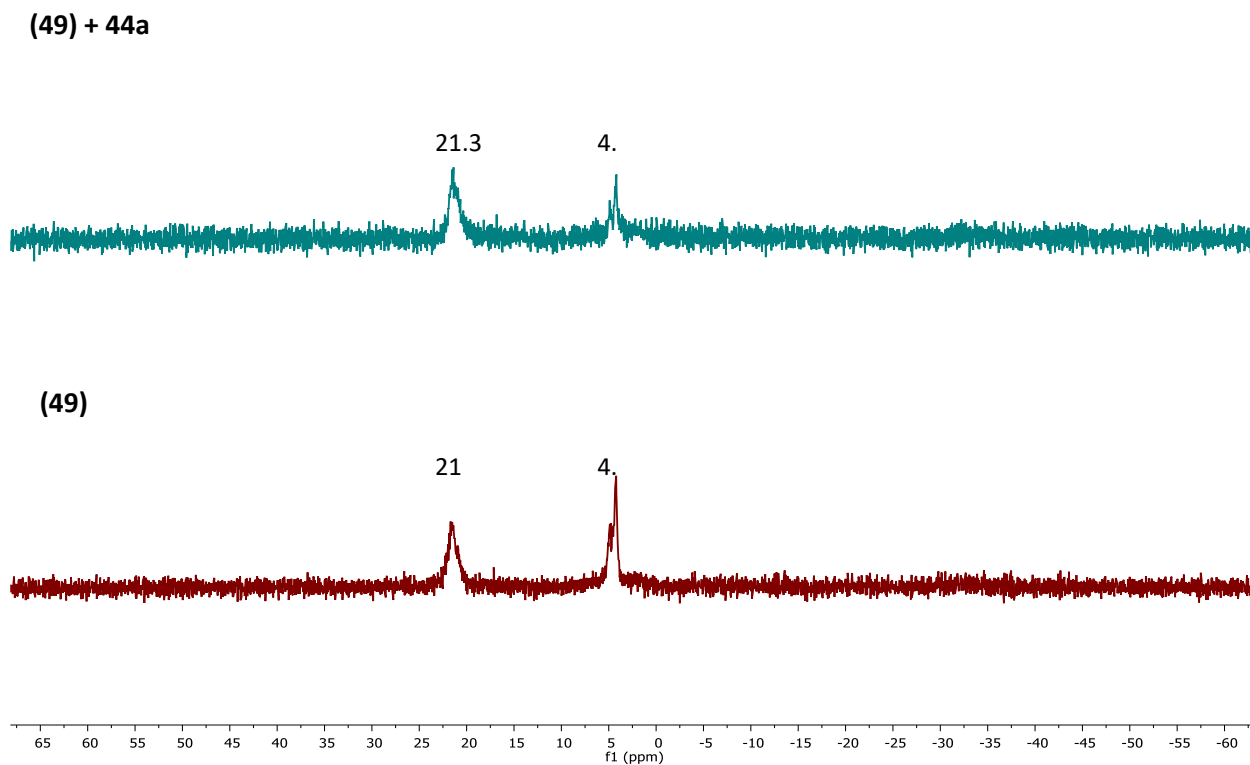


Figure 2.30. ^{11}B NMR of stoichiometric reaction. (**Top**): ^{11}B NMR after heating **(49)** + **44a** at 50°C for 2 hrs; (**Bottom**): ^{11}B NMR of **(49)**

2.7. References

1. Singh, A.; Shafiei-Haghighi, S.; Smith, C. R.; Unruh, D. K.; Findlater, M., Hydroboration of Alkenes and Alkynes Employing Earth-Abundant Metal Catalysts. *Asian Journal of Organic Chemistry* 2020, 9 (3), 416-420.
2. Tamang, S. R.; Singh, A.; Bedi, D.; Bazkiaei, A. R.; Warner, A. A.; Glogau, K.; McDonald, C.; Unruh, D. K.; Findlater, M., Polynuclear lanthanide–diketonato clusters for the catalytic hydroboration of carboxamides and esters. *Nature Catalysis* 2020, 3 (2), 154-162.
3. Crockett, M. P.; Tyrol, C. C.; Wong, A. S.; Li, B.; Byers, J. A., Iron-Catalyzed Suzuki–Miyaura Cross-Coupling Reactions between Alkyl Halides and Unactivated Arylboronic Esters. *Organic Letters* 2018, 20 (17), 5233-5237.
4. Hartwig, J. F., Borylation and silylation of C–H bonds: a platform for diverse C–H bond functionalizations. *Accounts of Chemical Research* 2012, 45 (6), 864-873.
5. Sato, M.; Miyaura, N.; Suzuki, A., Cross-coupling reaction of alkyl- or arylboronic acid esters with organic halides induced by thallium (I) salts and palladium-catalyst. *Chemistry Letters* 1989, 18 (8), 1405-1408.
6. Brown, H. C.; Chen, J., Hydroboration. 57. Hydroboration with 9-borabicyclo [3.3. 1] nonane of alkenes containing representative functional groups. *The Journal of Organic Chemistry* 1981, 46 (20), 3978-3988.
7. Brown, H. C.; Rao, B. S., A New Powerful Reducing Agent—Sodium Borohydride in the Presence of Aluminum Chloride and Other Polyvalent Metal Halides^{1, 2}. *Journal of the American Chemical Society* 1956, 78 (11), 2582-2588.
8. Brown, H. C.; Rao, B. S., Hydroboration. I. The reaction of olefins with sodium borohydride-aluminum chloride. A convenient route to organoboranes and the anti-Markownikoff hydration of olefins. *Journal of the American Chemical Society* 1959, 81 (24), 6423-6428.
9. Yamamoto, Y.; Fujikawa, R.; Umemoto, T.; Miyaura, N., Iridium-catalyzed hydroboration of alkenes with pinacolborane. *Tetrahedron* 2004, 60 (47), 10695-10700.
10. Crudden, C. M.; Hleba, Y. B.; Chen, A. C., Regio- and enantiocontrol in the room-temperature hydroboration of vinyl arenes with pinacol borane. *Journal of the American Chemical Society* 2004, 126 (30), 9200-9201.
11. Juliette, J. J.; Rutherford, D.; Horváth, I. T.; Gladysz, J., Transition metal catalysis in fluorous media: practical application of a new immobilization principle to rhodium-catalyzed hydroborations of alkenes and alkynes. *Journal of the American Chemical Society* 1999, 121 (12), 2696-2704.
12. Caballero, A.; Sabo-Etienne, S., Ruthenium-catalyzed hydroboration and dehydrogenative borylation of linear and cyclic alkenes with pinacolborane. *Organometallics* 2007, 26 (5), 1191-1195.
13. Gunanathan, C.; Hölscher, M.; Pan, F.; Leitner, W., Ruthenium catalyzed hydroboration of terminal alkynes to Z-vinylboronates. *Journal of the American Chemical Society* 2012, 134 (35), 14349-14352.
14. Huang, J.; Yan, W.; Tan, C.; Wu, W.; Jiang, H., Palladium-catalyzed regioselective hydroboration of aryl alkenes with B₂pin₂. *Chemical Communications* 2018, 54 (14), 1770-1773.
15. Bismuto, A.; Thomas, S. P.; Cowley, M. J., Aluminum Hydride Catalyzed Hydroboration of Alkynes. *Angewandte Chemie International Edition* 2016, 55 (49), 15356-15359.
16. Greenhalgh, M. D.; Jones, A. S.; Thomas, S. P., Iron-catalysed hydrofunctionalisation of alkenes and alkynes. *ChemCatChem* 2015, 7 (2), 190-222.
17. Lyaskovskyy, V.; de Bruin, B., Redox non-innocent ligands: versatile new tools to control catalytic reactions. *Acs Catalysis* 2012, 2 (2), 270-279.

18. Frühauf, H. W.; Landers, A.; Goddard, R.; Krüger, C., New Compounds from 1, 4-Diaza-1, 3-dienes and Iron Carbonyls: Hexacarbonyl (1, 4-diazadiene) diiron and Substituted 2 (3H)-Imidazolones. *Angewandte Chemie International Edition in English* 1978, *17* (1), 64-65.
19. Small, B. L.; Brookhart, M.; Bennett, A. M., Highly active iron and cobalt catalysts for the polymerization of ethylene. *Journal of the American Chemical Society* 1998, *120* (16), 4049-4050.
20. Bart, S. C.; Chłopek, K.; Bill, E.; Bouwkamp, M. W.; Lobkovsky, E.; Neese, F.; Wieghardt, K.; Chirik, P. J., Electronic structure of bis (imino) pyridine iron dichloride, monochloride, and neutral ligand complexes: a combined structural, spectroscopic, and computational study. *Journal of the American Chemical Society* 2006, *128* (42), 13901-13912.
21. Rosa, V.; Carabineiro, S. A.; Avilés, T.; Gomes, P. T.; Welter, R.; Campos, J. M.; Ribeiro, M. R., Synthesis, characterisation and solid state structures of α -diimine cobalt (II) complexes: Ethylene polymerisation tests. *Journal of Organometallic Chemistry* 2008, *693* (4), 769-775.
22. Brown, L. A.; Wekesa, F. S.; Unruh, D. K.; Findlater, M.; Long, B. K., BIAN-Fe (η^6 -C₆H₆): Synthesis, characterization, and l-lactide polymerization. *Journal of Polymer Science Part A: Polymer Chemistry* 2017, *55* (17), 2824-2830.
23. Supej, M. J.; Volkov, A.; Darko, L.; West, R. A.; Darmon, J. M.; Schulz, C. E.; Wheeler, K. A.; Hoyt, H. M., Aryl-substituted BIAN complexes of iron dibromide: Synthesis, X-ray and electronic structure, and catalytic hydrosilylation activity. *Polyhedron* 2016, *114*, 403-414.
24. Villa, M.; Miesel, D.; Hildebrandt, A.; Ragaini, F.; Schaarschmidt, D.; Jacobi von Wangelin, A., Synthesis and Catalysis of Redox-Active Bis (imino) acenaphthene (BIAN) Iron Complexes. *ChemCatChem* 2017, *9* (16), 3203-3209.
25. Wekesa, F. S.; Arias-Ugarte, R.; Kong, L.; Sumner, Z.; McGovern, G. P.; Findlater, M., Iron-catalyzed hydrosilylation of aldehydes and ketones under solvent-free conditions. *Organometallics* 2015, *34* (20), 5051-5056.
26. Yu, X.; Zhu, F.; Bu, D.; Lei, H., Ferrous complexes supported by sterically encumbered asymmetric bis (arylimino) acenaphthene (BIAN) ligands: synthesis, characterization and screening for catalytic hydrosilylation of carbonyl compounds. *RSC advances* 2017, *7* (25), 15321-15329.
27. Männig, D.; Nöth, H., Catalytic hydroboration with rhodium complexes. *Angewandte Chemie International Edition in English* 1985, *24* (10), 878-879.
28. Zhang, L.; Peng, D.; Leng, X.; Huang, Z., Iron-Catalyzed, Atom-Economical, Chemo- and Regioselective Alkene Hydroboration with Pinacolborane. *Angewandte Chemie* 2013, *125* (13), 3764-3768.
29. Obligacion, J. V.; Chirik, P. J., Highly selective bis (imino) pyridine iron-catalyzed alkene hydroboration. *Organic letters* 2013, *15* (11), 2680-2683.
30. Espinal-Viguri, M.; Woof, C. R.; Webster, R. L., Iron-Catalyzed Hydroboration: Unlocking Reactivity through Ligand Modulation. *Chemistry—A European Journal* 2016, *22* (33), 11605-11608.
31. MacNair, A. J.; Millet, C. R.; Nichol, G. S.; Ironmonger, A.; Thomas, S. P., Markovnikov-selective, activator-free iron-catalyzed vinylarene hydroboration. *ACS Catalysis* 2016, *6* (10), 7217-7221.
32. Chen, X.; Cheng, Z.; Lu, Z., Iron-catalyzed, Markovnikov-selective hydroboration of styrenes. *Organic letters* 2017, *19* (5), 969-971.
33. Su, W.; Qiao, R.-X.; Jiang, Y.-Y.; Zhen, X.-L.; Tian, X.; Han, J.-R.; Fan, S.-M.; Cheng, Q.; Liu, S., Ligand-free iron-catalyzed regioselectivity-controlled hydroboration of aliphatic terminal alkenes. *ACS Catalysis* 2020, *10* (20), 11963-11970.

34. Saini, A.; Smith, C. R.; Wekesa, F. S.; Helms, A. K.; Findlater, M., Conversion of aldimines to secondary amines using iron-catalysed hydrosilylation. *Organic & Biomolecular Chemistry* 2018, *16* (48), 9368-9372.
35. Tamang, S. R.; Cozzolino, A. F.; Findlater, M., Iron catalysed selective reduction of esters to alcohols. *Organic & Biomolecular Chemistry* 2019, *17* (7), 1834-1838.
36. Labre, F.; Gimbert, Y.; Bannwarth, P.; Olivero, S.; Dunach, E.; Chavant, P. Y., Application of Cooperative Iron/Copper Catalysis to a Palladium-Free Borylation of Aryl Bromides with Pinacolborane. *Organic letters* 2014, *16* (9), 2366-2369.
37. Andersson, P. G.; Munslow, I. J., *Modern reduction methods*. John Wiley & Sons: 2008.
38. Zhou, S.; Junge, K.; Addis, D.; Das, S.; Beller, M., A Convenient and General Iron-Catalyzed Reduction of Amides to Amines. *Angewandte Chemie* 2009, *121* (50), 9671-9674.
39. Werkmeister, S.; Junge, K.; Beller, M., Catalytic hydrogenation of carboxylic acid esters, amides, and nitriles with homogeneous catalysts. *Organic process research & development* 2014, *18* (2), 289-302.
40. Igarashi, M.; Fuchikami, T., Transition-metal complex-catalyzed reduction of amides with hydrosilanes: a facile transformation of amides to amines. *Tetrahedron Letters* 2001, *42* (10), 1945-1947.
41. Volkov, A.; Tinnis, F.; Slagbrand, T.; Trillo, P.; Adolfsson, H., Chemoselective reduction of carboxamides. *Chemical Society Reviews* 2016, *45* (24), 6685-6697.
42. Cheng, C.; Brookhart, M., Iridium-catalyzed reduction of secondary amides to secondary amines and imines by diethylsilane. *Journal of the American Chemical Society* 2012, *134* (28), 11304-11307.
43. Das, S.; Addis, D.; Junge, K.; Beller, M., Zinc-Catalyzed Chemoselective Reduction of Tertiary and Secondary Amides to Amines. *Chemistry—A European Journal* 2011, *17* (43), 12186-12192.
44. Gudun, K. A.; Segizbayev, M.; Adamov, A.; Plessow, P. N.; Lyssenko, K. A.; Balanay, M. P.; Khalimon, A. Y., POCN Ni (ii) pincer complexes: synthesis, characterization and evaluation of catalytic hydrosilylation and hydroboration activities. *Dalton Transactions* 2019, *48* (5), 1732-1746.
45. Hanada, S.; Ishida, T.; Motoyama, Y.; Nagashima, H., The ruthenium-catalyzed reduction and reductive N-alkylation of secondary amides with hydrosilanes: practical synthesis of secondary and tertiary amines by judicious choice of hydrosilanes. *The Journal of Organic Chemistry* 2007, *72* (20), 7551-7559.
46. Lampland, N. L.; Hovey, M.; Mukherjee, D.; Sadow, A. D., Magnesium-catalyzed mild reduction of tertiary and secondary amides to amines. *ACS Catalysis* 2015, *5* (7), 4219-4226.
47. Park, S.; Brookhart, M., Development and mechanistic investigation of a highly efficient iridium (V) silyl complex for the reduction of tertiary amides to amines. *Journal of the American Chemical Society* 2012, *134* (1), 640-653.
48. Reeves, J. T.; Tan, Z.; Marsini, M. A.; Han, Z. S.; Xu, Y.; Reeves, D. C.; Lee, H.; Lu, B. Z.; Senanayake, C. H., A practical procedure for reduction of primary, secondary and tertiary amides to amines. *Advanced Synthesis & Catalysis* 2013, *355* (1), 47-52.
49. Smith, A. M.; Whyman, R., Review of methods for the catalytic hydrogenation of carboxamides. *Chemical Reviews* 2014, *114* (10), 5477-5510.
50. Balaraman, E.; Gnanaprakasam, B.; Shimon, L. J.; Milstein, D., Direct hydrogenation of amides to alcohols and amines under mild conditions. *Journal of the American Chemical Society* 2010, *132* (47), 16756-16758.

51. Barrios-Francisco, R.; Balaraman, E.; Diskin-Posner, Y.; Leitus, G.; Shimon, L. J.; Milstein, D., PNN ruthenium pincer complexes based on phosphinated 2, 2'-dipyridinemethane and 2, 2'-oxobispyridine. metal–ligand cooperation in cyclometalation and catalysis. *Organometallics* 2013, 32 (10), 2973-2982.
52. Cabrero-Antonino, J. R.; Alberico, E.; Drexler, H.-J.; Baumann, W.; Junge, K.; Junge, H.; Beller, M., Efficient base-free hydrogenation of amides to alcohols and amines catalyzed by well-defined pincer imidazolyl–ruthenium complexes. *Acs Catalysis* 2016, 6 (1), 47-54.
53. Szostak, M.; Spain, M.; Eberhart, A. J.; Procter, D. J., Highly chemoselective reduction of amides (primary, secondary, tertiary) to alcohols using SmI₂/amine/H₂O under mild conditions. *Journal of the American Chemical Society* 2014, 136 (6), 2268-2271.
54. Zhang, B.; Li, H.; Ding, Y.; Yan, Y.; An, J., Reduction and reductive deuteration of tertiary amides mediated by sodium dispersions with distinct proton donor-dependent chemoselectivity. *The Journal of Organic Chemistry* 2018, 83 (11), 6006-6014.
55. Gribble, G. W., Sodium borohydride in carboxylic acid media: a phenomenal reduction system. *Chemical Society Reviews* 1998, 27 (6), 395-404.
56. Li, Y.; Molina de La Torre, J. A.; Grabow, K.; Bentrup, U.; Junge, K.; Zhou, S.; Brückner, A.; Beller, M., Selective reduction of amides to amines by boronic acid catalyzed hydrosilylation. *Angewandte Chemie International Edition* 2013, 52 (44), 11577-11580.
57. Blondiaux, E.; Cantat, T., Efficient metal-free hydrosilylation of tertiary, secondary and primary amides to amines. *Chemical Communications* 2014, 50 (66), 9349-9352.
58. Li, B.; Sortais, J.-B.; Darcel, C., Unexpected selectivity in ruthenium-catalyzed hydrosilylation of primary amides: synthesis of secondary amines. *Chemical Communications* 2013, 49 (35), 3691-3693.
59. Bhunia, M.; Sahoo, S. R.; Das, A.; Ahmed, J.; Sreejyothi, P.; Mandal, S. K., Transition metal-free catalytic reduction of primary amides using an abnormal NHC based potassium complex: integrating nucleophilicity with Lewis acidic activation. *Chemical science* 2020, 11 (7), 1848-1854.
60. Yao, W.; Wang, J.; Zhong, A.; Wang, S.; Shao, Y., Transition-metal-free catalytic hydroboration reduction of amides to amines. *Organic Chemistry Frontiers* 2020, 7 (21), 3515-3520.
61. Bisai, M. K.; Gour, K.; Das, T.; Vanka, K.; Sen, S. S., Lithium compound catalyzed deoxygenative hydroboration of primary, secondary and tertiary amides. *Dalton Transactions* 2021, 50 (7), 2354-2358.
62. Kumar, R.; Bisai, M. K.; Jain, S.; Vanka, K.; Sen, S. S., Deoxygenative hydroboration of primary and secondary amides: a catalyst-free and solvent-free approach. *Chemical Communications* 2021, 57 (81), 10596-10599.
63. Boeyens, J. C. A.; de Villiers, J. P. R., Crystal structure of the basic erbium tetramethylheptanedionate, Er₈O(thd)₁₀(OH)₁₂. *J. Cryst. Mol. Struct.* 1972, 2 (4), 197-211.
64. Poncelet, O.; G. Hubert-Pfalzgraf, L., Reactivity of neodymium(III) Isopropoxide derivatives: synthesis, characterization and crystal structure of [Nd₄(μ₃-OH)₂(μ₂, μ₁-acac)₆(acac)₄]. *Polyhedron* 1989, 8 (17), 2183-2188.
65. Plakatouras, J. C.; Baxter, I.; Hursthouse, M. B.; Malik, K. M. A.; McAleese, J.; Drake, S. R., Synthesis and structural characterisation of two novel Gdβ-diketonates [Gd₄(μ₃-OH)₄(μ₂-H₂O)₂(H₂O)₄(hfpd)₈]·2C₆H₆·H₂O 1 and [Gd(hfpd)₃(Me₂CO)(H₂O)] 2(hfpd–H = 1,1,1,5,5,5-hexafluoropentane-2,4-dione). *J. Chem. Soc., Chem. Commun.* 1994, (21), 2455-2456.

66. Xiong, R.-G.; Zuo, J.-L.; Yu, Z.; You, X.-Z.; Chen, W., $\text{Eu}_5(\mu_4\text{-OH})(\mu_3\text{-OH})_4(\mu\text{-DBM})_4(\text{DBM})_6$ (DBM=dibenzoylmethide): a novel Eu_5 square-pyramid polynuclear complex with a rare $\mu_4\text{-OH}$ bridging mode. *Inorg. Chem. Commun.* 1999, 2 (10), 490-494.
67. Ma, X.; Yang, W.; Chen, L.; Zhao, J., Significant developments in rare-earth-containing polyoxometalate chemistry: synthetic strategies, structural diversities and correlative properties. *CrystEngComm* 2015, 17 (43), 8175-8197.
68. Yan, D.; Dai, P.; Chen, S.; Xue, M.; Yao, Y.; Shen, Q.; Bao, X., Highly efficient hydroboration of carbonyl compounds catalyzed by tris(methylcyclopentadienyl)lanthanide complexes. *Org. Biomol. Chem.* 2018, 16 (15), 2787-2791.
69. Zhu, Z.; Dai, P.; Wu, Z.; Xue, M.; Yao, Y.; Shen, Q.; Bao, X., Lanthanide aryloxides catalyzed hydroboration of aldehydes and ketones. *Catal. Commun.* 2018, 112, 26-30.
70. Solorzano, C.; Antonietti, F.; Duranti, A.; Tontini, A.; Rivara, S.; Lodola, A.; Vacondio, F.; Tarzia, G.; Piomelli, D.; Mor, M., Synthesis and Structure–Activity Relationships of N-(2-Oxo-3-oxetanyl)amides as N-Acylethanolamine-hydrolyzing Acid Amidase Inhibitors. *J. Med. Chem.* 2010, 53 (15), 5770-5781.
71. Pelletier, G.; Bechara, W. S.; Charette, A. B., Controlled and Chemoselective Reduction of Secondary Amides. *J. Am. Chem. Soc.* 2010, 132 (37), 12817-12819.
72. Das, S.; Addis, D.; Zhou, S.; Junge, K.; Beller, M., Zinc-Catalyzed Reduction of Amides: Unprecedented Selectivity and Functional Group Tolerance. *J. Am. Chem. Soc.* 2010, 132 (6), 1770-1771.
73. Xie, J.-H.; Yan, P.-C.; Zhang, Q.-Q.; Yuan, K.-X.; Zhou, Q.-L., Asymmetric Hydrogenation of Cyclic Imines Catalyzed by Chiral Spiro Iridium Phosphoramidite Complexes for Enantioselective Synthesis of Tetrahydroisoquinolines. *ACS Catal.* 2012, 2 (4), 561-564.
74. Labre, F.; Gimbert, Y.; Bannwarth, P.; Olivero, S.; Duñach, E.; Chavant, P. Y., Application of Cooperative Iron/Copper Catalysis to a Palladium-Free Borylation of Aryl Bromides with Pinacolborane. *Org. Lett.* 2014, 16 (9), 2366-2369.
75. Bleith, T.; Gade, L. H., Mechanism of the Iron(II)-Catalyzed Hydrosilylation of Ketones: Activation of Iron Carboxylate Precatalysts and Reaction Pathways of the Active Catalyst. *J. Am. Chem. Soc.* 2016, 138 (14), 4972-4983.

III. COBALT-CATALYZED ALKYLATION OF NITRILES WITH ALCOHOLS

Modified with permission from *Organometallics* **2022**, ASAP ARTICLES

Arpita Singh and Michael Findlater*

(<https://doi.org/10.1021/acs.organomet.1c00690>)

3.1. Introduction

Nitriles are an important class of nitrogen containing compounds which can easily be transformed to myriad of valuable molecules: amines,¹⁻² amides,³⁻⁴ acids,⁵ ketones⁶ etc. Furthermore, nitriles also have applications as drugs and medicines in their own right.⁷ Due to the wide applicability of nitriles in numerous fields, organic transformations of arylmethyl nitriles such as alkylation have garnered much interest in the recent past. α -alkylated nitriles have a plethora of applications; not only can a broad range of functional groups such as amines, acids, amides be accessed from nitriles but they are also important synthons in a number of important drug molecules (**Figure 3.1**). Isoaminile⁸⁻⁹ and phenylalkylamines (verapamil,¹⁰ devapamil and gallopamil) containing the α -alkylated nitrile moiety have been utilized as antitussives and for the treatment of arrhythmia and hypertension respectively.

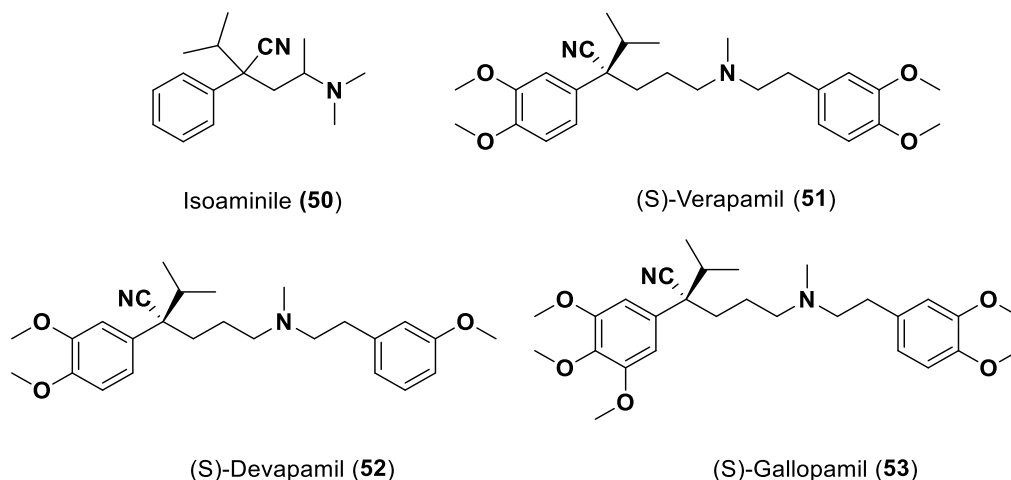


Figure 3.1. Representative examples of drugs containing the α -alkylated nitrile moiety.

Alkylation of nitriles employing alkyl halides as the alkylating agent has been well explored in the literature;¹¹ whereas examples of alkylation with alcohols remain limited. Alcohols are an excellent surrogate for alkyl halides as water is the sole by-product released after alkylation of nitriles with alcohols. Moreover, alkylation of nitriles with alcohols can be used as an alternative method for the introduction of an isopropyl group as opposed to the commonly employed use of alkylhalide and phase transfer catalyst.¹²

Traditionally, catalytic processes capable of effecting nitrile alkylation through the use of alcohols were limited to the use of 4- and 5d metals.¹³⁻¹⁸ More recently, due to their abundance,

low toxicity and reduced cost (typically), focus has now shifted to the use of 3d metals to catalyze this transformation (**Figure 3.2**).

Another challenge associated with nitrile alkylation is the sensitivity of the cyano- group towards water, which often results in the formation of undesired amide product. Additionally, formation of an alkene-nitrile by-product is also a major concern.¹⁹ The alkylation of nitriles using alcohols as an alkylating agent has been explored using platinum group metals: Ir^{13, 20}, Ru^{14-15, 17} and Os²¹ in the past decade. In contrast, examples of catalytic alkylation by 3d metals remain scant. The first example of base metal-catalyzed alkylation employed an Fe-PNP (PNP = Bis(2-(dicyclohexylphosphanyl)ethyl)amine) complex (**54**) and was reported by Wang and co-workers in 2018.²² In 2019, a manganese-PNP pincer (PNP = Bis(2-(diphenylphosphanyl)ethyl)amine) (**55**) was utilized by Rueping and co-workers to carry out the alkylation of nitriles; excellent yields of up to 99% were reported.²³ In 2020, Banerjee and co-workers reported the first example of nickel-catalyzed alkylation of aryl and alkyl nitriles with primary alcohols with yields up to 90% and excellent chemo-selectivity.²⁴ This was the first example where commercially available Ni(acac)₂ was used in conjunction with 1,10-phenanthroline ligand. Also in 2020, Sundararaju and coworkers employed Cp*Co(CO)I₂ (Cp* = pentamethylcyclopentadienyl ligand) (**56**) to carry out the alkylation of oxindoles, *N,N*-dimethyl barbituric acids, and phenyl acetonitrile with secondary alcohols; the scope of substrate for phenyl acetonitrile was limited to only 6 substrates.²⁵ In a notable development in 2020, Ding and co-workers developed an air stable cobalt complex (**57**) of a tetradentate mixed P/N donor ligand in the alkylation of nitriles using alcohols as the alkylating agent.²⁶

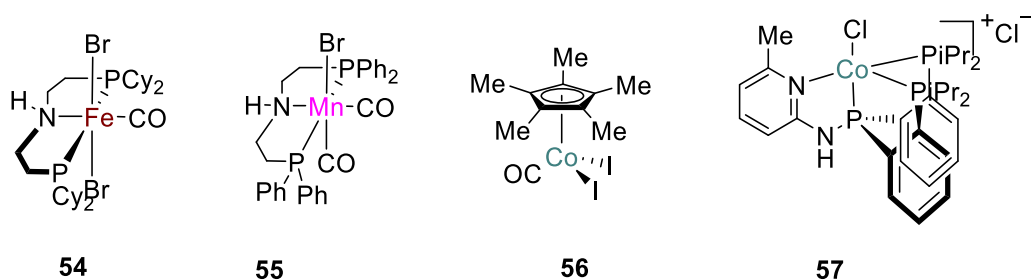


Figure 3.2. Representative examples of pre-catalysts used for alkylation of nitriles.

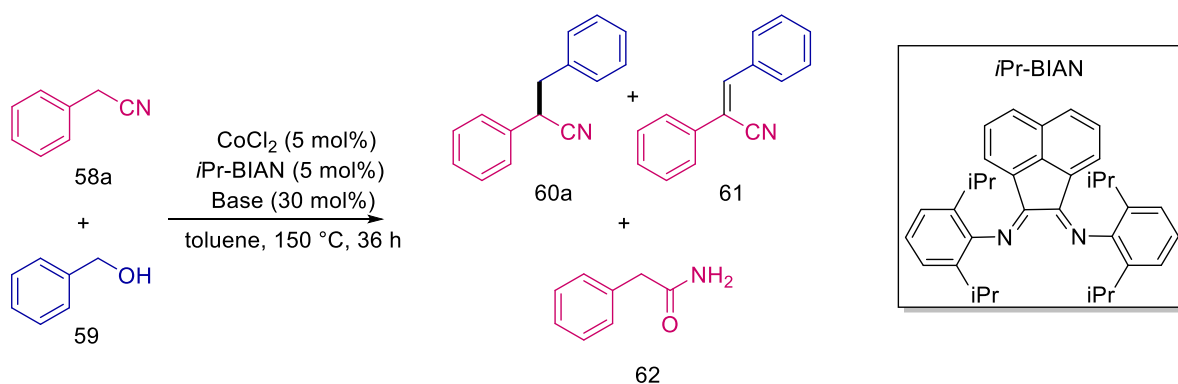
Given the relative scarcity of reports of base metal catalyzed alkylation of nitriles in the literature our own interest in base metal catalyzed transformations,²⁷⁻³³ and the promising results employing cobalt-based species, we resolved to explore the alkylation of nitriles with alcohols employing cobalt-based catalysts.

3.2. Results and Discussion

Our preliminary experiments focused on the use of commercially available cobalt salts as precatalysts in nitrile alkylation chemistry. No catalytic activity was observed employing CoCl₂ (5 mol%) in the presence of 0.25 mmol of phenyl acetonitrile (**58a**) and 0.5 mmol of benzylalcohol (**59a**) in toluene, even upon prolonged heating (150 °C after 36h). Due to our longstanding interest in the catalytic behavior of bis(arylimino)acenaphthene (BIAN) ligand supported transition metals,^{27-28, 30, 34-36} we began exploring the application of BIAN ligands in alkylation chemistry. BIAN ligands were first introduced to coordination chemistry by Elsevier and co-workers in 1994³⁷

and have gone on to be widely applied in catalysis³⁸⁻⁴⁰ and in the support of reactive main group species.⁴¹ They are a combination of an α,α' -diimine unit and the naphthalene system's p-framework and provide robust support for metal complexes. Upon introduction of *i*Pr-BIAN (*i*Pr-BIAN = bis(2,6-diisopropylaniline)acenaphthene) (5 mol%) and KO*t*Bu (30 mol%) to the above system, we were delighted to observe quantitative conversion of **58a** to the desired α -alkylated nitrile (**60a**). We subsequently studied what, if any, effect the identity of the base may play on the reaction outcome, thus, CsF, Cs₂CO₃, NaO*t*Bu, LiOMe and KHMDS were explored (**Table 3.1**) and it was found that no base was as effective as KO*t*Bu.

Table 3.1. Base screening for alkylation of nitriles.



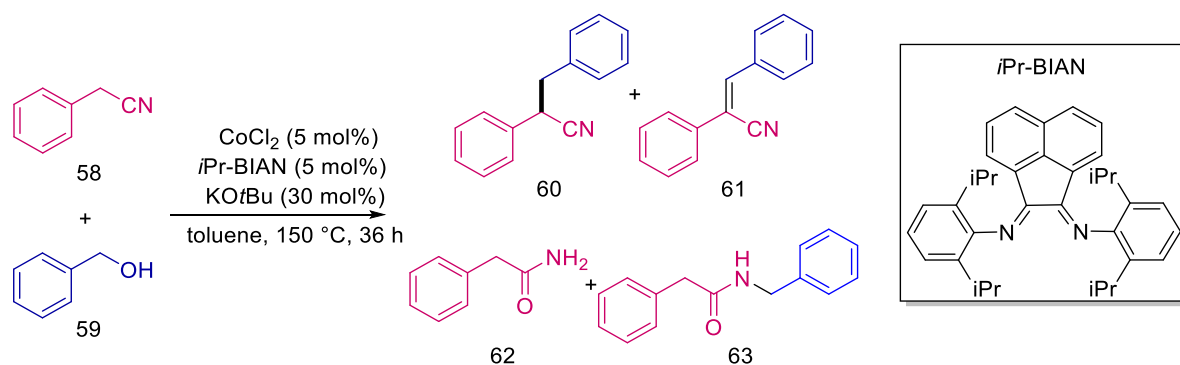
Entry	Bases	Conversion of 58 (%)	60 (%)	61 (%)	62 (%)
1.	K ₂ CO ₃	8	2	3	3
2.	LiOMe	6	3	2	1
3.	NaO <i>t</i> Bu	55	47	7	1
4.	Cs ₂ CO ₃	8	2	6	0
5.	CsF	7	2	3	2
6.	KHMDS	0			
7.	KO <i>t</i> Bu	100	100	0	0

Reaction conditions: **58a** (0.25 mmol), **59a** (0.5 mmol), base (30 mol%), CoCl₂ (2-5 mol%), *i*Pr-BIAN (2-5 mol%), toluene (1 mL). J-young tube in an oil bath (150 °C) for 36h. Conversion was determined by GC-MS.

We then examined the role of the solvent in the system by replacing toluene with several polar solvents: dimethylformamide (DMF), dimethylacetamide (DMA) and, 1,4-Dioxane were explored. In the alkylation of nitriles we discovered that toluene is the most appropriate solvent for this transformation (**Table 3.2, Entries 2-4**). Observed conversion of nitrile to alkylated product was decreased when lower temperatures were employed (**Table 3.2, Entries 5-6**). We also probed the effects of added alcohol on the conversion to alkylated product by varying the amount of alcohol; both 1 and 1.5 equiv. of benzyl alcohol afforded diminished conversion to the desired product (**Table 3.2, Entries 7-8**). Similarly, upon reduction of catalyst loading from 5 to 2 and 3 mol % (**Table 3.2, Entries 13-14**, respectively) lower conversion values were observed. Finally, we compared our catalytic system with other commercially available cobalt precursors namely

Co(acac)₃ and Co(benzoate)₂ (**Table 3.2, Entries 10-12**). We observed 100 % conversion of **58a** with exclusive formation of alkylated product **60a** when using Co(acac)₃ in the absence of BIAN ligand (**Table 3.2, Entry 10**). Similarly, use of Co(benzoate)₂ (**Table 3.2, Entry 12**) also afforded alkylated product exclusively and in good, albeit reduced yield (74 %).

Table 3.2. Optimization of the reaction conditions for nitrile alkylation.

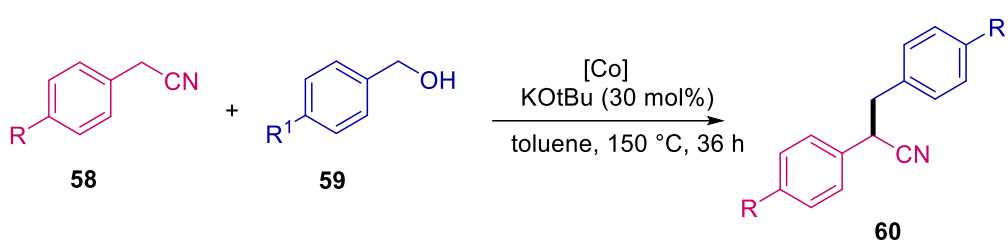


Entry	Deviation from conditions	Conversion (%)			
		60	61	62	63
1	None	100	-	-	-
2	DMF	-	-	-	-
3	DMA	14	-	-	-
4	1,4-dioxane	76	-	-	-
5	130 °C	67	-	-	-
6	140 °C	80	-	-	-
7	1 eq. ROH	62	-	-	-
8	1.5 eq. ROH	73	-	-	-
9	Only KOtBu	57	1	1	2
10	Co(acac) ₃ / no BIAN	100	-	-	-
11	CoBr ₂	98	-	-	-
12	Co(benzoate) ₂ / no BIAN	74	-	-	-
13	[Co] / BIAN (2 mol%)	75	-	3	3
14	[Co] / BIAN (3 mol%)	80	-	2	4
15	24 h	81	-	-	-

Reaction conditions: **58a** (0.25 mmol), **59a** (0.25-0.5 mmol), base (30 mol%), [Co] (2-5 mol%), *i*Pr-BIAN (2-5 mol%), toluene (1 mL). J-young tube in an oil bath (150 °C) for 36h. Conversion was determined by GC-MS.

Initially, we had mixed feelings about these results; although excited about the discovery of a simplified system in $\text{Co}(\text{acac})_3$ which was highly effective, we were disappointed to see that BIAN ligand appeared unnecessary for the reaction to proceed. We resolved to explore the usefulness of the BIAN ligand with a short substrate screen (Table 3.3) in which a head-to-head comparison of the “ligand-free” $\text{Co}(\text{acac})_3$ vs. the BIAN-supported cobalt system. This screen revealed that in each case, superior conversion was observed when employing BIAN ligand in the catalytic system. Furthermore, in one case a small enhancement of product selectivity was also observed (Table 3.3).

Table 3.3. Comparison between $\text{Co}(\text{acac})_3$ and $\text{CoCl}_2/\text{BIAN}$.



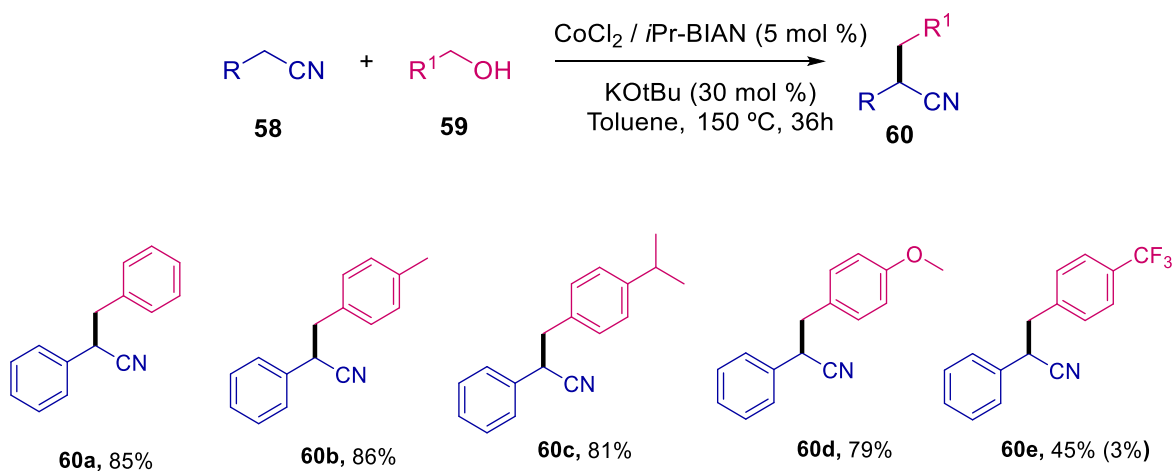
Entry	$\text{Co}(\text{acac})_3$	$\text{CoCl}_2 / i\text{Pr-BIAN}$
R = <i>p</i> -Me, R ¹ = H	91 %	100 %
R = <i>p</i> -F, R ¹ = H	62 %	76 %
R = H, R ¹ = <i>p</i> -Me	95 % (4 %)	100 %
R = H, R ¹ = <i>p</i> -OMe	63 %	91 %

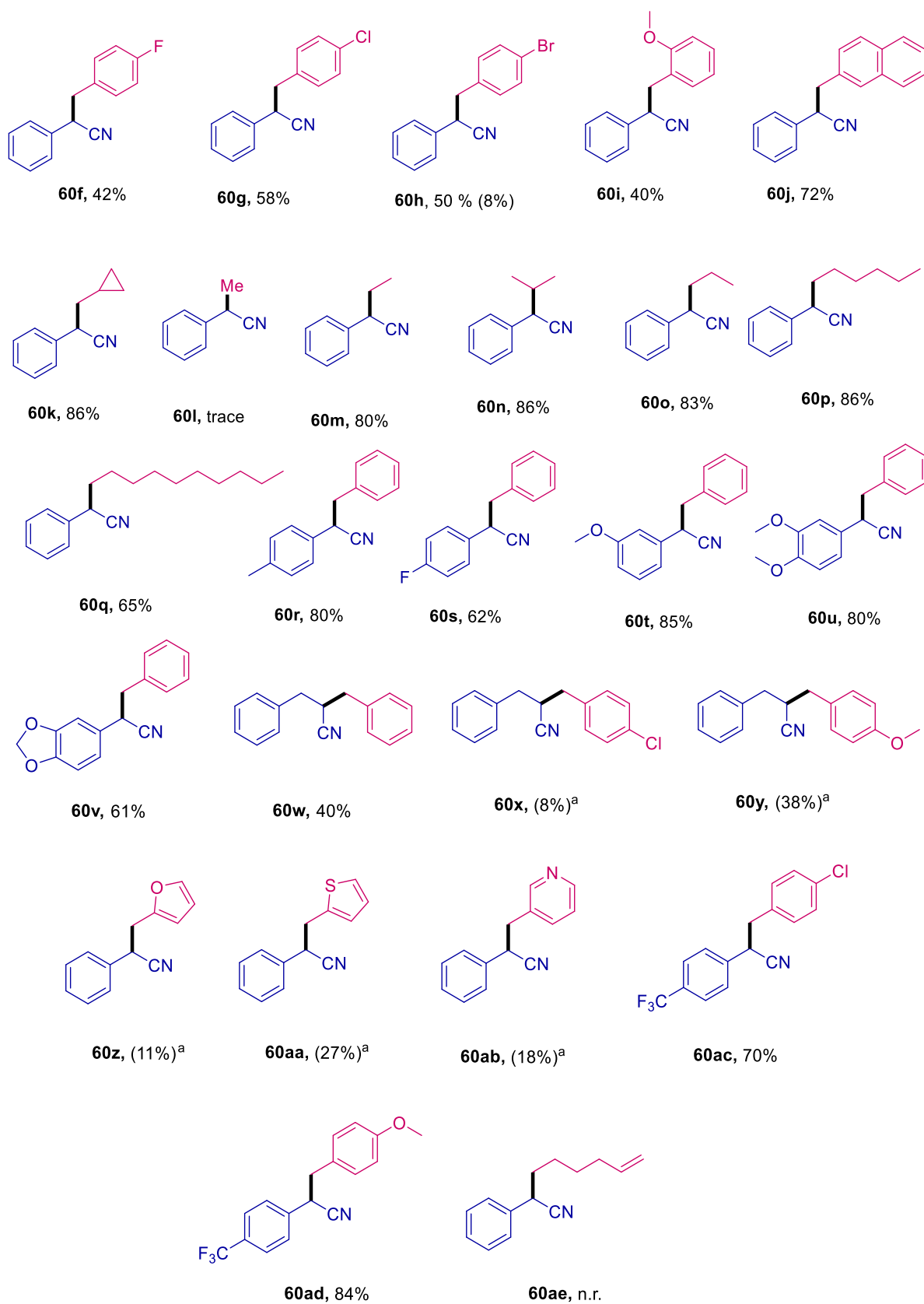
Reaction conditions: **58** (0.25 mmol), **59** (0.5 mmol), base (30 mol%), [Co] (5 mol%), *i*Pr-BIAN (5 mol%), toluene (1 mL). J-young tube in an oil bath (150 °C) for 36h. Conversion was determined by GC-MS.

With optimized conditions in hand, we began exploring the scope of alcohol substrate amenable to nitrile alkylation under these conditions. The model reaction readily allowed the isolation of alkylated nitrile in good yield (85%). Initially, we explored variation in the identity of the alcohol. The presence of electron donating substituents in the *para*-position of the benzyl alcohols (**59b-d**) i.e. *p*-methyl, *p*-isopropyl and *p*-methoxy, lead to similarly good yields of alkylated nitriles (86%, 81%, and 79% isolated yields, respectively). In the case of *p*-trifluoromethylbenzylalcohol **59e** (an electron-withdrawing substituent) the α -alkylated nitrile **60e** was obtained in only 45% isolated yield along with the formation of 2-phenylacetamide (3%). Interestingly, *p*-halide substituted benzyl alcohols (F, Cl, Br) afforded the products (**60f-h**) in 42%, 58% and 50% isolated yields respectively; 8% conversion of phenylacetone nitrile to 2,3-diphenylpropanenitrile **60a** was observed along with **60h**. In a more sterically hindered substrate like *o*-methoxybenzylalcohol **59i**, product **60i** was obtained in 40 % yield. 1-naphthylmethanol (**59j**) on reaction with phenyl acetonitrile (**58a**) afforded **60j** in 72% isolated yield. Cyclopropylmethanol **59k** on treatment with **58a** led to the formation of **60k** in 86% isolated yield. No ring-opened products were observed which suggests a non-radical mechanism is operative. We then explored the reaction between nitriles and linear alcohols. Only trace amounts of α -alkylated nitrile **60l** was obtained employing the potential C1-source, methanol. In contrast, ethanol afforded product **60m** in 80% isolated yield. Upon further increasing the chain length of the alcohols up to three and six carbons, 83% and 86% isolated yield

of **60o** and **60p** was obtained respectively. A small drop in isolated yield (65%) was observed in the case of **60q** which was obtained employing 1-decanol (**59q**) as the alkylating agent. As the catalytic system worked well for primary alcohols, we further tested the ability of the system to carry out alkylation of phenyl acetonitrile with the secondary alcohol 2-propanol (**59n**), and we were delighted to obtain product **60n** in 86% isolated yield. We subsequently investigated the generality of the nitrile substrate by exploring a range of functional groups and substitution patterns. Both electron-withdrawing and electron-donating features were tolerated, (*p*-methylphenyl)acetonitrile and (*p*-fluorophenyl)acetonitrile were smoothly converted to alkylated nitrile products (**60r** and **60s**, respectively) in modest to good yields. Similarly, the aryl ethers (*m*-methoxyphenyl)acetonitrile (**58t**), 2-(3,4-dimethoxyphenyl)acetonitrile (**58u**) and 1,3-Benzodioxole-5-acetonitrile (**58v**) were readily alkylated using benzyl alcohol in good to excellent yields (61 – 85% isolated yields). We extended our investigation of nitriles to include hydrocinnamonitrile, typically such substrates perform poorly in nitrile alpha-alkylation reactions. In contrast to the recent report of Ding and co-workers,²⁶ we found 3-phenylpropanenitrile (**58w**) to be a competent nitrile substrate for alkylation using benzylalcohol, albeit affording product **60w** in diminished yield (40%). Intrigued by this surprising result, we explored the effect of electronics on the reaction; *p*-chlorobenzylalcohol and *p*-methoxybenzylalcohol were independently treated with the hydrocinnamonitrile to afford products **60x** and **60y** in low yield which precluded isolation and characterization by NMR (8% and 38% conversion, respectively, was observed by GC-MS).

Heterocyclic alcohols were found to be poor substrates for nitrile alkylation. Only 11% conversion (GC-MS) of phenylacetonitrile to product **60z** was observed upon treatment with furan-2-ylmethanol. Similarly, with both thiophene- and pyridine-based substrates poor conversion to alkylated products were obtained (**60aa** and **60ab**). When substituents were introduced on both the nitrile and alcohol substrates good yields were still accessible. Treatment of 2-(4-(trifluoromethyl)phenyl)acetonitrile with *p*-chlorobenzylalcohol or *p*-methoxybenzylalcohol affords alkylated products **60ac** and **60ad** in 70% and 84% yield, respectively. The reaction of hex-5-en-1-ol with phenyl acetonitrile was unsuccessful. In general, the presence of electron-donating substituents (especially on the alcohol substrate) delivers a moderate boost in overall reaction yield.





Scheme 3.1. Substrate scope for alkylation of nitriles.

(a) Conversions determined from GC-MS.

The formation of the known *i*Pr-BIANCoCl₂ complex⁴²⁻⁴³ is assumed to occur in-situ followed by subsequent activation by KO^tBu to afford a catalytically active cobalt species. The use of *i*Pr-BIANCoCl₂ in catalytic reactions ranging from polymerization to hydrogenation have been demonstrated.⁴³⁻⁴⁵ The work of Ding and co-workers have established an attractive mechanistic possibility, however, at this stage the reaction mechanism is unknown to us. Intriguingly, the Co(III) and Co(II) precursors Co(acac)₃ and Co(benzoate)₂ are also competent catalysts under otherwise identical conditions thus begging the question of the identity of the active catalyst. However, it is evident the acac and benzoate ligands must play an important role since CoCl₂ alone was *not* an effective catalyst.

3.3. Conclusion

We have disclosed an inexpensive and facile catalytic system for nitrile alkylation, employing alcohols to afford α -alkylated nitriles, which uses a readily available cobalt source-CoCl₂ in conjunction with the well-studied *i*Pr-BIAN ligand. The catalytic system works well for a wide variety of substrates and is both regio- and chemoselective.

3.4. Experimental Section

3.4.1. General considerations

All reactions were performed in oven dried apparatus under the atmosphere of Argon. All metal salts, nitriles and alcohols were purchased from commercial vendors (Strem, Alfa Aesar and Sigma Aldrich). ¹H, ¹³C spectra were recorded on a Jeol 400 MHz spectrometer at 300K unless otherwise noted. ¹H NMR spectra were referenced to the solvent residual peak (CDCl₃, δ 7.26 ppm), and ¹³C{¹H} NMR spectra were referenced to the solvent residual peak (CDCl₃, δ 77.16 ppm). Coupling constants *J* are reported in Hz. NMR multiplicities are as follows: s = singlet, d = doublet, t = triplet, m = multiplet, sept = septet, dd = doublet of doublet, dq = doublet of quartet. GC-MS data were acquired using Thermo Scientific ISQ Single Quadrupole system.

3.4.2. General procedure for alkylation of nitriles

An oven dried J-young tube was charged with CoCl₂ (3.24 mg, 0.025 mmol), *i*Pr-BIAN (12.5 mg, 0.025 mmol), KO^tBu (16.82 mg, 0.15 mmol), alcohol (1.0 mmol) and nitrile (0.5 mmol) and 0.7-0.8 mL toluene. The reaction mixture was then placed on a preheated oil bath at 150 degrees. The progress of the reaction was monitored by GC-MS. The reaction mixture was cooled down to room temperature and was subjected to column chromatography using pentane/ diethyl ether 98:2 (v/v) to afford the pure alkylated nitrile.

3.5. Appendix

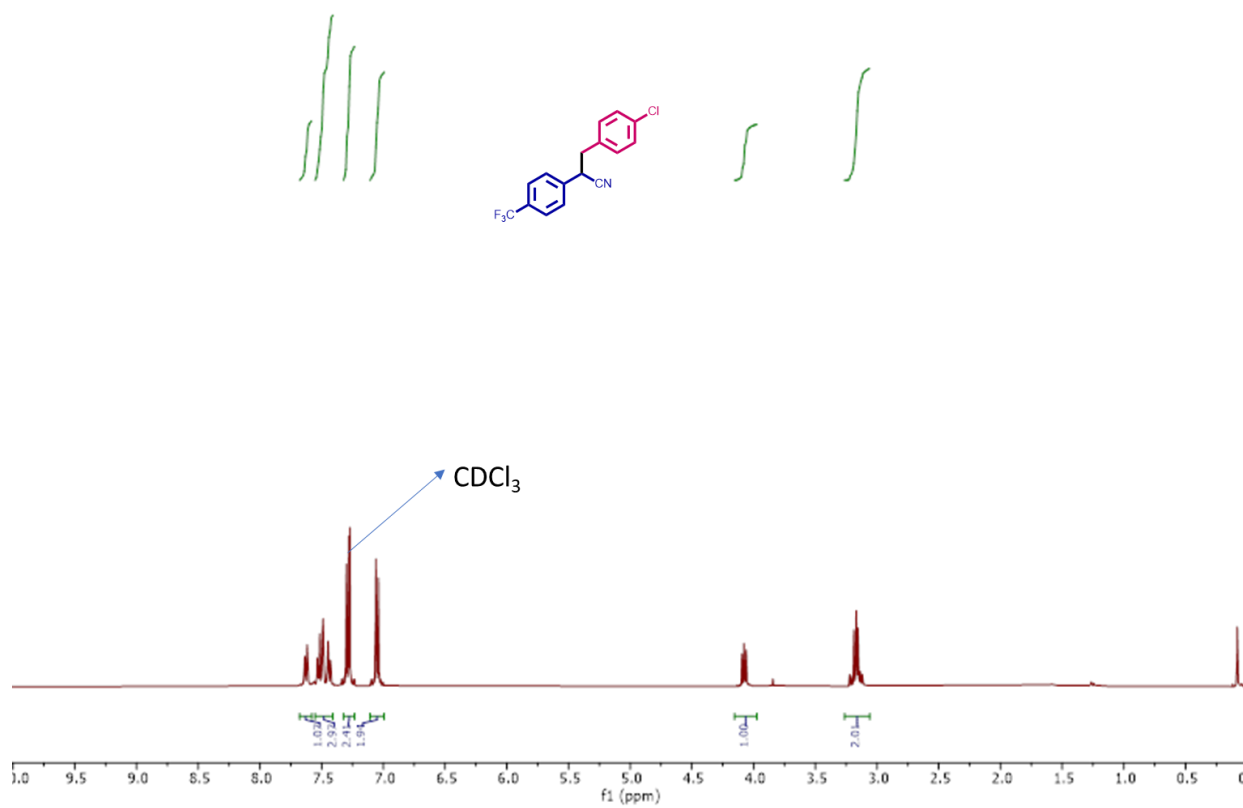


Figure 3.3. ^1H NMR of 3-(4-chlorophenyl)-2-(4-(trifluoromethyl)phenyl)propanenitrile (**60ac**)

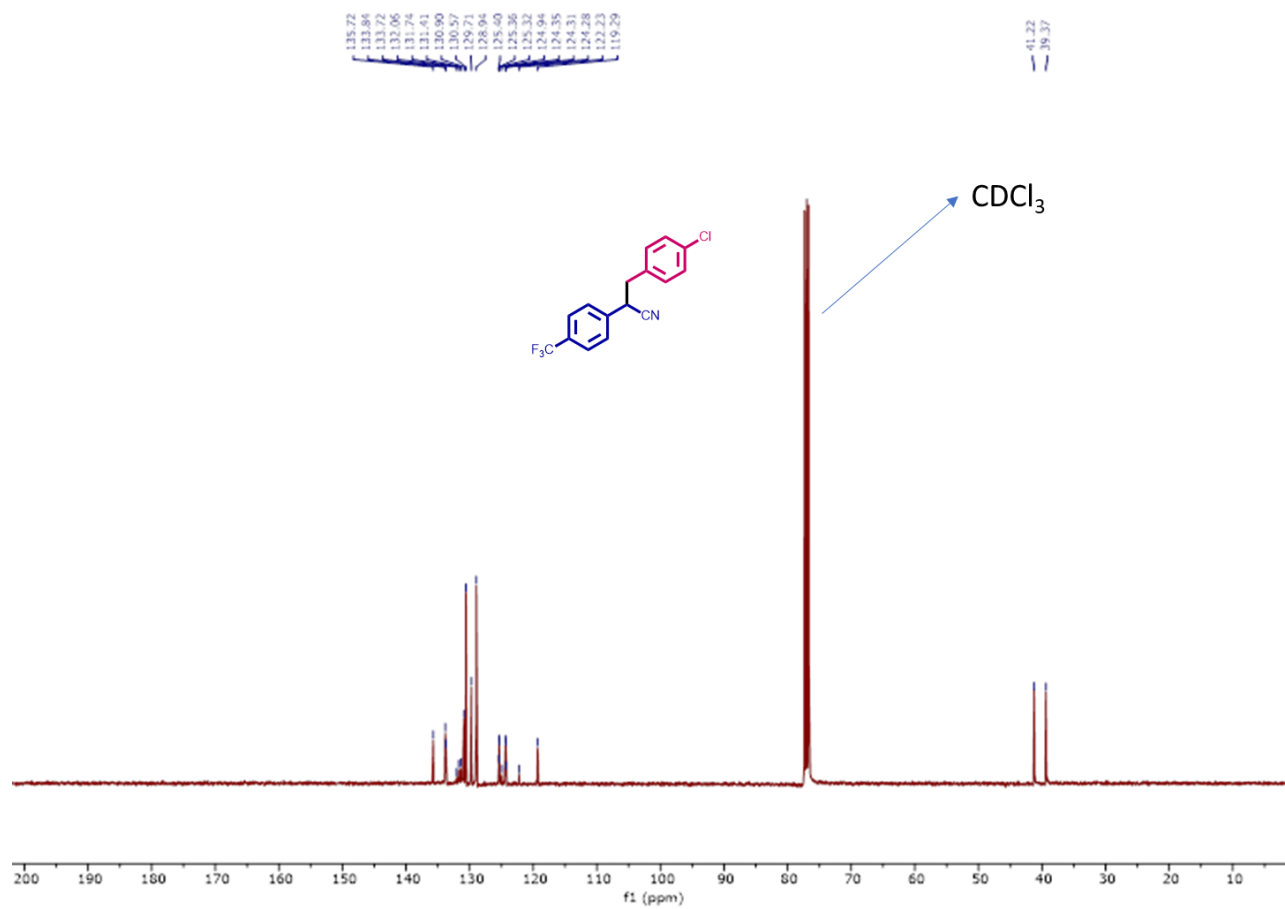


Figure 3.4. ^{13}C NMR of 3-(4-chlorophenyl)-2-(4-(trifluoromethyl)phenyl)propanenitrile (**60ac**)

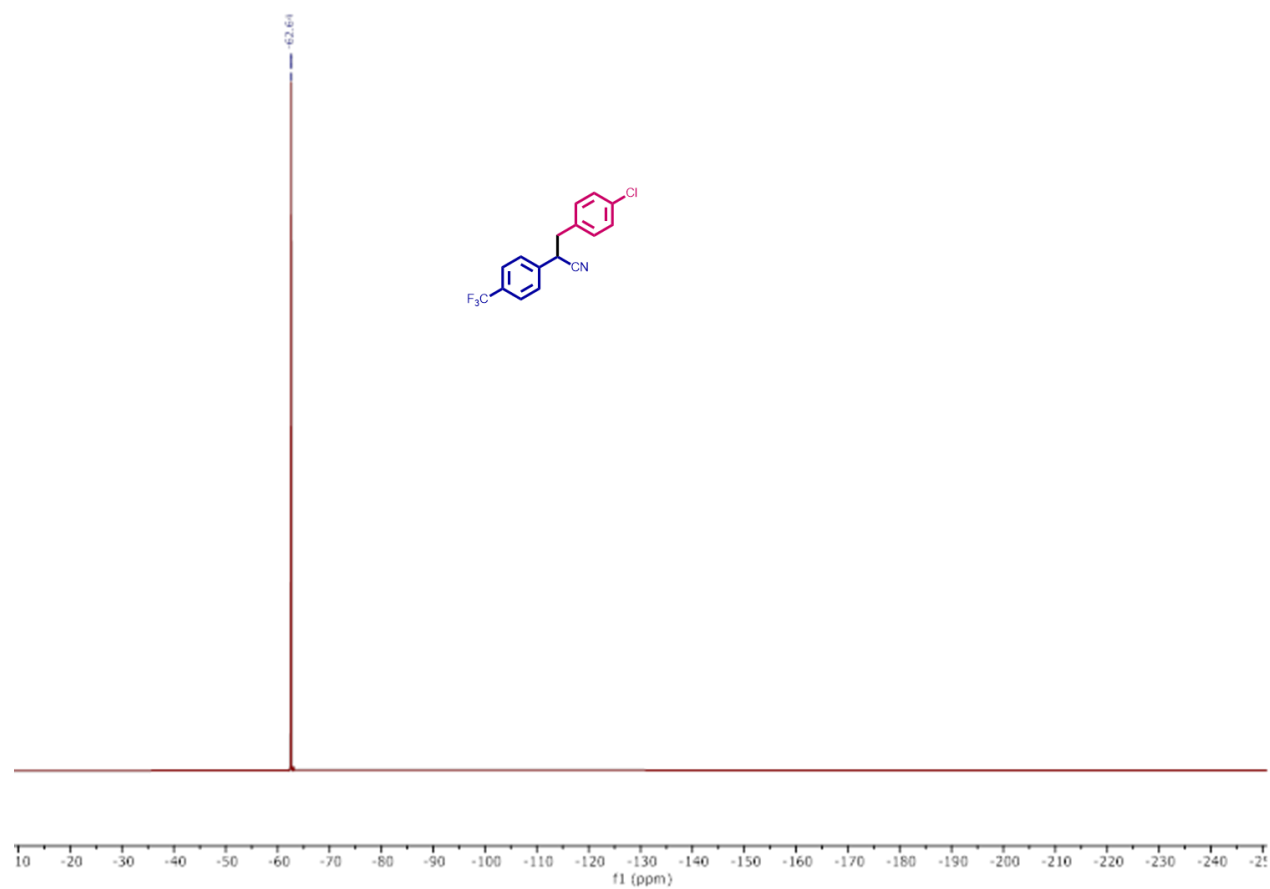


Figure 3.5. ^{19}F NMR of 3-(4-chlorophenyl)-2-(4-(trifluoromethyl)phenyl)propanenitrile (**60ac**)

3.6. References

1. Haddenham, D.; Pasumansky, L.; DeSoto, J.; Eagon, S.; Singaram, B., Reductions of aliphatic and aromatic nitriles to primary amines with diisopropylaminoborane. *The Journal of organic chemistry* **2009**, *74* (5), 1964-1970.
2. Mukherjee, A.; Srimani, D.; Chakraborty, S.; Ben-David, Y.; Milstein, D., Selective hydrogenation of nitriles to primary amines catalyzed by a cobalt pincer complex. *Journal of the American Chemical Society* **2015**, *137* (28), 8888-8891.
3. Moorthy, J. N.; Singhal, N., Facile and highly selective conversion of nitriles to amides via indirect acid-catalyzed hydration using TFA or AcOH– H₂SO₄. *The Journal of organic chemistry* **2005**, *70* (5), 1926-1929.
4. Reddy, N. N. K.; Rao, S. N.; Patil, R. D.; Adimurthy, S., Transition metal-free hydration of nitriles to amides mediated by NaOH.
5. Lignier, P.; Estager, J.; Kardos, N.; Gravouil, L.; Gazza, J.; Naffrechoux, E.; Draye, M., Swift and efficient sono-hydrolysis of nitriles to carboxylic acids under basic condition: role of the oxide anion radical in the hydrolysis mechanism. *Ultrasonics sonochemistry* **2011**, *18* (1), 28-31.
6. Taber, D. F.; Cai, L., Preparation of ketones from nitriles and phosphoranes. *The Journal of organic chemistry* **2005**, *70* (12), 4887-4888.
7. Wang, Y.; Du, Y.; Huang, N., A survey of the role of nitrile groups in protein–ligand interactions. *Future medicinal chemistry* **2018**, *10* (23), 2713-2728.
8. Antonietti, F.; Brenna, E.; Fuganti, C.; Gatti, F. G.; Giovenzana, T.; Grande, V.; Malpezzi, L., Synthesis of isoaminile mediated by enzymes. *Synthesis* **2005**, *2005* (07), 1148-1156.
9. Diwan, J.; Dhand, R.; Jindal, S.; Malik, S.; Sharma, P., A comparative randomized double-blind clinical trial of isoaminile citrate and chlophedianol hydrochloride as antitussive agents. *International journal of clinical pharmacology, therapy, and toxicology* **1982**, *20* (8), 373-375.
10. Barattin, R.; Gerby, B.; Bourges, K.; Hardy, G.; Olivares, J.; Boutonnat, J.; Arnoult, C.; d'Hardemare, A. D. M.; Ronot, X., Iodination increases the activity of verapamil derivatives in reversing PGP multidrug resistance. *Anticancer research* **2010**, *30* (7), 2553-2559.
11. Savoia, D.; Trombini, C.; Umani-Ronchi, A., Potassium-graphite (C₈K) as a metallation reagent. Alkylation of nitriles and esters with alkyl halides under heterogeneous conditions. *Tetrahedron Letters* **1977**, *18* (7), 653-656.
12. Barbry, D.; Pasquier, C.; Faven, C., Alkylation and hydrolysis of phenylacetone nitriles under microwave irradiation. *Synthetic communications* **1995**, *25* (19), 3007-3013.
13. Anxionnat, B.; Gomez Pardo, D.; Ricci, G.; Cossy, J., First intramolecular alkylation of nitriles with primary and secondary alcohols catalyzed by iridium complexes. *European journal of organic chemistry (Print)* **2012**, (24), 4453-4456.
14. Huang, S.; Hong, X.; Sun, Y.; Cui, H. Z.; Zhou, Q.; Lin, Y. J.; Hou, X. F., Ru (II)-PBTNNXN complex bearing functional 2-(pyridin-2-yl) benzo [d] thiazole ligand catalyzed α -alkylation of nitriles with alcohols. *Applied Organometallic Chemistry* **2020**, *34* (4), e5451.
15. Kuwahara, T.; Fukuyama, T.; Ryu, I., synthesis of alkylated nitriles by [RuHCl(CO)(PPh₃)₃]-catalyzed alkylation of acetonitrile using primary alcohols. *Chemistry Letters* **2013**, *42* (10), 1163-1165.
16. Sawaguchi, T.; Obora, Y., Iridium-catalyzed α -Alkylation of Acetonitrile with Primary and Secondary Alcohols. *Chemistry letters* **2011**, *40* (9), 1055-1057.
17. Thiyagarajan, S.; Gunanathan, C., Facile ruthenium (II)-catalyzed α -alkylation of arylmethyl nitriles using alcohols enabled by metal–ligand cooperation. *ACS Catalysis* **2017**, *7* (8), 5483-5490.

18. Turnbull, B. W.; Evans, P. A., Enantioselective rhodium-catalyzed allylic substitution with a nitrile anion: Construction of acyclic quaternary carbon stereogenic centers. *Journal of the American Chemical Society* **2015**, *137* (19), 6156-6159.
19. Paudel, K.; Xu, S.; Ding, K., Switchable Cobalt-Catalyzed α -Olefination and α -Alkylation of Nitriles with Primary Alcohols. *Organic Letters* **2021**.
20. Anxionnat, B.; Gomez Pardo, D.; Ricci, G.; Cossy, J., Monoalkylation of acetonitrile by primary alcohols catalyzed by iridium complexes. *Organic letters* **2011**, *13* (15), 4084-4087.
21. Buil, M. L.; Esteruelas, M. A.; Herrero, J.; Izquierdo, S.; Pastor, I. M.; Yus, M., Osmium catalyst for the borrowing hydrogen methodology: α -alkylation of arylacetonitriles and methyl ketones. *ACS Catalysis* **2013**, *3* (9), 2072-2075.
22. Ma, W.; Cui, S.; Sun, H.; Tang, W.; Xue, D.; Li, C.; Fan, J.; Xiao, J.; Wang, C., Iron-Catalyzed Alkylation of Nitriles with Alcohols. *CHEMISTRY-A EUROPEAN JOURNAL* **2018**, *24* (50), 13118-13123.
23. Borghs, J. C.; Tran, M. A.; Sklyaruk, J.; Rueping, M.; El-Sepelgy, O., Sustainable alkylation of nitriles with alcohols by manganese catalysis. *The Journal of organic chemistry* **2019**, *84* (12), 7927-7935.
24. Bera, S.; Bera, A.; Banerjee, D., Nickel-catalyzed hydrogen-borrowing strategy: chemo-selective alkylation of nitriles with alcohols. *Chemical Communications* **2020**, *56* (50), 6850-6853.
25. Chakraborty, P.; Garg, N.; Manoury, E.; Poli, R.; Sundararaju, B., C-alkylation of various carbonucleophiles with secondary alcohols under CoIII-catalysis. *ACS Catalysis* **2020**, *10* (14), 8023-8031.
26. Paudel, K.; Xu, S.; Ding, K., α -Alkylation of Nitriles with Primary Alcohols by a Well-Defined Molecular Cobalt Catalyst. *The Journal of Organic Chemistry* **2020**, *85* (23), 14980-14988.
27. Saini, A.; Smith, C. R.; Wekesa, F. S.; Helms, A. K.; Findlater, M., Conversion of aldimines to secondary amines using iron-catalysed hydrosilylation. *Organic & Biomolecular Chemistry* **2018**, *16* (48), 9368-9372.
28. Singh, A.; Shafiei-Haghighi, S.; Smith, C. R.; Unruh, D. K.; Findlater, M., Hydroboration of Alkenes and Alkynes Employing Earth-Abundant Metal Catalysts. *Asian Journal of Organic Chemistry* **2020**, *9* (3), 416-420.
29. Tamang, S. R.; Bedi, D.; Shafiei-Haghighi, S.; Smith, C. R.; Crawford, C.; Findlater, M., Cobalt-catalyzed hydroboration of alkenes, aldehydes, and ketones. *Organic letters* **2018**, *20* (21), 6695-6700.
30. Tamang, S. R.; Cozzolino, A. F.; Findlater, M., Iron catalysed selective reduction of esters to alcohols. *Organic & Biomolecular Chemistry* **2019**, *17* (7), 1834-1838.
31. Tamang, S. R.; Findlater, M., Iron catalyzed hydroboration of aldehydes and ketones. *The Journal of organic chemistry* **2017**, *82* (23), 12857-12862.
32. Tamang, S. R.; Singh, A.; Unruh, D. K.; Findlater, M., Nickel-catalyzed regioselective 1, 4-hydroboration of N-heteroarenes. *ACS Catalysis* **2018**, *8* (7), 6186-6191.
33. Zhang, S.; Bedi, D.; Cheng, L.; Unruh, D. K.; Li, G.; Findlater, M., Cobalt (II)-catalyzed stereoselective olefin isomerization: facile access to acyclic trisubstituted alkenes. *Journal of the American Chemical Society* **2020**, *142* (19), 8910-8917.
34. Bazkiaei, A. R.; Wiseman, M.; Findlater, M., Iron-catalysed hydroboration of non-activated imines and nitriles: kinetic and mechanistic studies. *RSC Advances* **2021**, *11* (25), 15284-15289.
35. Brown, L. A.; Wekesa, F. S.; Unruh, D. K.; Findlater, M.; Long, B. K., BIAN-Fe (η^6 -C₆H₆): Synthesis, characterization, and l-lactide polymerization. *Journal of Polymer Science Part A: Polymer Chemistry* **2017**, *55* (17), 2824-2830.

36. Larson, P. J.; Wekesa, F. S.; Singh, A.; Smith, C. R.; Rajput, A.; McGovern, G. P.; Unruh, D. K.; Cozzolino, A. F.; Findlater, M., Synthesis, characterization, electrochemical properties and theoretical calculations of (BIAN) iron complexes. *Polyhedron* **2019**, *159*, 365-374.
37. van Asselt, R.; Vrieze, K.; Elsevier, C. J., Oxidative addition of organic halides to zerovalent palladium complexes containing rigid bidentate nitrogen ligands. *Journal of organometallic chemistry* **1994**, *480* (1-2), 27-40.
38. Bernauer, J.; Pölker, J.; Jacobi von Wangelin, A., Redox-active BIAN-based Diimine Ligands in Metal-Catalyzed Small Molecule Syntheses. *ChemCatChem*.
39. LaPointe, A. M.; Brookhart, M., Reactions of cationic palladium (II) methyl and vinyl complexes with alkynes. *Organometallics* **1998**, *17* (8), 1530-1537.
40. Liu, W.; Brookhart, M., Mechanistic studies of palladium (II)- α -diimine-catalyzed polymerizations of cis-and trans-2-butenes. *Organometallics* **2004**, *23* (26), 6099-6107.
41. Hill, N. J.; Vargas-Baca, I.; Cowley, A. H., Recent developments in the coordination chemistry of bis (imino) acenaphthene (BIAN) ligands with s-and p-block elements. *Dalton Transactions* **2009**, (2), 240-253.
42. Gomes, C. S.; Gomes, P. T.; Duarte, M. T., α -Diimine transition-metal complexes: Mechanochemistry— A new synthetic approach. *Journal of Organometallic Chemistry* **2014**, *760*, 101-107.
43. Rosa, V.; Carabineiro, S. A.; Avilés, T.; Gomes, P. T.; Welter, R.; Campos, J. M.; Ribeiro, M. R., Synthesis, characterisation and solid state structures of α -diimine cobalt (II) complexes: Ethylene polymerisation tests. *Journal of Organometallic Chemistry* **2008**, *693* (4), 769-775.
44. Sandl, S.; Maier, T. M.; van Leest, N. P.; Kröncke, S.; Chakraborty, U.; Demeshko, S.; Koszinowski, K.; de Bruin, B.; Meyer, F.; Bodensteiner, M., Cobalt-catalyzed hydrogenations via olefin cobaltate and hydride intermediates. *ACS Catalysis* **2019**, *9* (8), 7596-7606.
45. Wang, X.; Fan, L.; Huang, C.; Liang, T.; Guo, C. Y.; Sun, W. H., Highly cis-1, 4 selective polymerization of isoprene promoted by α -diimine cobalt (II) chlorides. *Journal of Polymer Science Part A: Polymer Chemistry* **2016**, *54* (22), 3609-3615.

IV. METAL-CATALYZED HYDROBORATION OF CARBONATES AND SEMI-HYDROGENATION OF ALKYNES

4.1. Metal-catalyzed hydroboration of carbonates

A large number of organic carbonates are used as solvents in synthesis and catalysis.¹ Although carbonates are considered to be green solvents and can increase chemical selectivity in some cases, removing them from reaction mixtures can be challenging;² in particular, cyclic carbonates typically have high boiling points. One of the most effective ways to overcome this challenge is to transform them to value added substrates via reduction. The reduction of carbonyl groups has garnered much interest in preceding decades;³ and progress has been made in the hydrogenation of ketones, aldehydes, and more recently, esters⁴ and amides.⁵ Recently, reduction of organic carbonates has drawn attention as they can be readily prepared from renewable C1 feedstock i.e.; CO and CO₂ and their reduction yields methanol.^{4,6} Cyclic organic carbonates in particular can be obtained by the coupling of CO₂ with epoxides; affords diols and methanol upon hydrogenation.⁶ The conversion of CO₂ to carbonates and further to diols presents a practical two-step approach for the conversion of greenhouse gas CO₂ into methanol and value-added diols. However, examples of reduction of organic carbonates remains scant. The catalytic hydrogenation of cyclic carbonates represents an excellent approach to a range of important diol molecules, however, it requires harsh reaction conditions, flammable gases, high temperature and transition metal catalysts based upon Ru, Mn and, Fe complexes.⁷⁻⁹

Hydroboration is an alternative to hydrogenation for the reduction of organic compounds and it does not require pressurized and flammable H₂ gas. Although, hydroboration of aldehydes, ketones, isocyanates, imines, amides, pyridines, nitriles, and alkynes has been well explored,^{7,10-11} examples of hydroboration of carbonates remain limited.

In 2018, Leitner and co-workers synthesized [Mn(Ph₂PCH₂SiMe₂)₂NH(CO)₂Br] (**64**) and utilized it for the hydroboration of carboxylic acids, carbonates and CO₂; the system worked well for both linear and cyclic carbonates.⁷ In 2019, Rueping and co-workers utilized Mg based complex MgBu₂ (**6**) for the reduction of the organic carbonates; yields upto >95% were reported. The catalytic system was also capable of recycling polycarbonates to diol and methanol.¹² Ma and co-workers used low valent Mg (I) complex (**65**) for the conversion of carbonates, polycarbonates, esters and CO₂ to alcohols; excellent yields of up to 99 % were reported.¹ Rüter and co-workers employed Mn(OTf)₂(CH₃CN)₂ for the hydroboration of esters, carbonates and nitriles; yields of up to 99% were reported. This catalytic system presented the first successful example of a catalyst which didn't require any ligand preparation.¹³ In 2021, Wangelin and co-workers deployed Mn(hmds)₂ for the catalytic hydroboration of nitriles, esters, amides, pyridines, carbodiimides and carbonates. The catalytic system was also capable of depolymerizing polycarbonates and polyesters.¹⁴ Very recently, Cantat and co-workers employed La[N(SiMe₃)₂]₃ in presence of HBpin for the depolymerization of polyesters and polycarbonates; alcohols and diols were obtained in high selectivity.¹⁵

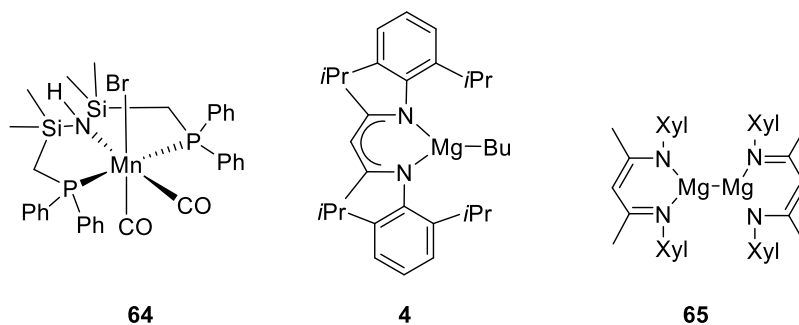
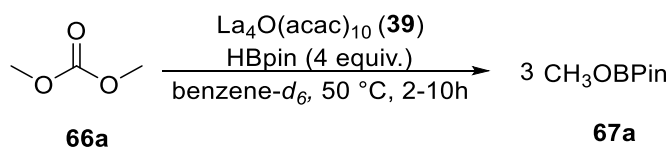


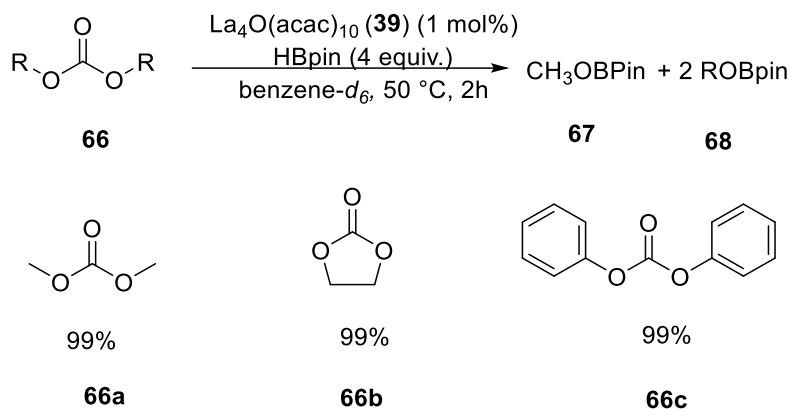
Figure 4.1. Selected examples of pre-catalysts for hydroboration of carbonates.

The ability and versatility of $\text{La}_4\text{O}(\text{acac})_{10}$ (**39**) to catalyze the hydroboration of a wide range of substrates (amides and esters)¹⁶ prompted us to test our previously developed catalytic system in the hydroboration of carbonates. Under similar catalytic conditions as employed for hydroboration of esters and increasing the amount of HBpin from 2.5 equiv. to 4 equiv., we began optimizing the reaction conditions. Using 0.1 mol% of **39**, excellent conversion of **66a** to **67a** was observed in 10 hours. Upon an increase in catalyst loading to 1 mol %, the reaction was observed to reach completion in ~2 hours. The catalytic system worked well for both cyclic and acyclic substrates and NMR yields of up to 99 % were obtained in all cases (**Scheme 4.1**).

Table 4.1. Optimization of hydroboration of carbonates

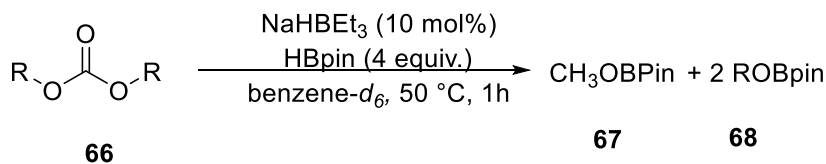


$\text{La}_4\text{O}(\text{acac})_{10}$ (mol %) (39)	67a Conversion (%), time
0.1	>99%, 10h
0.5	>99%, 4h
1.0	>99 %, 2h
1.5	>99 %, 2h



Scheme 4.1. Substrate scope for lanthanum-catalyzed hydroboration of carbonates

Our group previously reported on the ability of NaHBET_3 to catalyze the hydroboration of nitriles in 2020.¹⁷ We tested this catalytic system in the hydroboration of carbonates and compared it to the lanthanum-based catalytic system described above. Complete conversion of **66a** to **67a** was observed with 10 mol% NaHBET_3 in the presence of 4 equiv. HBpin. Quantitative yields were obtained for substrates **66a-c** in 1 hour of reaction time. Progress of the reaction of **66b** was monitored by ^1H NMR and full conversion of substrate was observed in about 40 minutes (**Figure 4.7**). No reaction was observed when the equimolar reaction of HBpin and ethylene carbonate (**Figure 4.8-4.9**) was carried out. Upon mixing equal amounts of ethylene carbonate and NaHBET_3 , a peak at -17.08 ppm was observed in the ^{11}B NMR spectrum, suggesting the formation of an $[\text{REt}_3\text{B}]^-$ type species (**Figure 4.10**). Monitoring the catalytic reaction using ^{11}B NMR revealed the presence of a peak at -85 ppm (**Figure 4.6**) suggesting that BEt_3 was evolved during the reaction. This prompted us to test the activity of NaH as it might be an active catalyst generated after the liberation of BEt_3 from NaHBET_3 , 77% conversion of **66b** was obtained after 24 hours. As reaction catalyzed by NaH is slower in comparison to NaHBET_3 , we believe that NaH might not be an active catalyst generated during the course of the reaction.



Scheme 4.2. General reaction for hydroboration of carbonates with NaHBET_3

4.2. Copper-catalyzed semi-hydrogenation of alkynes

Alkenes are a chemical feedstock and are used extensively in the production of alcohols, plastics and fuels. Some of the methods used to access C=C double bonds include witting reactions, olefin metathesis, and the semi-reduction of alkynes. The semi-reduction of alkynes to alkenes has garnered interest in the recent past, but there are challenges associated with this transformation. The two major problems associated with the semi-reduction of alkynes are over-reduction to alkanes and the generation of a mixture of Z/E alkene isomers. In the past decade, methods

Entry	Copper source/ solvent	Ligand	Conversion 73 (%)	Selectivity (74:74')
1.	CuF ₂ /THF	-	<5%	n.d.
2.	CuCl ₂ /THF	-	<5%	n.d.
3.	Cu(OTf) ₂ /THF	-	>99%	94:6
4.	Cu(OTf) ₂ /ACN	-	>99%	94:6
5.	Cu(OTf) ₂ /DMF	-	95%	96:4
6.	Cu(OTf) ₂ /THF	PCy ₃	98	94:6
7.	Cu(OTf) ₂ /THF	PPh ₃	>99%	94:6
8.	Cu(OTf) ₂ /THF	PCyp ₃	>99%	95:5
9.	Cu(OTf) ₂ /THF	2,2'-bipy	95%	94:6
10.	Cu(OTf) ₂ /THF	4,4-di-tert-butyl-2,2'-bipyridine	98%	94:6
11.	Cu(OTf) ₂ /THF	dppe	n.r.	-

Reaction conditions: Diphenylacetylene (44.5 mg, 0.25 mmol), [Cu] (0.0125 mmol), NaOtBu (2.4 mg, 0.025 mmol), BH₃.NH₃ (15.4 mg, 0.5 mmol, 2 equiv.) and 0.7 mL solvent. n.d-not determined.

4.3. Conclusion

Preliminary results have shown that both La₄O(acac)₁₀ and NaHBET₃ are potent pre-catalysts for the hydroboration of carbonates. Future experiments will focus on determining the applicability of these systems for hydroboration of polycarbonates, carbamates, and urea derivatives. Copper-catalyzed semi -hydrogenation of alkynes is reported; our system involves the usage of commercially available copper salts and no special ligand synthesis is required for this transformation. Future experiments will focus on the mechanistic studies and optimizing the catalytic system that can flip the selectivity from Z-alkene to E-alkene.

4.4. Experimental Section

4.4.1. General procedure for hydroboration of carbonates with La₄O(acac)₁₀

An oven dried J-Young tube was charged with La₄O(acac)₁₀ (3.9 mg, 0.0025mmol, 1 mol%), carbonate (0.25 mmol), HBpin (127.98mg, 144 uL, 1 mmol) and 0.7-0.8 mL benzene. The reaction mixture was then placed on a preheated oil bath at 50 °C. The progress of the reaction was monitored by ¹H NMR and ¹¹B NMR.

4.4.2. General procedure for hydroboration of carbonates with NaHBET₃

An oven dried J-Young tube was charged with carbonate (0.25 mmol), NaHBET₃ (25 uL, 0.025mmol, 10 mol%), HBpin (127.98mg, 144 uL, 1 mmol) and 0.7-0.8 mL benzene. The reaction mixture was then placed on a preheated oil bath at 50 °C. The progress of the reaction was monitored by ¹H NMR and ¹¹B NMR.

4.4.3. General procedure for semi-hydrogenation of alkynes

An oven dried vial was charged with diphenylacetylene (44.5 mg, 0.25 mmol), Cu(OTf)₂ (4.5 mg, 0.0125 mmol), NaOtBu (2.4 mg, 0.025 mmol), (BH₃.NH₃ (15.4 mg, 0.5 mmol, 2 equiv.) and 0.7 mL solvent. The reaction mixture was then placed on a preheated oil bath at 50 °C. The progress of the reaction was monitored by ¹H NMR.

4.5. Appendix

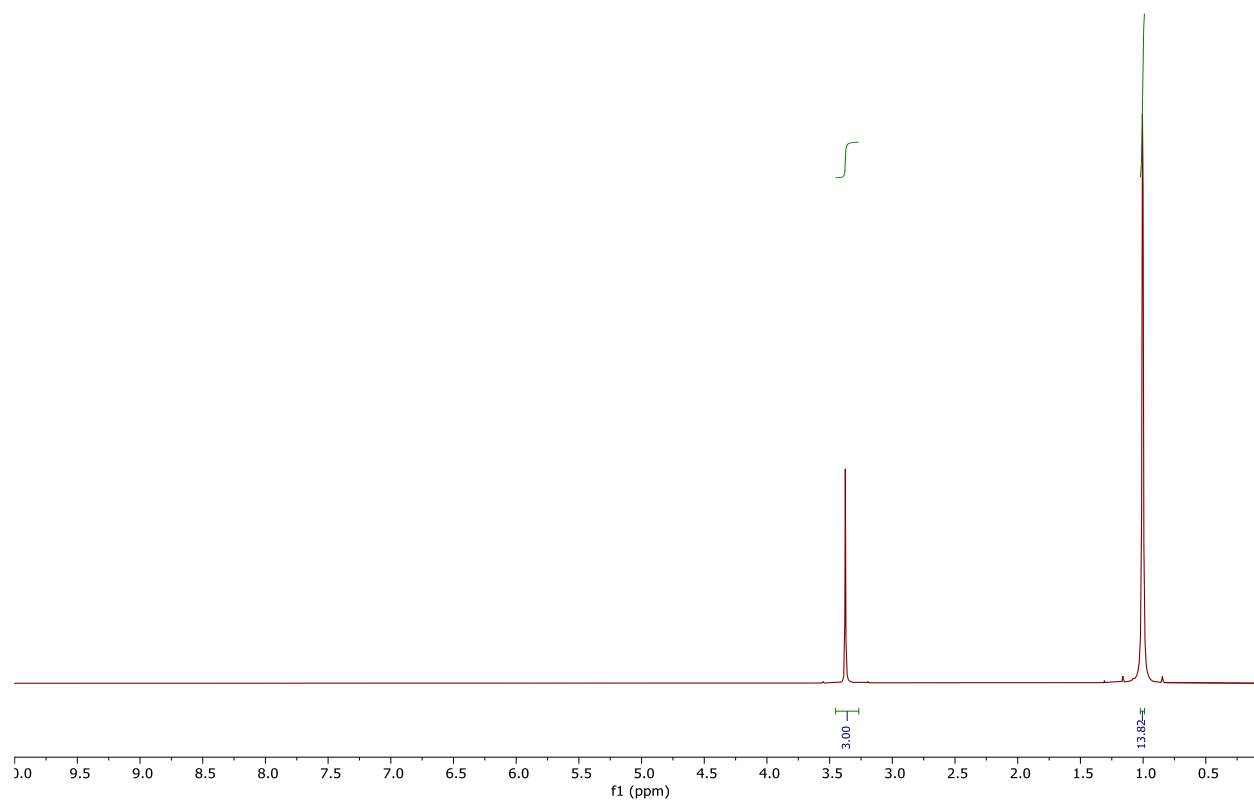


Figure 4.3. ^1H NMR for hydroboration of dimethyl carbonate with $\text{La}(\text{acac})_3$

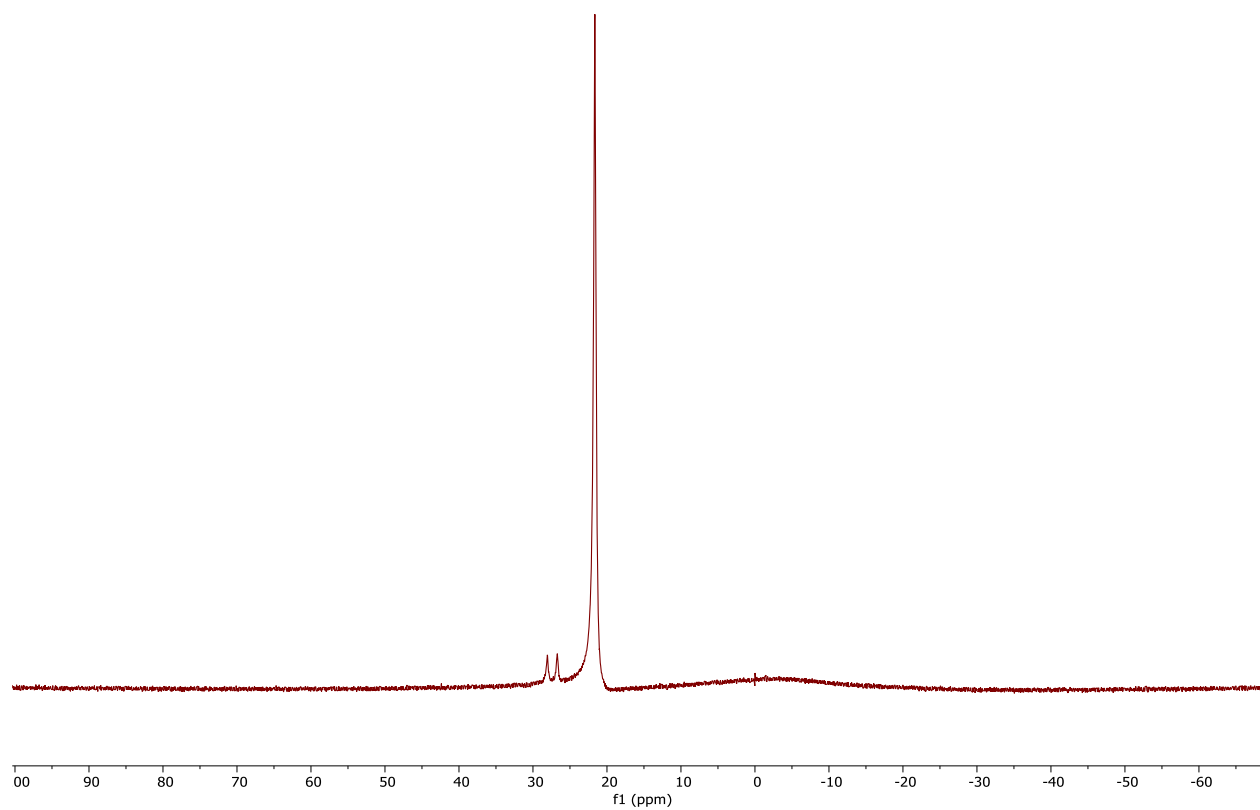


Figure 4.4. ^{11}B NMR for hydroboration of dimethyl carbonate with $\text{La}(\text{acac})_3$

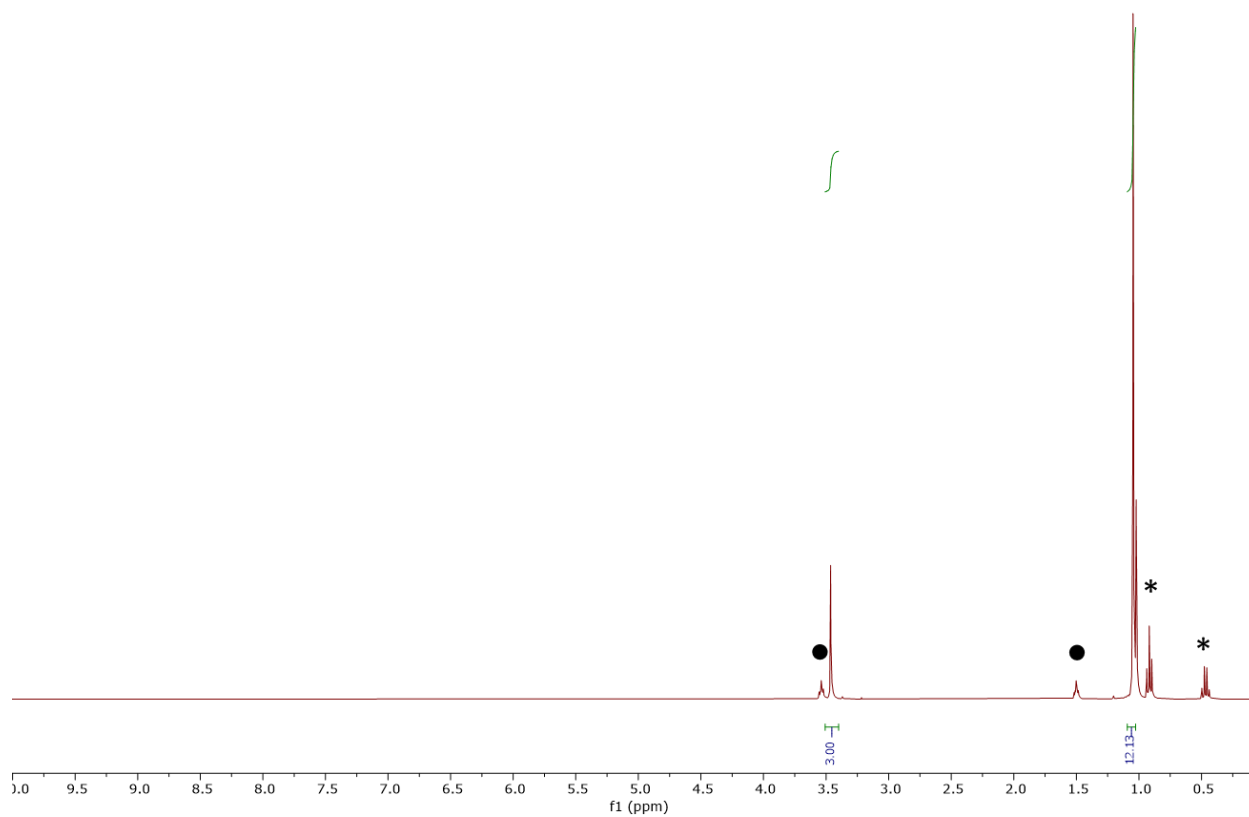


Figure 4.5. ^1H NMR for hydroboration of dimethyl carbonate with NaHBET_3 , ● represents NaHBET_3 and * represents internal standard

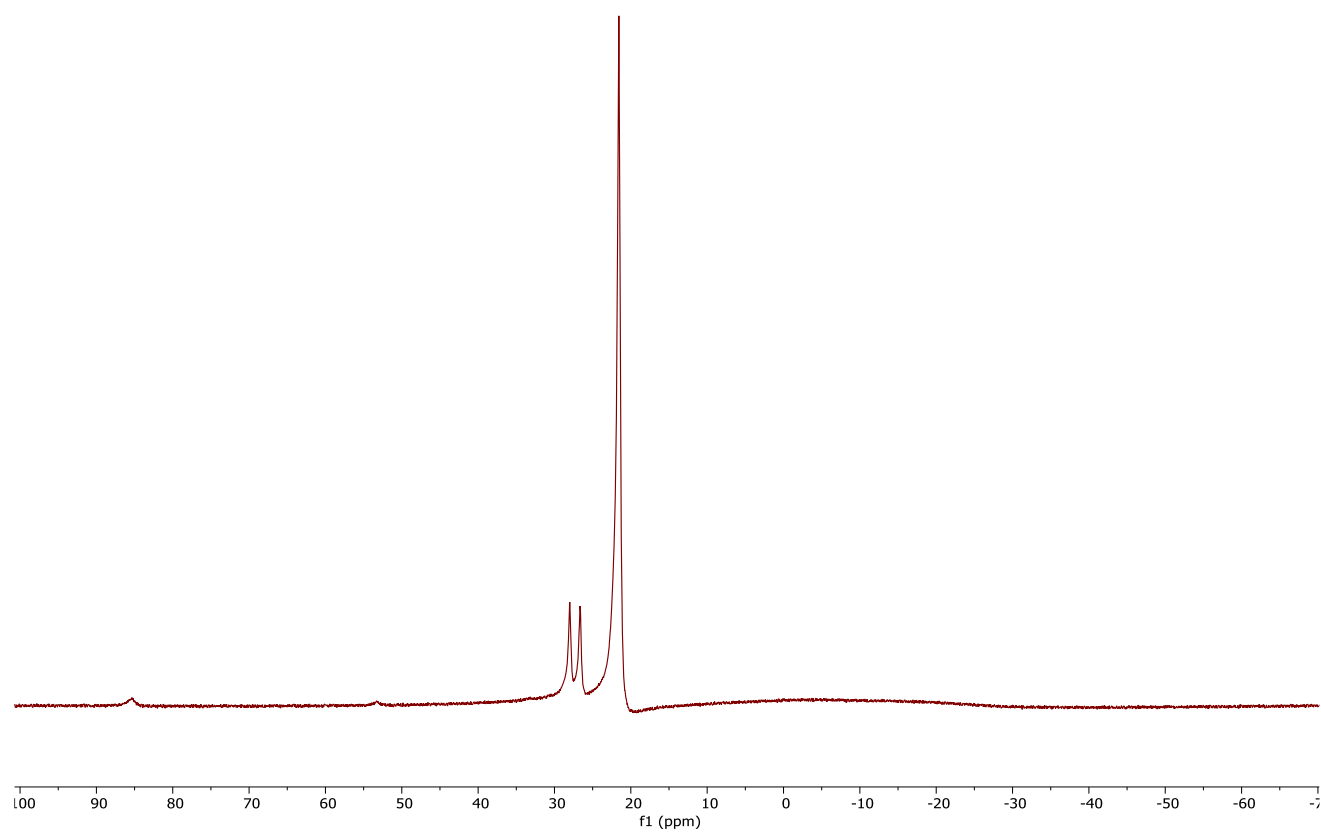


Figure 4.6. ^{11}B NMR for hydroboration of dimethyl carbonate with NaHBET_3

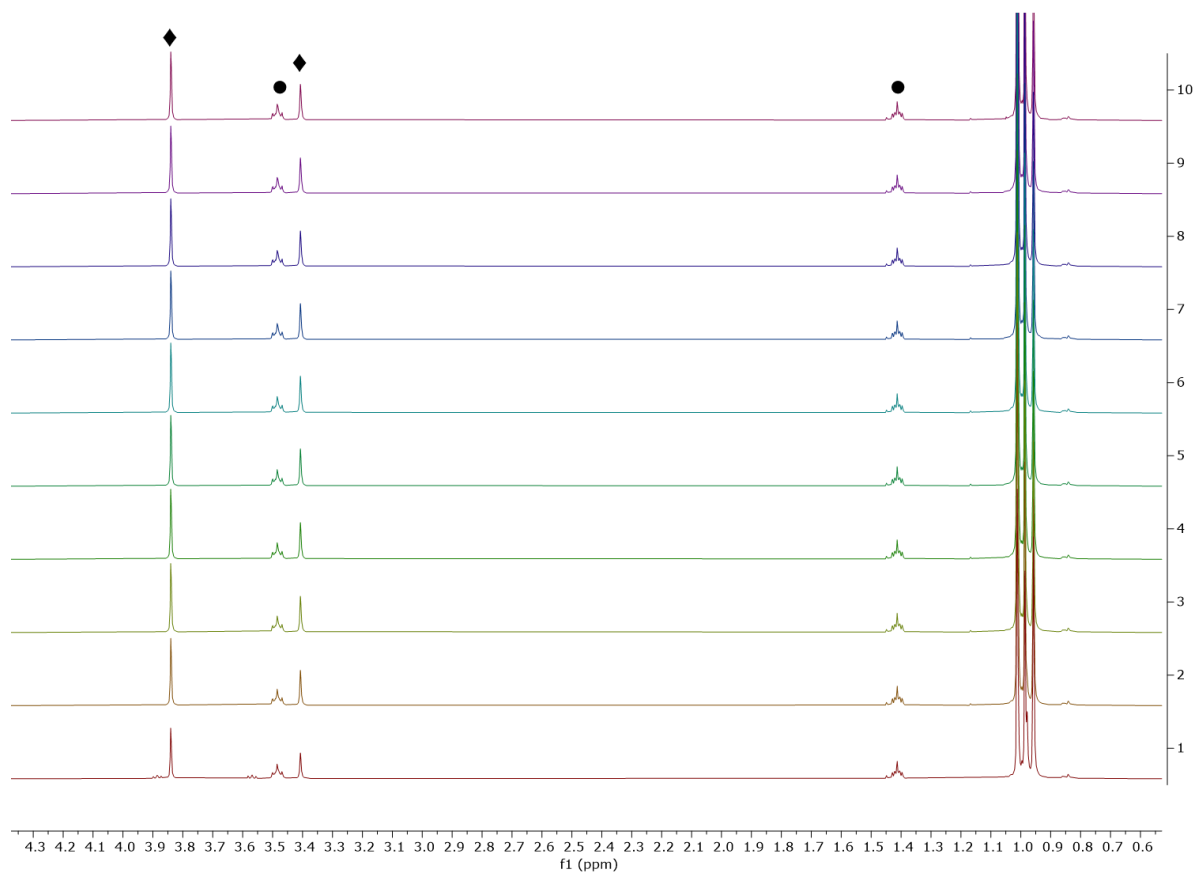


Figure 4.7. ^1H NMR for progress of hydroboration of ethylene carbonate with NaHBET_3 , ● represents NaHBET_3 and ♦ represents the products **67** and **68b**

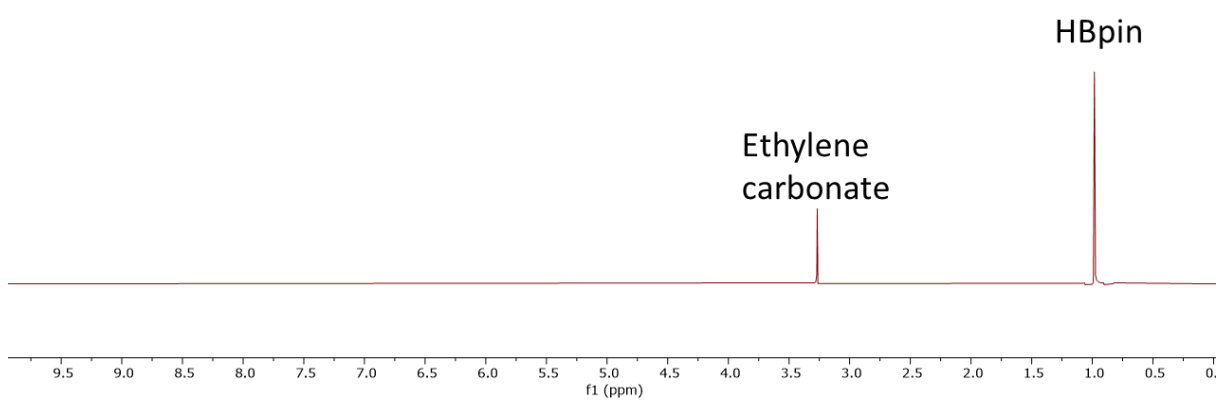


Figure 4.8. ^1H NMR of stoichiometric reaction of HBpin and ethylene carbonate

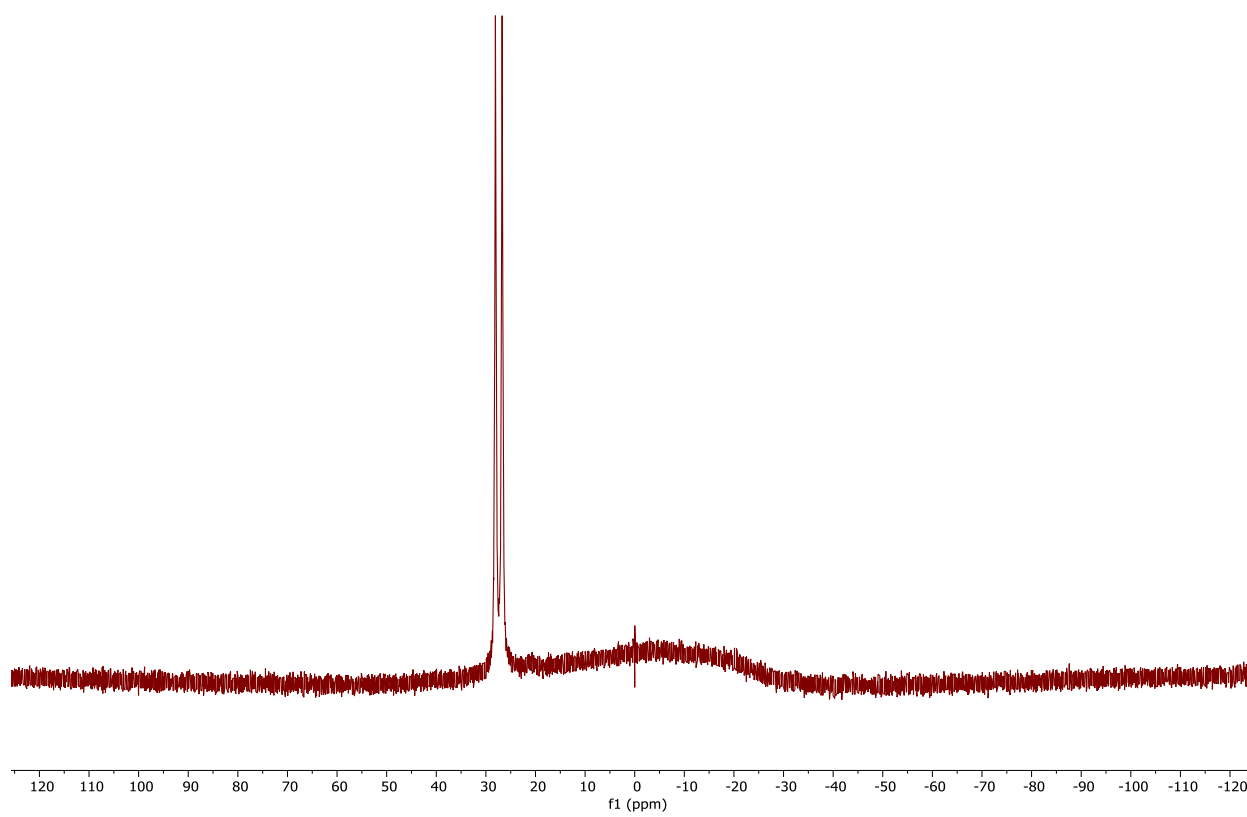


Figure 4.9. ^{11}B NMR of stoichiometric reaction of HBpin and ethylene carbonate

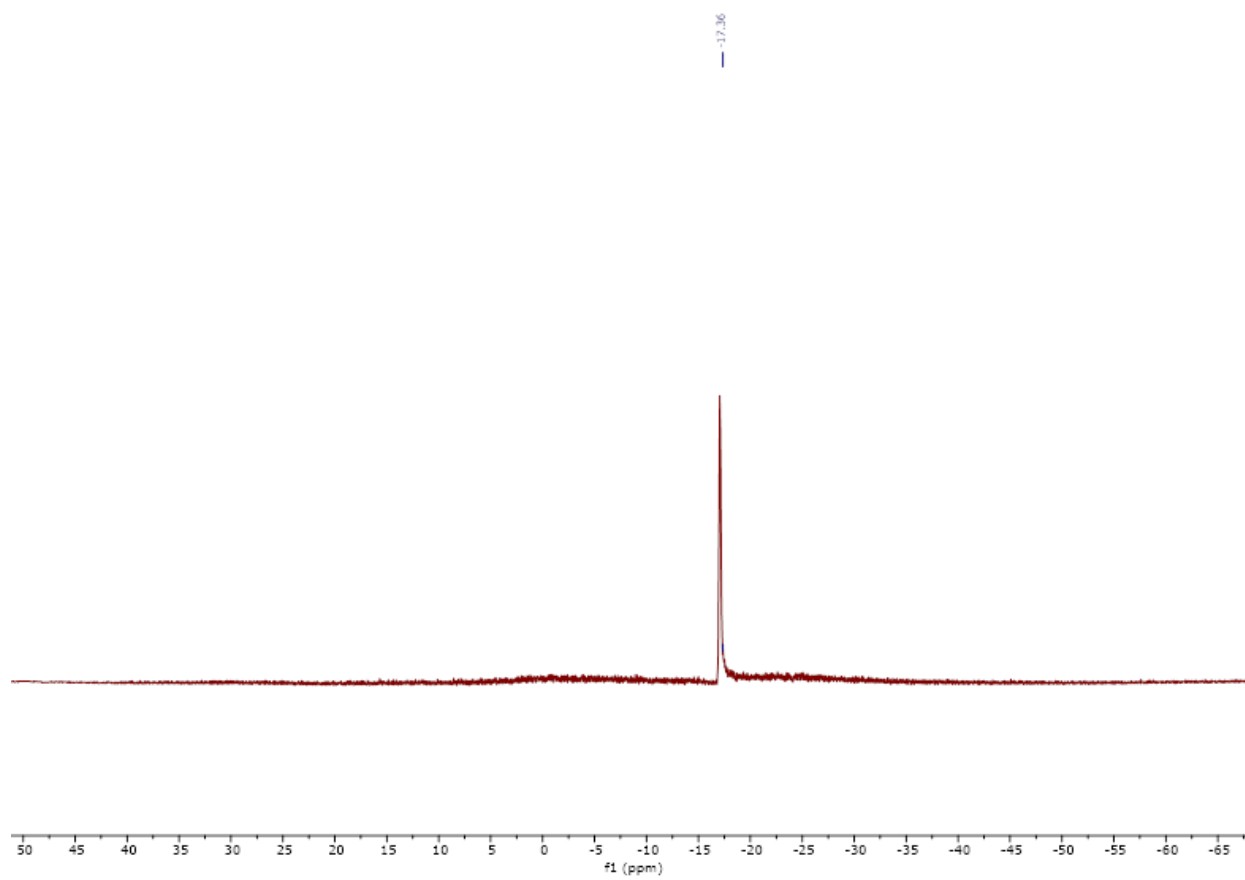


Figure 4.10. ^{11}B NMR of stoichiometric reaction of NaHBET_3 and ethylene carbonate

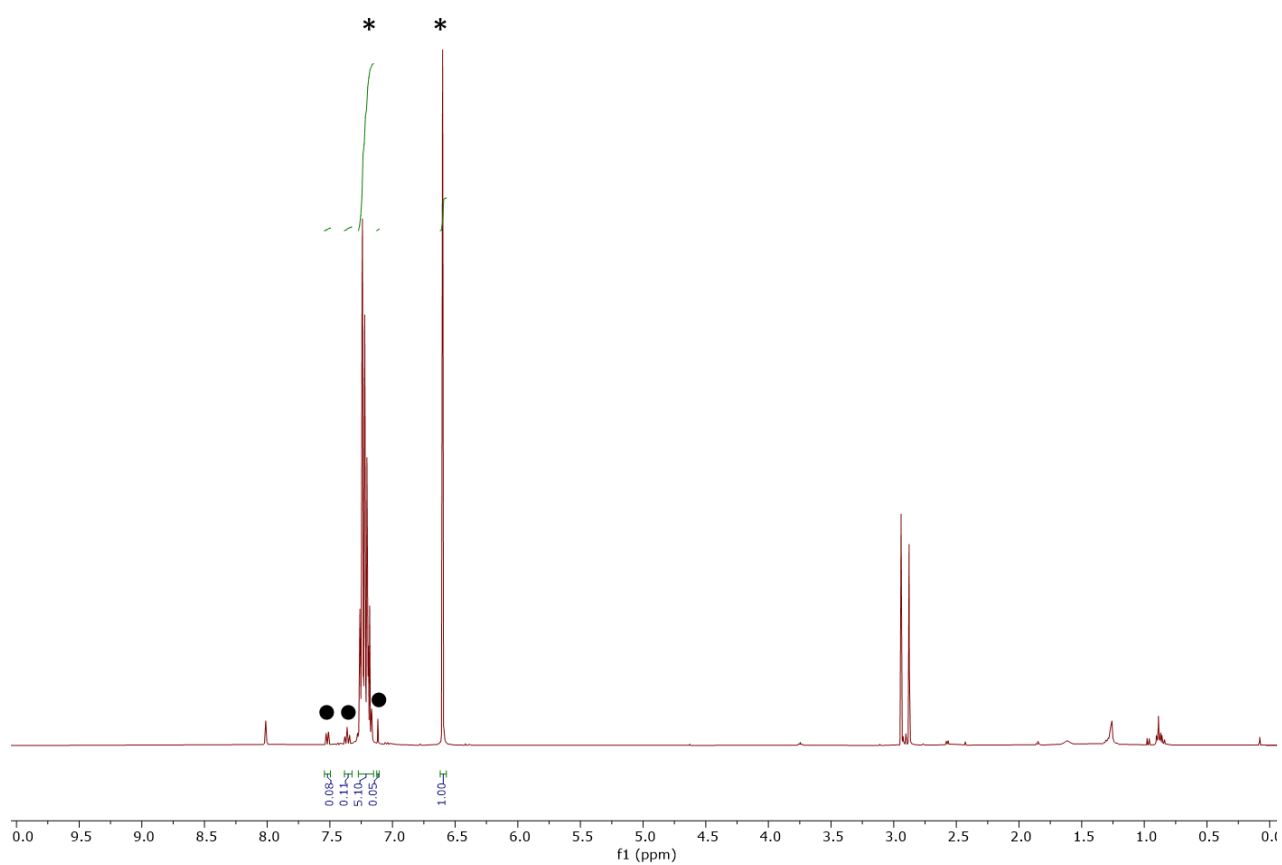


Figure 4.11. ^1H NMR of semi-reduction of diphenylacetylene in DMF, * represents Z-alkene, ● represents E-alkene

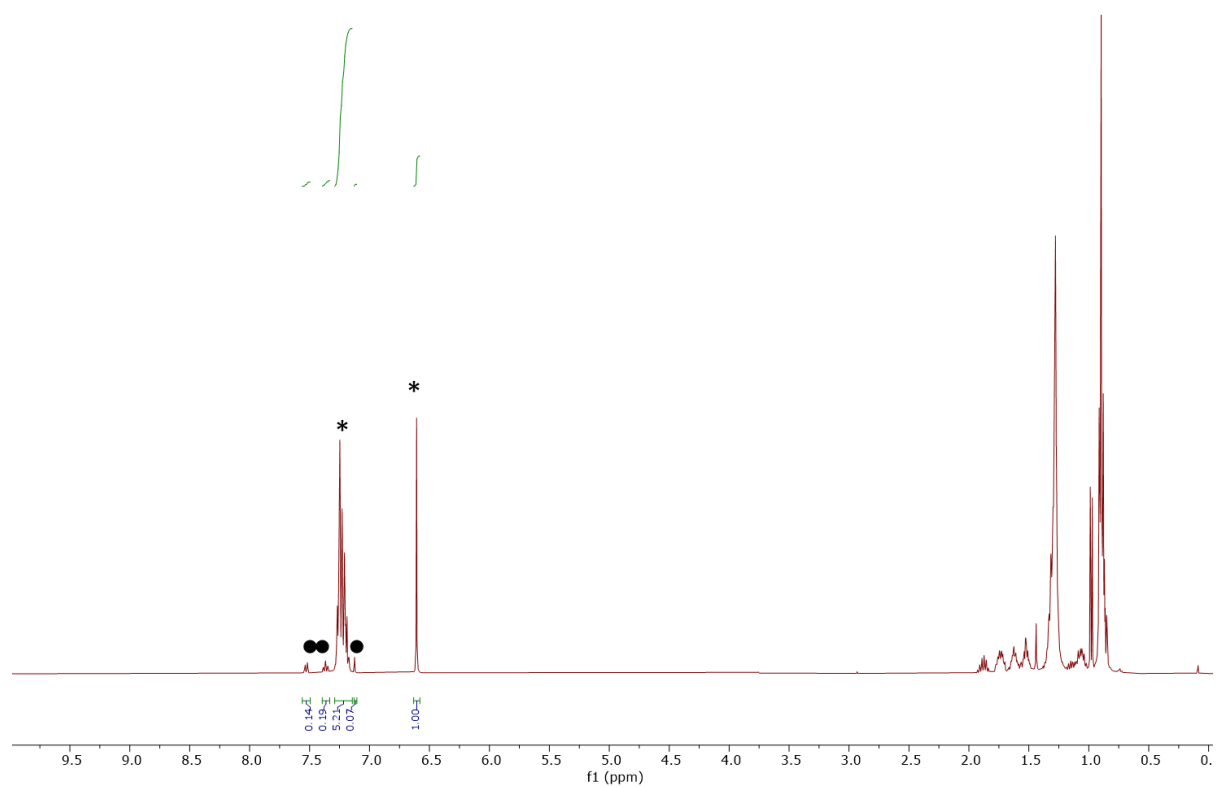


Figure 4.12. ^1H NMR of semi-reduction of diphenylacetylene in THF and 4, 4-ditertiarybutyl-2,2'-bipyridyl, * represents Z-alkene, ● represents E-alkene.

4.6. References

1. Cao, X.; Wang, W.; Lu, K.; Yao, W.; Xue, F.; Ma, M., Magnesium-catalyzed hydroboration of organic carbonates, carbon dioxide and esters. *Dalton Transactions* **2020**, 49 (9), 2776-2780.
2. Schaffner, B.; Schaffner, F.; Verevkin, S. P.; Borner, A., Organic carbonates as solvents in synthesis and catalysis. *Chemical reviews* **2010**, 110 (8), 4554-4581.
3. Clapham, S. E.; Hadzovic, A.; Morris, R. H., Mechanisms of the H₂-hydrogenation and transfer hydrogenation of polar bonds catalyzed by ruthenium hydride complexes. *Coordination Chemistry Reviews* **2004**, 248 (21-24), 2201-2237.
4. Zhang, J.; Leitus, G.; Ben-David, Y.; Milstein, D., Efficient homogeneous catalytic hydrogenation of esters to alcohols. *Angewandte Chemie* **2006**, 118 (7), 1131-1133.
5. Magro, A. A. N.; Eastham, G. R.; Cole-Hamilton, D. J., The synthesis of amines by the homogeneous hydrogenation of secondary and primary amides. *Chemical communications* **2007**, (30), 3154-3156.
6. Han, Z.; Rong, L.; Wu, J.; Zhang, L.; Wang, Z.; Ding, K., Catalytic hydrogenation of cyclic carbonates: a practical approach from CO₂ and epoxides to methanol and diols. *Angewandte Chemie* **2012**, 124 (52), 13218-13222.
7. Erken, C.; Kaithal, A.; Sen, S.; Weyhermüller, T.; Hölscher, M.; Werlé, C.; Leitner, W., Manganese-catalyzed hydroboration of carbon dioxide and other challenging carbonyl groups. *Nature communications* **2018**, 9 (1), 1-9.
8. Kim, S. H.; Hong, S. H., Transfer hydrogenation of organic formates and cyclic carbonates: an alternative route to methanol from carbon dioxide. *ACS Catalysis* **2014**, 4 (10), 3630-3636.
9. Kumar, A.; Janes, T.; Espinosa-Jalapa, N. A.; Milstein, D., Manganese catalyzed hydrogenation of organic carbonates to methanol and alcohols. *Angewandte Chemie International Edition* **2018**, 57 (37), 12076-12080.
10. Geier, S. J.; Vogels, C. M.; Westcott, S. A., Current developments in the catalyzed hydroboration reaction. In *Boron Reagents in Synthesis*, ACS Publications: 2016; pp 209-225.
11. Yoshida, H., Borylation of alkynes under base/coinage metal catalysis: some recent developments. *ACS Catalysis* **2016**, 6 (3), 1799-1811.
12. Szewczyk, M.; Magre, M.; Zubar, V.; Rueping, M., Reduction of cyclic and linear organic carbonates using a readily available magnesium catalyst. *ACS Catalysis* **2019**, 9 (12), 11634-11639.
13. Thenarukandiyil, R.; Satheesh, V.; Shimon, L. J.; de Ruiter, G., Hydroboration of Nitriles, Esters, and Carbonates Catalyzed by Simple Earth-Abundant Metal Triflate Salts. *Chemistry—An Asian Journal* **2021**, 16 (8), 999-1006.
14. Ghosh, P.; Jacobi von Wangelin, A., Manganese-Catalyzed Hydroborations with Broad Scope. *Angewandte Chemie* **2021**, 133 (29), 16171-16179.
15. Kobylarski, M.; Berthet, J.-C.; Cantat, T., Reductive depolymerization of polyesters and polycarbonates with hydroboranes by using a lanthanum (III) tris (amide) catalyst. *Chemical communications (Cambridge, England)*.
16. Tamang, S. R.; Singh, A.; Bedi, D.; Bazkiaei, A. R.; Warner, A. A.; Glogau, K.; McDonald, C.; Unruh, D. K.; Findlater, M., Polynuclear lanthanide–diketonato clusters for the catalytic hydroboration of carboxamides and esters. *Nature Catalysis* **2020**, 3 (2), 154-162.
17. Bedi, D.; Brar, A.; Findlater, M., Transition metal-and solvent-free double hydroboration of nitriles. *Green Chemistry* **2020**, 22 (4), 1125-1128.
18. Semba, K.; Fujihara, T.; Xu, T.; Terao, J.; Tsuji, Y., Copper-Catalyzed Highly Selective Semihydrogenation of Non-Polar Carbon-Carbon Multiple Bonds using a Silane and an Alcohol. *Advanced Synthesis & Catalysis* **2012**, 354 (8), 1542-1550.

19. Cox, N.; Dang, H.; Whittaker, A. M.; Lalic, G., NHC–copper hydrides as chemoselective reducing agents: catalytic reduction of alkynes, alkyl triflates, and alkyl halides. *Tetrahedron* **2014**, *70* (27-28), 4219-4231.
20. Korytiaková, E.; Thiel, N. O.; Pape, F.; Teichert, J. F., Copper (I)-catalysed transfer hydrogenations with ammonia borane. *Chemical Communications* **2017**, *53* (4), 732-735.
21. Bao, H.; Zhou, B.; Jin, H.; Liu, Y., Diboron-Assisted Copper-Catalyzed Z-Selective Semihydrogenation of Alkynes Using Ethanol as a Hydrogen Donor. *The Journal of Organic Chemistry* **2019**, *84* (6), 3579-3589.
22. Fu, S.; Chen, N.-Y.; Liu, X.; Shao, Z.; Luo, S.-P.; Liu, Q., Ligand-controlled cobalt-catalyzed transfer hydrogenation of alkynes: Stereodivergent synthesis of Z- and E-alkenes. *Journal of the American Chemical Society* **2016**, *138* (27), 8588-8594.

Appendix: Copyrights

Nickel-Catalyzed Regioselective 1,4-Hydroboration of N-Heteroarenes

Author: Sem Raj Tamang, Arpita Singh, Daniel K. Unruh, et al

Publication: ACS Catalysis

Publisher: American Chemical Society

Date: Jul 1, 2018

Copyright © 2018, American Chemical Society



PERMISSION/LICENSE IS GRANTED FOR YOUR ORDER AT NO CHARGE

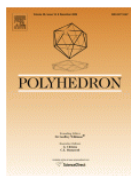
This type of permission/license, instead of the standard Terms and Conditions, is sent to you because no fee is being charged for your order. Please note the following:

- Permission is granted for your request in both print and electronic formats, and translations.
- If figures and/or tables were requested, they may be adapted or used in part.
- Please print this page for your records and send a copy of it to your publisher/graduate school.
- Appropriate credit for the requested material should be given as follows: "Reprinted (adapted) with permission from {COMPLETE REFERENCE CITATION}. Copyright {YEAR} American Chemical Society." Insert appropriate information in place of the capitalized words.
- One-time permission is granted only for the use specified in your RightsLink request. No additional uses are granted (such as derivative works or other editions). For any uses, please submit a new request.

If credit is given to another source for the material you requested from RightsLink, permission must be obtained from that source.

BACK

CLOSE WINDOW



Synthesis, characterization, electrochemical properties and theoretical calculations of (BIAN) iron complexes

Author:

Patrick J. Larson, Francis S. Wekesa, Arpita Singh, Cecilia R. Smith, Amit Rajput, Gregory P. McGovern, Daniel K. Unruh, Anthony F. Cozzolino, Michael Findlater

Publication: Polyhedron

Publisher: Elsevier

Date: 1 February 2019

© 2018 Elsevier Ltd. All rights reserved.

Journal Author Rights

Please note that, as the author of this Elsevier article, you retain the right to include it in a thesis or dissertation, provided it is not published commercially. Permission is not required, but please ensure that you reference the journal as the original source. For more information on this and on your other retained rights, please visit: <https://www.elsevier.com/about/our-business/policies/copyright#Author-rights>

BACK

CLOSE WINDOW

License Number 5297471048494

[Printable Details](#)

License date Apr 28, 2022

Licensed Content

Licensed Content Publisher John Wiley and Sons
Licensed Content Publication Asian Journal of Organic Chemistry
 Hydroboration of Alkenes and Alkynes
 Employing Earth-Abundant Metal
 Catalysts
Licensed Content Title
Licensed Content Author Michael Findlater, Daniel K. Unruh, Cecilia
 R. Smith, et al
Licensed Content Date Nov 28, 2019
Licensed Content Volume 9
Licensed Content Issue 3
Licensed Content Pages 5

Order Details

Type of use Dissertation/Thesis
Requestor type Author of this Wiley article
Format Print and electronic
Portion Full article
Will you be translating? No

About Your Work

Title Hydroboration of Alkenes and Alkynes
 Employing Earth-Abundant Metal
 Catalysts
Institution name UC Merced
Expected presentation date Jun 2022

Additional Data

Polynuclear lanthanide–diketonato clusters for the catalytic hydroboration of carboxamides and esters



Author: Sem Raj Tamang et al

Publication: Nature Catalysis

Publisher: Springer Nature

Date: Jan 6, 2020

Copyright © 2020. The Author(s). under exclusive licence to Springer Nature Limited

Author Request

If you are the author of this content (or his/her designated agent) please read the following. If you are not the author of this content, please click the Back button and select no to the question "Are you the Author of this Springer Nature content?".

Ownership of copyright in original research articles remains with the Author, and provided that, when reproducing the contribution or extracts from it or from the Supplementary Information, the Author acknowledges first and reference publication in the Journal, the Author retains the following non-exclusive rights:

To reproduce the contribution in whole or in part in any printed volume (book or thesis) of which they are the author(s).

The author and any academic institution, where they work, at the time may reproduce the contribution for the purpose of course teaching.

To reuse figures or tables created by the Author and contained in the Contribution in oral presentations and other works created by them.

To post a copy of the contribution as accepted for publication after peer review (in locked Word processing file, of a PDF version thereof) on the Author's own web site, or the Author's institutional repository, or the Author's funding body's archive, six months after publication of the printed or online edition of the Journal, provided that they also link to the contribution on the publisher's website.

Authors wishing to use the published version of their article for promotional use or on a web site must request in the normal way.

If you require further assistance please read Springer Nature's online [author reuse guidelines](#).

For full paper portion: Authors of original research papers published by Springer Nature are encouraged to submit the author's version of the accepted, peer-reviewed manuscript to their relevant funding body's archive, for release six months after publication. In addition, authors are encouraged to archive their version of the manuscript in their institution's repositories (as well as their personal Web sites), also six months after original publication.

v1.0

BACK

CLOSE WINDOW

Cobalt-Catalyzed Alkylation of Nitriles with Alcohols

Author: Arpita Singh, Michael Findlater

Publication: Organometallics

Publisher: American Chemical Society

Date: Feb 1, 2022

Copyright © 2022, American Chemical Society



PERMISSION/LICENSE IS GRANTED FOR YOUR ORDER AT NO CHARGE

This type of permission/license, instead of the standard Terms and Conditions, is sent to you because no fee is being charged for your order. Please note the following:

- Permission is granted for your request in both print and electronic formats, and translations.
- If figures and/or tables were requested, they may be adapted or used in part.
- Please print this page for your records and send a copy of it to your publisher/graduate school.
- Appropriate credit for the requested material should be given as follows: "Reprinted (adapted) with permission from {COMPLETE REFERENCE CITATION}. Copyright (YEAR) American Chemical Society." Insert appropriate information in place of the capitalized words.
- One-time permission is granted only for the use specified in your RightsLink request. No additional uses are granted (such as derivative works or other editions). For any uses, please submit a new request.

If credit is given to another source for the material you requested from RightsLink, permission must be obtained from that source.

[BACK](#)

[CLOSE WINDOW](#)